FUNCTIONAL COMPARTMENTATION OF RIBONUCLEIC ACID PRECURSORS IN *E. COLI*

by

James Edward Summerton

A Dissertation Submitted to the Faculty of the

COMMITTEE ON BIOCHEMISTRY

In Partial Fulfillment of the Requirements
For the Degree of

DOCTOR OF PHILOSOPHY

In the Graduate College

THE UNIVERSITY OF ARIZONA

1 9 7 3

THE UNIVERSITY OF ARIZONA

GRADUATE COLLEGE

I hereby recommend that this dissertation prepared under my direction by James Edward Summerton

entitled Functional Compartmentation of Ribonucleic Acid Precursors in E. coli

be accepted as fulfilling the dissertation requirement of the degree of Doctor of Philosophy

Christopher K. Mathews — 4/4/73
Dissertation Director — Date

After inspection of the final copy of the dissertation, the following members of the Final Examination Committee concur in its approval and recommend its acceptance:*

Christopher K. Mathews	4/4/73
Mark R. Haussler	4/4/73
W. S. Sachsman	4 Apr 73
Karen Dey Stark	4/6/73
Gordon Tollin	4/6/73

*This approval and acceptance is contingent on the candidate's adequate performance and defense of this dissertation at the final oral examination. The inclusion of this sheet bound into the library copy of the dissertation is evidence of satisfactory performance at the final examination.

STATEMENT BY AUTHOR

This dissertation has been submitted in partial fulfillment of requirements for an advanced degree at The University of Arizona and is deposited in the University Library to be made available to borrowers under rules of the Library.

Brief quotations from this dissertation are allowable without special permission, provided that accurate acknowledgment of source is made. Requests for permission for extended quotation from or reproduction of this manuscript in whole or in part may be granted by the head of the major department or the Dean of the Graduate College when in his judgment the proposed use of the material is in the interests of scholarship. In all other instances, however, permission must be obtained from the author.

SIGNED: James Edward Summerton

ACKNOWLEDGMENTS

I wish to express my sincere appreciation to the many persons throughout The University of Arizona who have so generously contributed their time and expertise to the development of this dissertation. Special thanks are extended to Dr. W. P. Cosart of the Chemical Engineering Department and to Mr. Larry Norrid, formerly of the Systems Engineering Department, for their extensive and invaluable assistance in developing several of the key equations used in the computer simulations. I am particularly indebted to Mr. R. A. Norling of the University Hospital Systems Engineering Department for incorporating my kinetic equations into two functioning FORTRAN programs.

Several persons have provided innumerable positive criticisms and suggestions throughout the course of this study. I have benefited especially from discussions with Dr. Marshall Dinowitz of the Microbiology Department, Drs. Kaoru Matsuda, W. V. Zucker, and Konrad Keck, all of the Biological Sciences Department, and Mr. M. J. Hewlett of the Biochemistry Department.

Finally, I would like to express my gratitude to Dr. C. K. Mathews for his astute guidance of this work, for intellectual stimulation, and for his enduring patience during my numerous pursuits along nonproductive tangents.

This investigation was supported by the U.S. Public Health Service Grant GMO 1982 to the Department of Biochemistry of the College

of Medicine, The University of Arizona, and the American Heart Association Grant 701013.

TABLE OF CONTENTS

TABLE OF CONTENTS--Continued

TABLE OF CONTENTS--Continued

LIST OF ILLUSTRATIONS

LIST OF ILLUSTRATIONS--Continued

LIST OF ILLUSTRATIONS--Continued

ABSTRACT

Computer simulations of RNA metabolism combined with isotopic labeling experiments were performed to verify and characterize the precursor compartmentation present in Escherichia coli B labeled with radioactive uracil. RNA precursors are shown to be compartmentalized in such a manner that both stable and unstable classes of RNA are synthesized from precursors of equivalent specific activities.

A method has been developed for measuring the pool size and synthesis rate of the unstable RNA fraction. This method is independent of both RNA-DNA hybridization efficiencies and the type of precursor compartmentation present in E. coli. A means of accurately measuring the specific activity of the stable RNA fraction is presented. This procedure relies on rifampicin to stop quickly the synthesis of short transcriptons and to allow either elongation and stabilization or degradation of all interfering RNA chains.

It is suggested that this method for measuring the pool size and synthesis rate of the unstable RNA fraction in a procaryotic organism may be of value in eucaryotic organisms where low hybridization efficiencies and precursor compartmentation are major obstacles to making kinetic measurements of RNA metabolism.

INTRODUCTION

Ribonucleic acid metabolism in microorganisms has been the subject of a great number of studies since the late 1950's. Such studies have shown that stable species of RNA (ribosomal and transfer RNA's) function as part of the machinery used in protein synthesis and unstable species of RNA (messenger RNA) function as agents which carry information, originally stored in the DNA, which is used to specify the sequence of amino acids in the proteins of the cell.

Once RNA had been implicated in the utilization of the information stored in DNA, a great deal of interest arose concerning the control of this information transfer. In studying the control of RNA metabolism, it is important to be able to measure such parameters as pool size, synthesis rate, and decay rate, for the various classes of RNA. A substantial number of methods for measuring these parameters have been developed in recent years. An overwhelming majority of these methods rely in part or totally on the use of isotopically labeled RNA precursors. For the most part these labeling methods fall into two categories.

In one category are those methods where labeled precursor is added for a brief period and then the total RNA is fractionated into its component classes or species. After fractionation, the various components are compared with respect to the amount of label incorporated. Such comparisons give information about relative rates of synthesis, pool sizes, rates of decay, etc. The methods for fractionating the RNA include hybridization to homologous DNA (Kennell, 1968; Midgley, 1969;

Norris and Koch, 1972), separation on the basis of molecular (or complex) weight (Mangiarotti and Schlesinger, 1967), and separation on the basis of stability (Levinthal, Keynan, and Higa, 1962; Schwartz, Craig, and Kennell, 1970). The major problem in these experiments generally lies in the fractionation procedure. For instance, hybridization reactions seldom proceed to more than 75% completion (Kennell, 1968). Fractionation, on the basis of molecular weight, such as when polysomes are separated from ribosomes and ribosomal subunits (Mangiarotti and Schlesinger, 1967; Zimmerman and Levinthal, 1967), often gives ambiguous or incomplete results. Ambiguity enters if the polysomes break down during their preparation and thereby contaminate the ribosomal or ribosomal subunit fractions. Incomplete fractionation can result when labeled RNA fractions are complexed to membrane (Maruo, Seto, and Nagata, 1969). When RNA is fractionated on the basis of its stability, such as in uracil deprivation of uracil auxotrophs (Lindahl and Forchhammer, 1969), recycling of label introduces considerable error into the rate estimation.

When metabolic inibitors are used to stop synthesis and allow decay of the unstable RNA fraction (Levinthal et al., 1962; Pato and Meyenburg, 1970), it is often difficult or impossible to determine if the resulting rate estimations correspond to the desired normal rates. For instance, actinomycin D has been used to stop RNA synthesis (Levinthal et al., 1962; Pastan and Perlman, 1969). Actinomycin D is believed to block RNA synthesis by stopping the translocation of RNA polymerase along the DNA template. In these experiments the amount and rate of decay of unstable RNA are measured. There is, however, evidence

indicating that the unstable RNA fraction decays abnormally in the presence of actinomycin (Fan, Higa, and Levinthal, 1964). Another metabolic inhibitor, rifampicin, has been used to block new RNA chain initiations (Schwartz et al., 1970; Pato and Meyenburg, 1970). This drug acts by binding to free RNA polymerase molecules. The resulting RNA polymerase-rifampicin complex is incapable of initiating new RNA chains. The synthesis of previously initiated RNA chains continues to completion in the presence of rifampicin (Umezawa et al., 1968). In such experiments, the maximum amount of label incorporated is assumed to be proportional to the rate of total RNA synthesis and the amount of label remaining after the unstable RNA has decayed is assumed to be proportional to the rate of stable RNA synthesis. The difference is presumed to be proportional to the rate of unstable RNA synthesis. The problem here is that the amount of label incorporated into any given RNA species is closely related to its transcripton length; hence, products of long transcriptons are grossly overestimated and products of short transcriptons are substantially underestimated. It would only be fortuitous if the results from such experiments correlated with relative synthesis rates. An additional problem with this approach derives from the fact that a very substantial amount (about 50%) of labeled unstable RNA decays from the time labeled precursor is added to the time when the maximum amount of label has been incorporated (my unpublished results from a computer simulation of RNA labeling and decay in the presence of rifampicin). The decay during this interval results in a gross underestimation of the relative rate of unstable RNA synthesis.

Labeling experiments in the second category center around the relationship between precursor and product. Methods which make use of this precursor-product relationship can be divided into three classes.

In one class are those methods which require measurement of the specific or total activity of the precursor and only minimal information, such as pool size, about the product. Salser, Janin, and Levinthal (1968) and Nierlich and Vielmetter (1968) have used such a technique to estimate the rate of syntheis, pool size, and rate of decay of the unstable RNA fraction.

In a second class are those methods which require a measurement of the specific or total activity of the product and only minimal information about the precursor. Early work along this line was done by McCarthy and Britten (1962). More recently, Koch (1968, 1971a, 1971b) has developed means for evaluating the early labeling kinetics of RNA in the absence of precise information about its precursor.

In the third class are those experiments which require measurement of the specific or total activities of both the precursor and the product. Procedures of this type require far fewer assumptions and approximations and as a result have gained favor in the last few years. One important factor contributing to the popularity of experiments in this third class are the recent advances in nucleotide fractionation techniques (Randerath and Randerath, 1967).

Mueller and Bremer (1968) formulated the basic ideas involved in experiments in this class. They measured, as a function of time after labeling, the specific activities of both the immediate precursor to RNA and of RNA. If one knows the specific activity of the immediate precursor and the rate of change of the specific activity of the product, then it is a simple matter to calculate the rate of synthesis. Furthermore, they reasoned that the value of this calculated synthesis rate, when

extrapolated to zero labeling time, would correspond to the total or gross synthesis rate and the value at very long labeling times would correspond to the net synthesis rate (net synthesis rate equals total synthesis rate minus decay rate). The decay rate is a good approximation of the rate of synthesis of the unstable RNA fraction.

Winslow and Lazzarini (1969) have utilized this basic idea in their procedure for estimating RNA chain elongation rates. Pato and Meyenburg (1970) have used a variation of this basic idea in experiments in which they added simulatneously both rifampicin and labeled uracil. They then measured the amount of label incorporated into the various stable RNA fractions and the specific activity of the UTP pool as a function of time after labeling. From this information they drew conclusions about linkage of the genes coding for stable RNA species. Chaney and Boyer (1972) have used a rather exotic variation of the basic idea in their ^{18}O experiments. Oxygen has the unique property of entering RNA via two pathways. One pathway involves addition during endogenous synthesis of the RNA precursors and the second pathway involves entrance into precursors during hydrolytic cleavage of unstable RNA. From their measured steady-state specific activity values they were able to estimate the gross synthesis rate of RNA.

There is a universal but seldom stated assumption which underlies experiments utilizing labeled RNA precursors. The assumption is that all classes of RNA are synthesized from precursors of equivalent specific activities. Experiments which are centered around the relationship between precursor and product rest on the more general assumption that the precursor to RNA is not compartmentalized.

If RNA precursor is compartmentalized, then this compartmentation would introduce error into those labeling schemes deriving information from the precursor product relationship. Furthermore, experimental approaches involving fractionation of RNA into its component classes or species would also be in error if different classes of RNA were synthesized from precursors of different specific activities.

Several lines of evidence appear to contradict the assumption of noncompartmentation of RNA precursor. In any system of sequential reactions where a labeled precursor is supplied at a continuous rate, the concentration of label must be highest in the most proximal reactant, next highest in the next most proximal reactant, and so forth. This condition of a precursor having a higher specific activity than its product holds until all components are completely labeled. It is believed that when bacteria take up uracil the uracil is first incorporated into UMP, and then by successive phosphorylation steps it enters UDP, then UTP, after which it is incorporated into RNA. If such is the case, then one would expect in a continuous labeling experiment that, up to the time at which all components were completely labeled, the order of the specific activities of the uracil-containing nucleotides would be: UMP $>$ UDP $>$ UTP. Mueller and Bremer (1968) have measured the specific activities of the UMP, UDP, and UTP pools of the bacterium Escherichia coli as a function of time after labeling a culture with radioactive uracil. They find that after the first 10 seconds of labeling the specific activity of the UTP is higher than the specific activity of its precursor pools of UMP and UDP. The most likely explanation for this finding is that the precursors are compartmentalized.

In an experiment where labeled precursor is used, if one can measure as a function of time the specific activity of both the precursor and its product, then it is a simple matter to calculate the rate at which the precursor is being transformed into product.

In another labeling experiment Mueller and Bremer measured the specific activities of the UTP pool and the RNA pool. They then used these values to calculate the apparent rate of RNA synthesis and found that the apparent rate was much higher than could be accounted for by the sum of the rates of unstable and stable RNA synthesis. Again, precursor compartmentation can be used to explain this apparent discrepancy.

If the precursors of RNA are indeed compartmentalized, then it is important that this compartmentation be characterized so that its effect on RNA labeling kinetics can be properly taken into account. Herein I detail my work in which I have both verified and characterized RNA precursor compartmentation in *E. coli* B. In addition, I have developed a method for measuring the pool size and the rate of synthesis of unstable RNA in the presence of this type of precursor compartmentation. And finally, I have devised a means of determining the specific activity of that portion of the precursor pool which is being used for RNA synthesis.

CHAPTER II

THEORETICAL CONSIDERATIONS

Evidence for Compartmentation of RNA Precursors

The sequence of reactions leading from exogenous uracil to RNA is believed to be that shown in Figure 1 (Davidson, 1969).

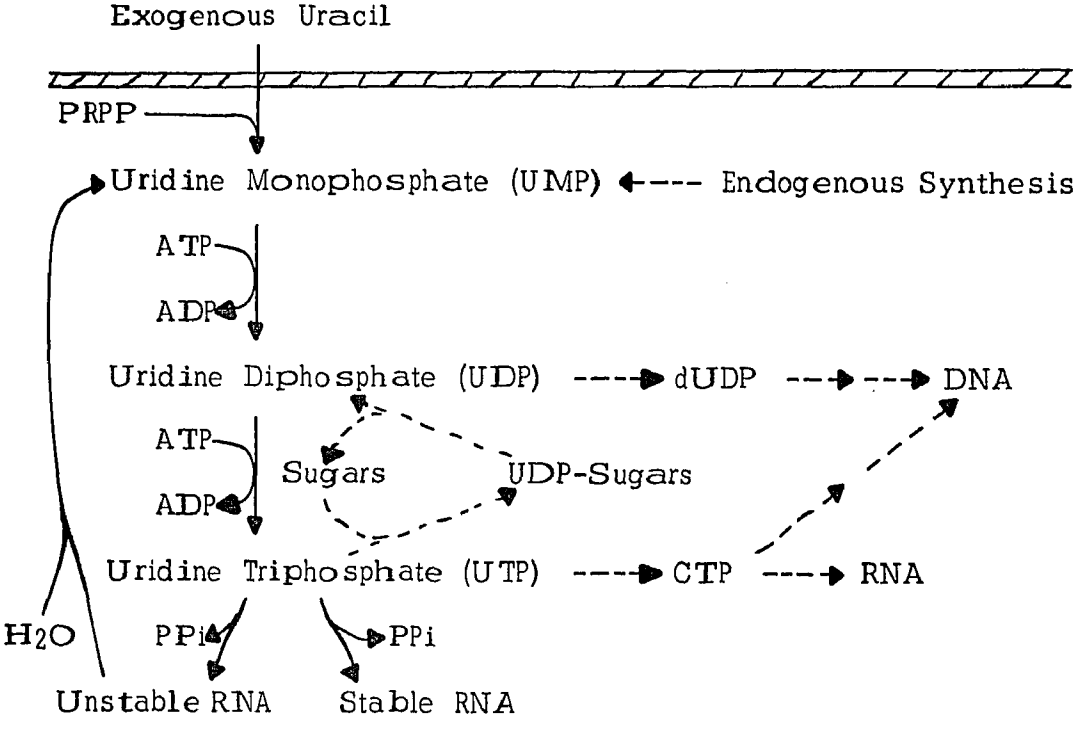

Figure 1. Sequence of Reactions from Uracil to RNA

At this point I would like to define the term "unstable RNA." Jacob and Monod (1961) postulated a metabolically unstable class of RNA which acts as a template from which protein is synthesized. Such a

class, termed "messenger RNA," has been found and extensively characterized with respect to both the composite class, Geiduschek and Haselkorn (1969), and individual species composing the class, Schwartz, Craig, and Kennell (1970); Mosteller and Yanofsky (1970); Leive and Kollin (1967). A common feature of most if not all species of messenger RNA in microorganisms is their metabolic instability characterized by exponential decay with a half-life of several minutes. Because of this instability, most workers dealing with microbial systems have equated messenger RNA with unstable RNA. This assumption of equivalence may be in error.

There may be some messenger species which are reasonably stable. Messenger RNA coding for penicillinase in the organism Bacillus subtilis appears to be reasonably stable (Pollock, 1963). Salser (1966) has presented evidence for some relatively long-lived messenger RNA species in B. subtilus. Many higher organisms have specialized messengers, such as that coding for hemoglobin, which are stable for several days or longer.

In higher organisms there are several classes of RNA which are unstable but probably are not used as templates for protein synthesis. One of these classes is the heterogeneous nuclear RNA. This fraction is synthesized and degraded at a relatively high rate, but it never leaves the nucleus and presumably does not perform as a template for protein synthesis (Darnell, 1968). Analogous types of RNA may be present in microorganisms. Also in higher organisms, ribosomal and transfer RNA's are transcribed in longer than final segments, which are then cleaved during the molecular maturation process (Darnell, 1968).

In summary, it is quite possible that in bacterial systems not all messenger RNA is unstable and not all unstable RNA is messenger. I am, therefore, operationally defining two mutually exclusive RNA fractions. Unstable RNA will refer to that fraction of RNA which degrades to components soluble in cold 5% trichloroacetic acid (TCA) during a 60-minute incubation with the drug rifampicin. Stable RNA is that fraction of RNA which remains TCA insoluble in the presence of rifampicin. I have chosen the metabolic inhibitor rifampicin because it is believed to allow both the normal decay of those RNA species which are normally unstable and the maturation processes which lead to stabilization of those species which are normally stable (Mosteller and Yanofsky, 1970).

Mueller and Bremer (1968) have presented data indicating that in E. coli labeled with [^{3}H]uracil, the UTP pool has, after 10 seconds of labeling, a higher specific activity than the UMP and UDP pools. This can be reasonably explained in any of three ways. First, UMP may not be a precursor to UTP. Second, some compounds, which I shall denote as UMP-X and UDP-Y, may be labeled at a substantially slower rate than are UMP and UDP. During extraction and fractionation, these compounds may be cleaved to UMP and UDP. These relatively unlabeled residues would now dilute the specific activities of the final UMP and UDP preparations. Third, the precursors may be compartmentalized.

In vitro studies seem to rule out the first explanation (Hurwitz and August, 1963). The second explanation would appear more reasonable since the conditions used by Mueller and Bremer (1968) in the extraction and fractionation procedures (temperatures to 100°C and pH down to about 1) could easily cause cleavage of mono-, di- and

triphosphonucleoside compounds to give mono- and diphosphonucleosides. I tested this second possibility by repating their precursor labeling experiments. The extraction and fractionation of the nucleotides were carried out at 4°C and neutral pH. My results (see Chapter V) differ from those of Mueller and Bremer with respect to the specific activity of the UDP pool; but I consistently find that after very short periods of labeling, the specific activity of the UTP pool is significantly higher than that of the UMP pool. For example, at two minutes after labeling, UTP has a specific activity 30% greater than that of UMP. Thus, the remaining explanation--that of precursor compartmentation--appears to be the most likely one.

The second line of evidence leading Mueller and Bremer to propose compartmentation of RNA precursors consisted of a calculated rate of total RNA synthesis much higher than the expected sum of the rates of unstable and stable RNA synthesis. The extra component appeared to have a half-life of about 10 seconds and an exceedingly high rate of synthesis. Several explanations could account for this rather unexpected finding. The component could be a real class of RNA characterized by a very short half-life and an exceedingly high rate of synthesis, or, alternatively, it could be an artifact of the method used for determing the total rate of synthesis.

The total rate of synthesis of RNA can be determined by plotting as a function of time after labeling the value of the ratio: rate of change of RNA specific activity divided by precursor specific activity (Mueller and Bremer, 1968). The value of this ratio when extrapolated to zero time gives the gross synthesis rate if the proper criteria are met. The

precursor assayed must be the most proximal precursor and must be homogeneous throughout the cell with respect to specific activity.

The value of the total rate of RNA synthesis calculated from the specific activities of cytidine triphosphate and the cytidine monophosphate residues of RNA (Mueller and Bremer, 1968) appears to rule out the presence of a fraction of RNA with a very high synthesis rate and a 10-second half-life unless this fraction contains no CMP residues. In Chapter V, I present evidence indicating that there is no detectable uracil-containing fraction with a 10-second half-life. This information is derived from a labeling function (the proportional synthesis function) which is relatively independent of precursor compartmentation. The four ribonucleoside triphosphates are the substrates from which RNA polymerase synthesizes RNA (Hurwitz and August, 1963). This seems to rule out the explanation that the UTP pool is not the immediate precursor to the UMP residues in RNA. The remaining explanation--that of inhomogeneity of precursor specific activity (compartmentalized precursor)--appears to be the only reasonable one.

Possible Types of Precursor Compartmentation

With respect to labeling kinetics, there are only two types of precursor compartmentation in the context of RNA metabolism. In Type I, both classes of RNA, stable and unstable, are synthesized from precursors of equivalent specific activity. Figure 2 illustrates one variation of this Type I compartmentation. In both Figure 2 and Figure 3, pools A and B are chemically identical but spatially separated.

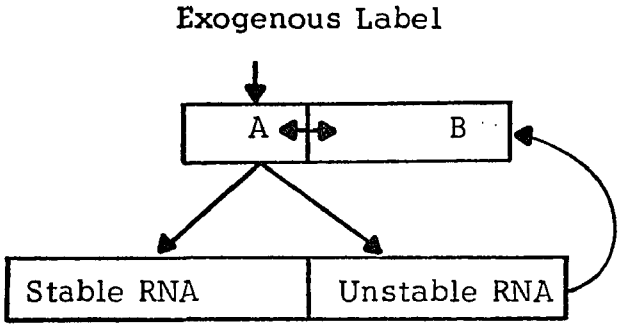

Figure 2. One Variation of Type I Precursor Compartmentation

The important characteristic of Type I precursor compartmentation is that all classes of RNA are synthesized from the same precursor pool, i.e., they are synthesized from precursors of equivalent specific activities.

In Type II precursor compartmentation, different classes of RNA are synthesized from precursors of different specific activities. Figure 3 illustrates one variation of Type II compartmentation.

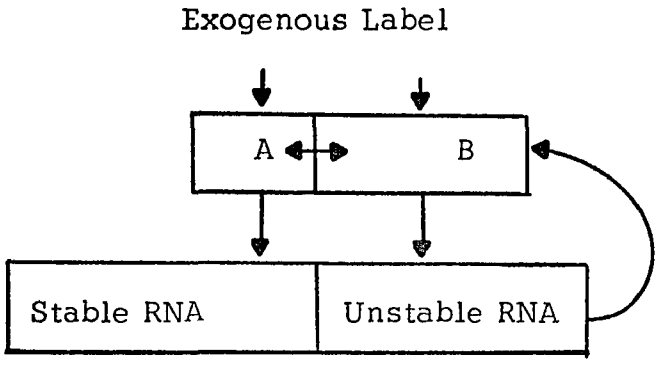

Figure 3. One Variation of Type II Precursor Compartmentation

The important characteristic of Type II precursor compartmentation is that one or more classes of RNA are synthesized from precursor of one specific activity and one or more classes are synthesized from precursor of either a higher or a lower specific acitivty.

In both types of compartmentation the difference between the specific activities of the various precursor compartments is greatest immediately after labeling and decreases with time due to mixing of the pools. Essentially all methods for measuring rate of unstable RNA synthesis rely heavily on measurements made on samples taken very soon after labeling. Because of this fact, any precursor compartmentation phenomenon has a potential for introducing serious error into the rate estimations.

It is important to determine which type of compartmentation actually prevails in vivo. If Type I dominates, then those methods for measuring rate of synthesis of unstable RNA which are dependent on a knowledge of precursor specific activity or pool size will give erroneous results. If, on the other hand, Type II compartmentation prevails, then essentially all methods for measuring unstable RNA synthesis rate will give erroneous results.

Computer Simulation of Three Variations of RNA Precursor Metabolism

I have considered three models of RNA precursor metabolism: a noncompartmentalized model, a Type I compartmentalized model, and a Type II compartmentalized model. In developing these models, a number of simplifying approximations were necessary. I have disregarded endogenous synthesis in all models. This simplification is valid if the

external precursor specific activity never enters into the final answer. Since my experimental work is concerned only with relative specific activities of cellular components and does not require a comparison of internal and external specific activities, this required condition is satisfied.

I have also disregarded those side reactions, such as synthesis of deoxy-UDP (dUDP) and CTP, which do not return uracil residues to the main sequence (see Figure 1). Those side reactions which do not return uracil residues to the main sequence have the effect of increasing to a small extent the rate of labeling of the precursor pool and hence quantiatively increase the rate of labeling of RNA. Approximately 12% of the exogenously supplied uracil is shunted into dUDP (Mueller and Bremer, 1968) and approximately 40% passes into CTP (McCarthy and Britten, 1962). Since I am primarily interested in comparative values between the three models rather than quantitative effects in any one model, I believe that this is an acceptable simplification.

In the living cell there are probably three or more chemically distinct pools in sequence leading from exogenous precursor to RNA (Fig. 1). In addition, there are a number of pools, such as the UDP-sugars, out of the main sequence but believed to be in relatively rapid equilibrium with the main sequence pools (Salser, 1966). In the computer-simulated models, I have combined all of these pools into a single composite pool. This single precursor pool approximation has the effect of increasing the initial rate of RNA labeling as compared to the rate of RNA labeling in a system having several sequential precursor pools. Combining the precursors into a composite pool will therefore introduce

significant qualitative errors into the output from each model. However, since the resulting errors will be quite similar in each of the three models, they will effectively cancel when one compares the output from them. In the computer simulations I am only secondarily interested in the absolute specific activity values from any one model. The major interest lies in a comparison of the outputs from the three different models. In summary, I believe that these comparisons are reasonably accurate in spite of the simplifications and approximations used in these simulation programs.

The first model assumes noncompartmentalized precursors. In this model labeled precursor enters the cell from the exogenous pool. Once inside the cell, it is chemically transformed in several steps into the immediate precursor to RNA. There is a thorough mixing at each stage of the chemical transformation, such that the specific activity of the molecules being transformed to the next stages are representative of the specific activity of their entire cellular pool. Decay products from the unstable RNA fraction feed into one of these cellular precursor pools and are reutilized in the same manner as that precursor coming directly from an exogenous source. This model is shown in Figure 4a. The simplified version shown in Figure 4b was used for the computer simulations.

The second model is an example of Type I precursor compartmentation. This model is essentially that proposed by Mueller and Bremer (1968) to explain an apparent paradox in their experimental data. In this model the labeled precursor enters at the cell periphery. There is at this point and after each subsequent chemical transformation a competition between chemical transformation of labeled precursor and diffusion of labeled precursor toward the central region of the cell. If

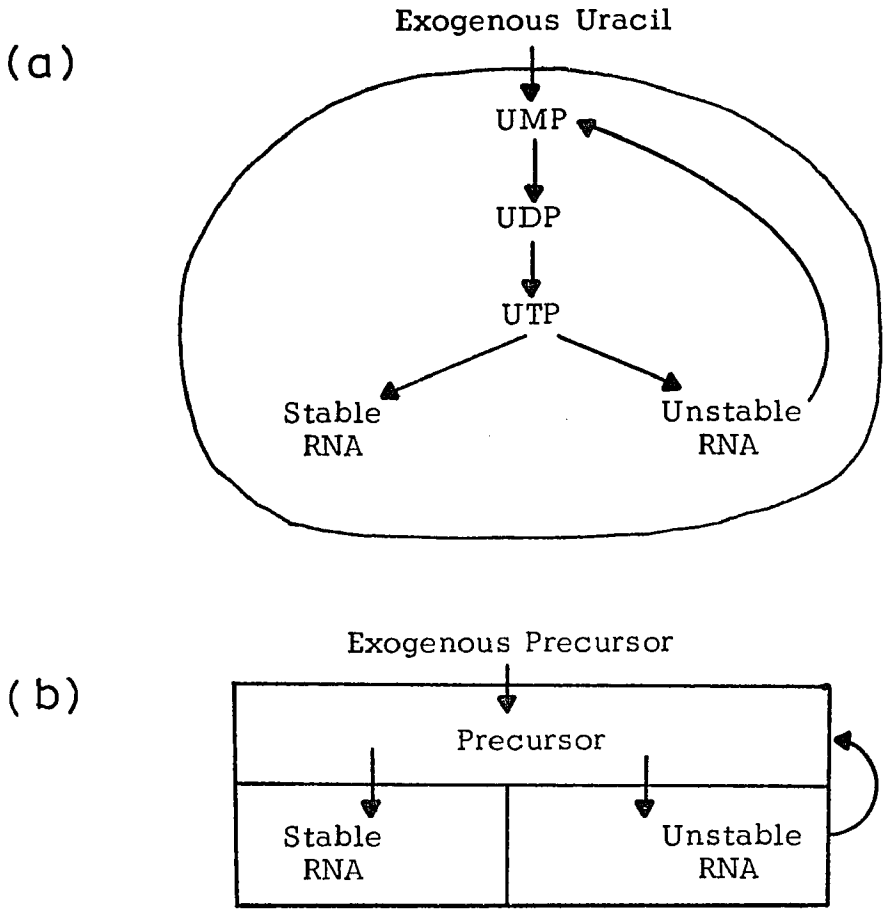

Figure 4. Noncompartmentalized Model

(a) Diagrammatic model; (b) Simplified model.

the rate of chemical transformation is of the same order of magnitude as the rate of diffusion, then at early times after labeling there will be a significant spatial inhomogeneity with respect to precursor specific activities. At early times after labeling, the precursors at the periphery of the cell will have a substantially higher specific activity than those of the central region. It is likely that RNA synthesis in bacteria occurs at the cell periphery (Roth and Daneo-Moore, 1971; Maruo et al., 1969; Varricchio, 1972). If this is the case, then RNA synthesis will, at early

times after labeling, utilize precursor whose specific activity is substantially higher than that of the average cellular precursor.

This second model is diagrammed in Figure 5a. The simplified version shown in Figure 5b was used for the computer simulations.

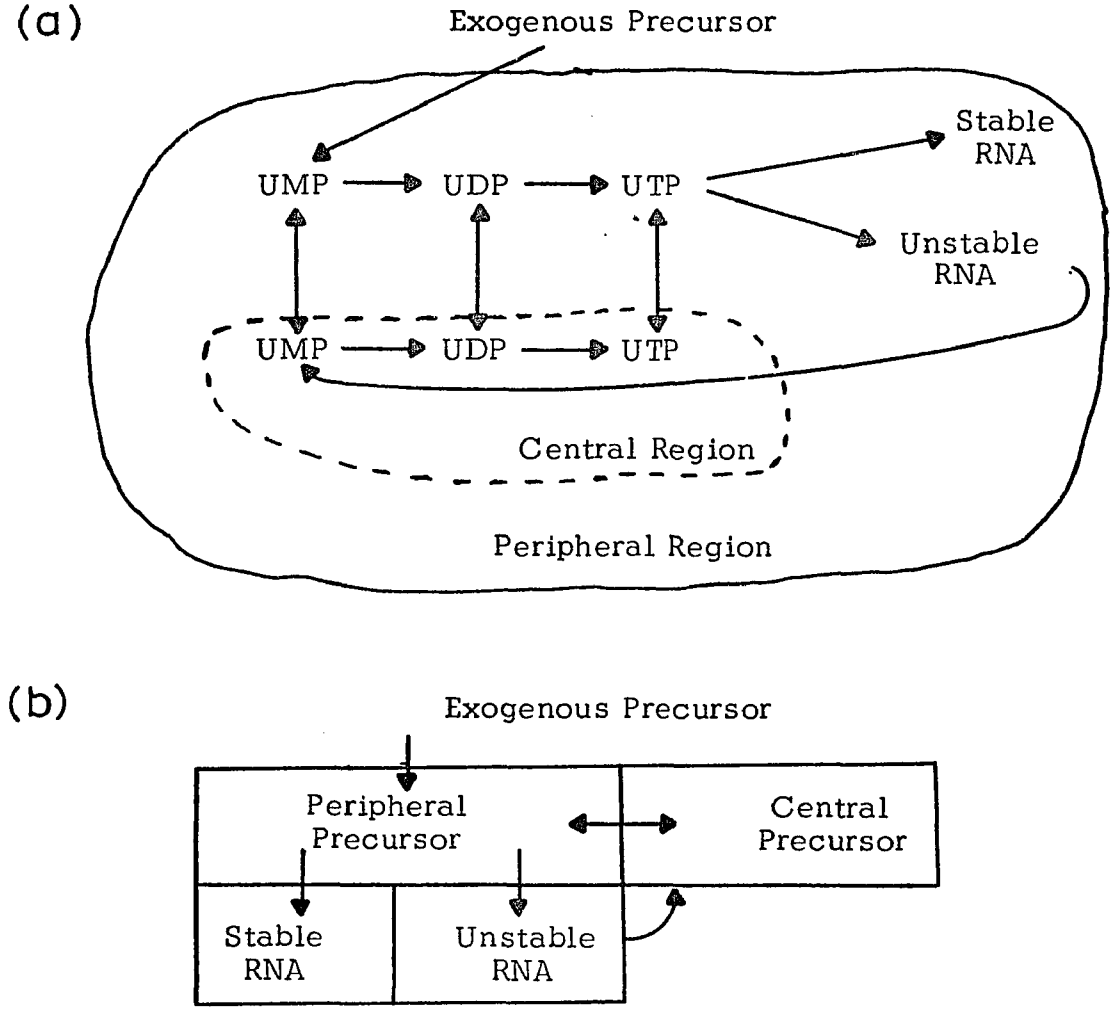

Figure 5. Peripherally Compartmentalized Model

(a) Diagrammatic model; (b) Simplified model.

The details of this model are not firmly established. It is possible that the nucleotide phosphorylation steps may occur only at the cell membrane. For example, Thomas, Weissbach, and Kaback (1971) have found that the γ phosphate of ATP is first incorporated into membrane-bound phosphatidic acid and then this membrane-bound phosphate is transferred to deoxynucleoside diphosphates. A similar phenomenon may occur in the phosphorylation of the ribonucleosides. Furthermore, it is conceivable that once the uracil has entered the cell, it remains bound to the membrane throughout the phosphorylation steps. Another possibility is that the peripheral precursor pool corresponds to the periplasmic space or to a mesosomal structure, whereas the central pool corresponds to the cytoplasmic region. An osmotically sensitive non-cytoplasmic pool has been characterized in E. coli. This pool contains a number of enzymes and appears to contain acid-soluble nucleotides (Rogers, 1970).

The important points in this model are twofold. First, both classes of RNA are synthesized from a common precursor pool. Second, this pool from which RNA is being synthesized has, at early times after labeling, a significantly higher specific activity than its chemically identical but spatially separate pool.

The third model is an example of Type II precursor compartmentation. In this variation of Type II compartmentation, the stable RNA fraction is synthesized from one precursor pool and the unstable RNA fraction is synthesized from a spatially separate precursor pool. In this model, I envision an area of the cell in which there is a high rate of precursor utilization and a separate area in which there is a low rate of

precursor utilization. The area of high precursor utilization corresponds to a region around those genes devoted to stable RNA synthesis. Kennell (1968) estimates that only 0.3% of the E. coli genome codes for stable RNA. Most or all of these genes are probably clustered fairly closely (Spadari and Ritossa, 1970; Cutler and Evans, 1967; Birnbaum and Kaplan, 1971).

The area of low precursor utilization is that region around the genes coding for unstable RNA. These gene sites are probably spread randomly throughout the remaining 99.7% of the genome. If stable RNA synthesis constitutes approximately half of the total RNA synthesis, then in the vicinity of the genes for stable RNA, precursor is being utilized more than 300 times as fast per unit genome as in the vicinity of the genes for unstable RNA.

The uptake of exogenous uracil appears to be strictly controlled (Bremer and Yuan, 1968a; Nierlich, 1968; O'Donovan and Neuhard, 1970), probably by feedback inhibition at the level of the permease. If the permease is the limiting factor in the uptake of exogenous uracil, it would seem reasonable to expect the permease to be least inhibited over regions where precursor utilization is the most rapid, i.e., over the genes coding for stable RNA. If this were true, those precursors feeding stable RNA synthesis should become labeled much more rapidly than those feeding unstable RNA synthesis. Since serious errors would result in essentially all labeling schemes if precursors are compartmentalized in this manner, I refer to this model as artifactually compartmentalized. This proposed compartment phenomenon is incorporated into the model shown

in Figure 6a. The simplified version shown in Figure 6b was used for the computer simulations

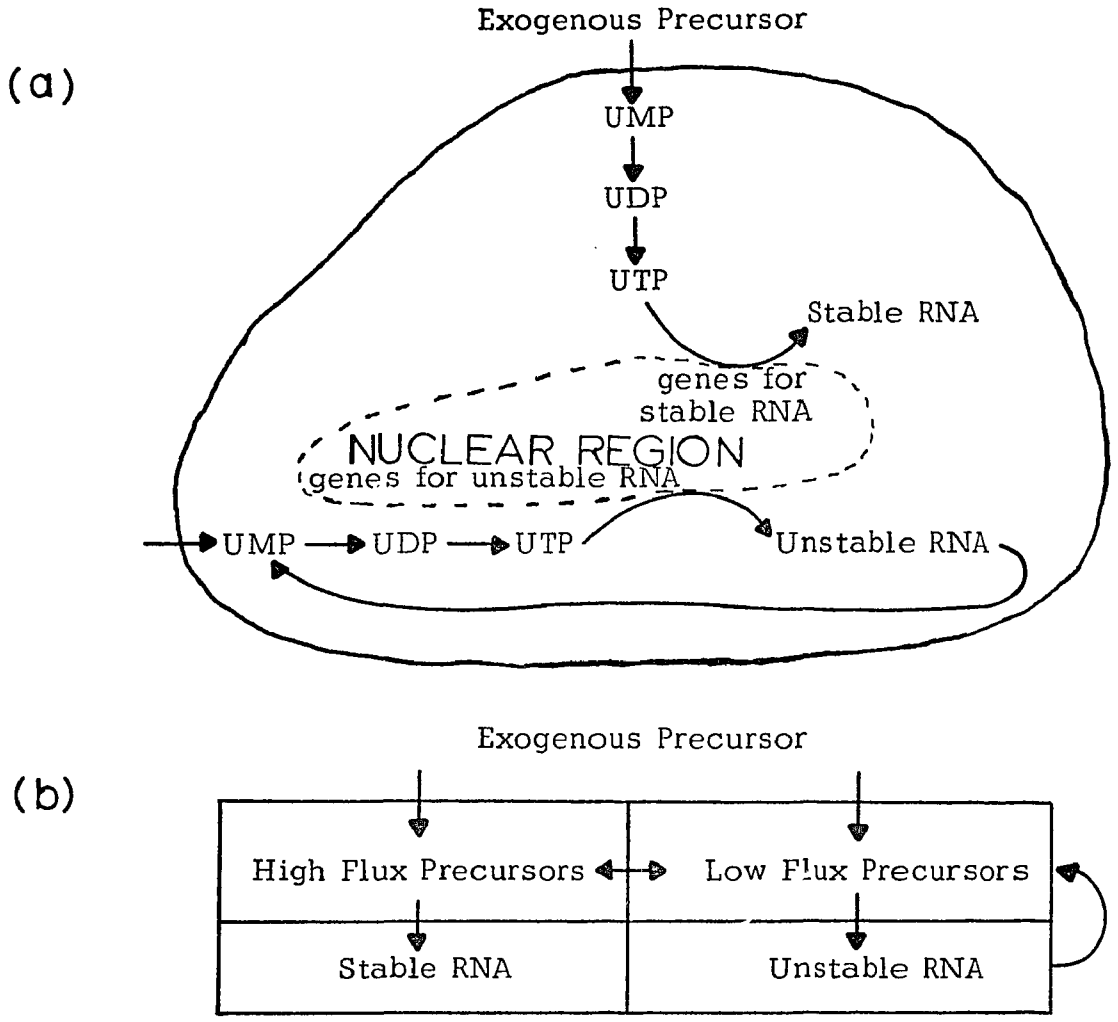

Figure 6. Artifactually Compartmentalized Model

(a) Diagrammatic model; (b) Simplified model.

The recycling of unlabeled nucleotides from unstable RNA decay would enhance this compartmentation of labeled precursor because the majority of nucleotides derived from unstable RNA (unlabeled at early

times after adding label) would appear in the area of low utilization simply because this area is much larger than the area of high utilization.

In the two compartmentalized models I am not assuming physical barriers separating the compartments but rather a specific activity gradient which is maintained to a decreasing extent for the first minute or so after labeling. This is a consequence of competition between diffusion of labeled precursor and chemical transformation of labeled precursor. A precedent for such functional compartmentation arising out of a competition between diffusion and chemical transformation has been characterized by Garfinkel and Lajtha (1963). They found that in kidney proximal tubule cells a product--hippuric acid--has at early times after labeling a higher specific activity than its precursor--cellular glycine. A somewhat similar phenomenon has been discovered by Berlin and Stadtman (1966). They found in adenine-labeled B. subtilus that after very short times, the cellular AMP had a higher specific activity than cellular adenine.

I have depicted the spatial inhomogeneities in precursor specific activities as being divided into distinct compartments, i.e., peripheral and central compartments or high-flux and low-flux compartments. These distinct compartments are simply approximations of a gradient. Without this two-compartment approximation of the gradients, the computer simulations would have been excessively long and involved. Of greater importance is the fact that in the context of these models two-compartment kinetics are qualitatively quite similar to the kinetics derived from a continuous gradient.

It is commonly accepted that unstable RNA decays in an exponential fashion, i.e., the probability for decay in a given time increment is the same for every phosphodiester bond in the unstable RNA pool. There are, however, theoretical considerations which argue strongly for at least partial linear decay of the unstable RNA pool. RNA synthesis proceeds from the 5' to the 3' end (Shigeura and Boxer, 1964; Bremer et al., 1965). Translation of messenger RNA likewise proceeds from the 5' to the 3' end (Wahba, Salas, and Stanley, 1966). If decay of a messenger RNA molecule were to begin at some random point more proximal to the 3' end of a gene than some ribosome involved in translation of that gene, the result would be a nonfunctional polypeptide fragment. Such a process would seem rather wasteful of energy and would clutter the cell with nonfunctional components.

Kuwano, Kwan, and Apirion (1969) have proposed a mechanism of messenger RNA decay whereby decay proceeds concurrently with or directly following the last ribosome to transverse the messenger. Such a decay process would proceed sequentially from the 5' end to the 3' end. This scheme is particularly attractive for several reasons. First, there would be no synthesis of nonfunctional polypeptide fragments. Second, a single process would be responsible for both functional and mass decay. Third, an agent--named RNase V by Kuwano et al. (1969) and believed by several workers to be ribosome-bound RNase II (Holmes and Singer, 1971; Bothwell and Apirion, 1971)--has been characterized which appears to degrade messenger RNA in the 5' to 3' direction. Its action seems to be coupled to ribosomal translocation.

If some or all of the unstable RNA fraction does indeed decay sequentially from the 5' to the 3' end, then one might expect at least partial linear decay rather than wholly exponential decay.

Because of these considerations I have developed two variations of each of the three models. One variation contains an exponentially decaying unstable RNA pool and the other variation contains a linearly decaying unstable RNA pool.

I defined the following notation for a generalized pool A:

PSA--pool size in moles of uracil-containing compound in pool A at time zero.

SAA_T--relative specific activity of pool A at time T, or counts per minute per mole of uracil-containing compound divided by counts per minute per mole of uracil in the exogenous pool.

RAB--rate of transfer of any uracil-containing compound from pool A to pool B at time zero.

I am considering nonsynchronized exponential phase bacterial cultures, and hence all pool sizes and rates are increasing exponentially. I specify nonsynchronous cultures because it has been shown that nucleotide pool sizes undergo dramatic changes during the cell growth cycle (Huzyk and Clark, 1971). Each rate and pool size is therefore multiplied by the factor $e^{T/G}$, where T is the time after labeling and G is the generation time, defined as the time required to increase cell mass or cell number e-fold. Where material is being transferred from pool A to pool B at the rate $(RAB)e^{T/G}$ (see Figure 7), the rate of transfer into pool B of labeled uracil containing compound is

$$(RAB)e^{T/G}(SAA)_T.$$

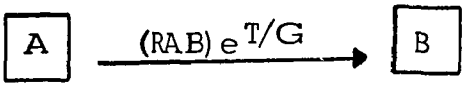

Figure 7. Synthesis of Pool B

In the special case where an unstable RNA pool is decaying in a linear fashion the flow of label from pool B (the linearly decaying RNA pool) to pool C (see Figure 8) is

$$(RBC)\, e^{T/G}\, (SAA_{T-L}).$$

The term, SAA_{T-L}, refers to the specific activity of pool A at L seconds before sampling. The value of L corresponds to the lifetime of a nucleotide in pool B.

Figure 8. Synthesis and Decay of Pool B

The specific activity of any pool at T seconds after adding labeled precursor is the summation from time zero to time T of all inflowing label minus all outflowing label: this summated quantity divided by the pool size. For example, the specific activity of pool B at time T in Figure 8 is described by equation (1).

$$SAB_T = \frac{\int_0^T \left[(RAB)\, e^{t/G}\, (SAA_t) - (RBC)\, e^{t/G}\, (SAB_t)\right] dt}{(PSB)\, e^{T/G}}. \qquad (1)$$

This equation can be modified by the procedure given in Appendix A to

describe the change in specific activity over a period of ΔT seconds as follows:

$$\Delta SAB \cong SAB_T(e^{-\Delta T/G} - 1) + G(1 - e^{-\Delta T/G}) \left[\frac{RAB(SAA_T + 1/2(SAA_T - SAA_{T-\Delta T}))}{PSB} - \frac{RBC(SAB_T + 1/2(SAB_T - SAB_{T-\Delta T}))}{PSB} \right] . \quad (2)$$

For a given interval ΔT, I define a constant, Y, as follows:

$$Y = (e^{-\Delta T/G} - 1) \quad (3)$$

and a second constant, Z, as follows:

$$Z = G(1 - e^{-\Delta T/G}) . \quad (4)$$

This result can now be generalized to give the change in specific activity of pool B over a time interval, ΔT:

$$\Delta SAB \cong Y(SAB_T) + Z\left(\frac{\sum(\text{inflows}) - \sum(\text{outflows})}{\text{pool size}}\right) . \quad (5)$$

Three additional equations are important in calculating flow rates in these models. The first equation gives the relationship between inflow (synthesis), outflow (degradation), pool size, and generation time.

$$\text{inflow} = \frac{\text{pool size}}{G} + \text{outflow} . \quad (6)$$

The second equation gives the relationship between inflow, half-life, pool size, and generation time for an exponentially decaying pool.

$$\text{pool size} = \frac{(\text{inflow})(\text{half-life})}{0.69315 + (1/G)(\text{half-life})} . \quad (7)$$

The third equation gives the relationship between inflow, lifetime, pool size, and generation time for a linearly decaying pool.

$$\text{pool size} = \frac{(\text{inflow})(1/2 \text{ lifetime})}{0.500 + (1/G)(1/2 \text{ lifetime})} . \quad (8)$$

The assumptions upon which these last three equations are based together with their derivations are given in Appendix A.

In simulating labeling experiments in the various models, the precursor and product pools were coupled in the desired manner; the zero time specific activity values were registered (usually zero values): and then exogenous precursor of specific activity 1.0 was introduced. The output consisted of the specific activities of each pool at each time increment and various ratios calculated from these specific activities. For example, the specific activity of total RNA was of interest. By letting pool C be unstable RNA and pool D be stable RNA, the specific activity of the combined pools was calculated as follows:

$$SA(C+D) = \frac{(SAC)(PSC) + (SAD)(PSD)}{(PSC) + (PSD)} . \qquad (9)$$

A FORTRAN IV program was written by Richard Norling (Systems Engineering Department, University Hospital) for the University of Arizona CDC 6400 to run these simulation models. I ran both long-term labeling simulations and pulse-chase simulations. In addition, I ran a number of simulations in which both the relative sizes of the precursor compartments and the diffusion rate between the cellular precursor pools were varied in a systematic manner. In one last set of simulations, I set the initial internal precursor pool(s) specific activity(ies) to 1.0. This experiment was designed to determine what functions were independent of precursor specific activity.

Determination of Unstable RNA Pool Size and Synthesis Rate in a Type I Compartmentalized System

In this section I shall use the following abbreviations:

SA--specific activity or counts-per-minute/mole

PS--pool size in moles

R---rate of synthesis in moles/second

un--unstable RNA

st--stable RNA

tot--total RNA

pre--RNA precursor.

I have shown that there is Type I precursor compartmentation in *E. coli* labeled with uracil. This will be covered in detail in Chapter V. Furthermore, the computer simulation studies show that the zero time intercept value of the function, SAun/SAtot, is unaffected by the presence of Type I precursor compartmentation. Again, this is shown in detail in Chapter V.

At early times after labeling, there is negligible loss of label from the unstable RNA pool and hence the specific activity of this pool is proportional to its rate of synthesis times the precursor specific activity divided by its pool size,

$$SAun : (Run)(SApre)/(PSun). \tag{10}$$

This relationship also holds for the specific activity of the total RNA pool. Therefore, the value of the function, SAun/SAtot, when extrapolation to zero time has the value

$$\left(\frac{SAun}{SAtot}\right)_{(T \to 0)} = \frac{(Run)(SApre)/(PSun)}{(Rtot)(SApre)/(PStot)} . \tag{11}$$

If both classes of RNA are being synthesized from precursors of equivalent specific activity (Type I precursor compartmentation) then the precursor specific activity terms cancel out of this expression. It is for this reason that zero time extrapolation of this function is unaffected by Type I compartmentation. I am defining both the rate of total RNA synthesis and the pool size of total RNA as unity. The unstable RNA synthesis rate will therefore take the form, fraction of total RNA synthesis; and the pool size of unstable RNA will take the form, fraction of the total RNA pool size. Equation (11) now becomes:

$$\left(\frac{SAun}{SAtot}\right)_{(T\to 0)} = \frac{Run}{PSun} . \tag{12}$$

Because the zero time intercept value of the function, SAun/SAtot, is related to the proportion of RNA synthesis which is devoted to unstable RNA I shall refer to this function as the proportional synthesis function.

The pool size of unstable RNA can be extracted from the following relationships:

$$SAtot = \frac{(SAun)(PSun) + (SAst)(PSst)}{(PSun) + (PSst)} \tag{13}$$

and

$$PSun + PSst = 1. \tag{14}$$

Algebraic manipulation gives:

$$PSun = \frac{SAtot - SAst}{SAun - SAst} . \tag{15}$$

This last relationship holds at all times after labeling, including during chase experiments, and in all types or the absence of compartmentation. Furthermore, it holds whether the unstable fraction

decays in an exponential or a linear manner and in spite of heterogeneity in decay rates.

I will now summarize my method for determining PSun and Run in either a noncompartmentalized or a Type I compartmentalized system. The values for SAun, SAst, and SAtot must be measured simultaneously at some time after labeling. Several determinations of SAun, and SAtot must be made within the first minute after labeling. This affords a precise extrapolation of this ratio, the proportional synthesis function, to the zero time intercept. Substitution of the SAun, SAst, and SAtot values into equation (15) will give the value for PSun. Graphical extrapolation of the proportional synthesis function, SAun/SAtot, to zero time will complete the procedure and allow calculation of Run using equation (12).

Procedures for experimental measurement of both SAtot and SAun offer few difficulties. Measurement of SAst, on the other hand, is fraught with potential difficulties. If a total cellular lysate is taken, one immediately runs into the problem of separating the stable fraction from the unstable fraction. All fractionation on the basis of molecular weight has the drawback that all stable species will be contaminated with nascent and partially degraded fragments of unstable species. Furthermore, if fractionated on the basis of molecular weight, the high molecular weight stable species (ribosomal) will be lacking their nascent chains which are of disproportionate importance in the specific activity value since they are the most highly labeled.

Fractionation by hybridization procedures are also unacceptable. As numerous workers have shown, it is not feasible to remove completely all unstable RNA from a mix of total RNA by the procedure of hybridization

(Kennell, 1968; Gillespie and Spiegelman, 1965). It might be possible to remove a very pure stable RNA fraction by hybridization with its respective DNA but preparing a clean preparation of DNA coding only for stable RNA is an exceedingly difficult task.

The drug actinomycin stops all RNA synthesis and allows decay of the unstable fraction. At first glance this would appear to be an ideal approach to measure SAst but a closer inspection argues otherwise. Several studies indicate that actinomycin protects a fraction of RNA which would normally be unstable (Fan, Higa, and Levinthal, 1964; Lindahl and Forchhammer (1969) and suggest that a fraction of RNA which would normally be stable is caused to decay in the presence of actinomycin (Schaechter, Previc, and Gillespie, 1965).

Another drug, rifampicin, acts by blocking initiation of new RNA chains. This drug allows normal decay of unstable RNA species and the normal processing which leads to stabilization of stable species. It has the disadvantage of allowing continued synthesis of all of those chains which were initiated prior to rifampicin treatment. Such continued synthesis will introduce substantial error in the specific activity value of all species of stable RNA whose synthesis is not completed a very short time after it is initiated. The work of Pato and Meyenburg (1970) indicates that the elapsed time between initiation and completion of synthesis is very short for transfer RNA species.

The procedure I have chosen for assaying SAst consists of adding a small volume of labeled culture to 10 volumes of ice-cold culture containing rifampicin and EDTA. The low temperature essentially stops RNA synthesis while allowing the drug to enter and bind to its

target. The EDTA enhances entrance of the drug (Leive, 1965). The culture is then warmed to 37°C and Mg^{++} is added to saturate the EDTA. After 60 minutes, the RNA is extracted and fractionated by disc gel electrophoresis. This procedure separates RNA on the basis of molecular weight. The transfer RNA peak is taken and its specific activity is measured. This peak should now be free of nascent ribosomal and 5 S RNA since these species will have elongated to their final length during the 60-minute post-treatment incubation. The transfer RNA peak should also be free of any unstable RNA because all unstable species will have decayed completely during the 60-minute treatment with rifampicin. Pato and Meyenburg (1970) have reported an RNA fraction whose synthesis is unaffected by rifampicin, but this fraction will not interfere in the specific activity assay since it has a molecular weight much greater than ribosomal and hence will be completely excluded from the transfer RNA peak.

Figure 9 shows a comparison of the specific activities of samples of a culture labeled for one minute and then either lysed or treated with actinomycin, or treated with rifampicin. As expected, the specific activity of the rifampicin-treated material is substantially lower than that of either the lysed or the actinomycin-treated material.

In this assay a slight error may be introduced if that nucleotide derived from transfer RNA which is used for the specific activity assay is either cytidine monophosphate or adenosine monophosphate. The reason for this is that a three-nucleotide segment containing two cytidines and an adenosine is added post-transcriptionally to transfer RNA species

Figure 9. Comparison of the Specific Activities of Low Molecular Weight RNA Prepared by Three Different Methods

An exponentially growing culture (tris glucose-amino acids medium) was incubated with $H_3{}^{32}PO_4$ (carrier free; 65 μc/ml.) for six doublings before [5-^{3}H] uracil (1.4 nmoles/ml.; 37 μC/ml.) was added. At one minute after ^{3}H labeling the culture was quickly chilled to 0°C. One 0.5 ml. aliquot was pipetted directly into a hot lysis mixutre. A second 0.5 ml. aliquot was added to an equal volume of 0°C medium containing 200 g/ml. actinomycin D and 4×10^{-3} M EDTA. A third 0.5 ml. aliquot was added to an equal volume of 0°C medium containing 600 μg/ml. rifampicin and 4×10^{-3} M EDTA. The latter two samples were warmed to 37°C and $MgCl_2$ was added to a final concentration of 4×10^{-3} M. These two cultures were then incubated an additional hour at 37°C. The cells from these two cultures were spun down and lysed. RNA was extracted from all three lysates and electrophoresed on 15% polyacrylamide gels. The gels were sliced (2 mm/slice) and the amounts of ^{3}H and ^{32}P in each slice assayed.

(a) The ^{32}P counts per minute are plotted for each slice in the 4 S to 5 S region of a gel containing the rifampicin-treated samples (— • —). The ratio, $^3H/^{32}P$, is plotted for each slice of this gel (— □ —).

(b) The 4 S regions (slices 63 to 67) of the three gels are compared with respect to the ratio, $^3H/^{32}P$. The samples are respectively: lysed (— o —); actinomycin-treated (— Δ —); and rifampicin-treated (— □ —).

The vertical arrows in each figure (slice 65) denotes the gel slice in the 4 S region which is used for assaying the specific activity of the stable RNA fraction.

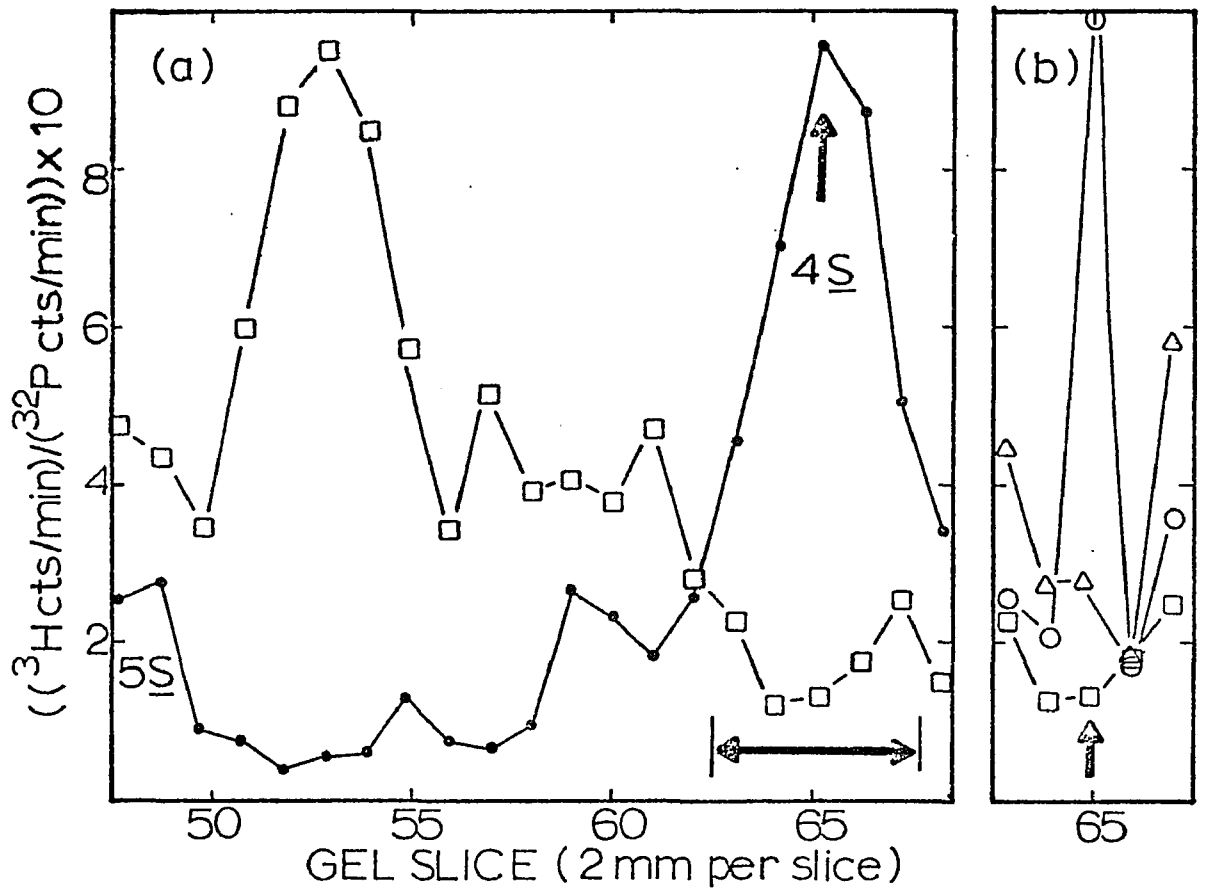

Figure 9. Comparison of the Specific Activities of Low Molecular Weight RNA Prepared by Three Different Methods

(Borek and Srinivasan, 1966). This added synthesis is probably not prevented by rifampicin treatment since rifampicin acts by binding to the DNA-dependent RNA polymerase.

Determination of the Specific Activity of That Precursor Feeding RNA Synthesis

A measure of the specific activity of that precursor feeding RNA synthesis would be of considerable value in a substantial number of labeling schemes. There is no technique currently available for measuring this function in systems having compartmentalized precursors. In some cases, a true measure of this specific activity function might lead to substantially altered conclusions. As a case in point, Pato and Meyenburg (1970) have drawn conclusions about gene linkage from experiments involving simultaneous labeling with [^{3}H]uracil and treatment with rifampicin. In essence, they measured both the amount of label incorporated into transfer RNA and the rise of precursor specific activity as a function of time after labeling. From these data they concluded that some transfer RNA genes are linked in polycistronic transcription units. If, as is the case in a compartmentalized system, their measured cellular precursor specific activity was substantially lower than the specific activity of that precursor feeding transfer RNA synthesis, then it is entirely possible that transfer RNA genes are not linked. A measurement of the correct specific activity function could resolve this question.

In other cases, a measurement of the correct precursor specific activity function might result in seriously altered rate estimations. For instance, Winslow and Lazzarini (1969) have developed a procedure for measuring RNA chain elongation rates. This procedure is based in part

on a measure of precursor specific activity. There estimations are quite possibly in serious error due to their having based their calculation on total cellular precursor specific activity in what may well be a compartmentalized system.

In other experimental systems, a measure of the correct specific activity function might remove the ambiguity from values obtained by extrapolation. For example, Mueller and Bremer (1968) have based their estimation of the rate of incorporation of labeled precursor into RNA on a measurement of the precursor specific activity. Because of compartmentalized precursors, their extrapolated zero time intercept value was unreasonably high, and they were forced to make a rough estimation of what the zero intercept value might have been in the absence of precursor compartmentation. The ambiguity of this estimation could be removed if a method were available for measuring the desired precursor specific activity function.

Below I detail a method for calculating the specific activity of the precursor which feeds RNA synthesis. This procedure is designed especially for determining specific activity functions for the first few minutes after labeling. This method can be applied to systems having either noncompartmentalized precursors or Type I compartmentalized precursors. Its principal usefulness is in the Type I compartmentalized system where direct measurement of this desired specific activity function is impossible.

As can be seen from equation (1), the specific activity of a product pool (pool B in the context of equation 1) is to a great degree proportional to the integral of its precursor specific activity. More

simply, this means that the specific activity of an RNA pool is nearly proportional to the integral of its true precursor specific activity. In a compartmentalized system, this true precursor specific activity will differ from the total cellular precursor specific activity. This difference is particularly great at early times after labeling.

The unstable RNA fraction is the fraction most amenable to specific activity assay during the first minute after labeling (see previous section for a discussion of the problems of measuring the specific activity of the stable RNA fraction), and so I have developed the following equations with respect to this fraction.

Equation (1) can be adapted, using the nomenclature of the previous section, to give the specific activity function for the unstable RNA fraction.

$$SAun_T = \frac{\int_0^T e^{t/G} \left[(Run)(SApre_t) - (Rdecay)(SAun_t)\right] dt}{(PSun)\, e^{T/G}}. \qquad (16)$$

Here, Rdecay refers to the rate of decay of the unstable RNA fraction. The units are in moles/second.

During the first minute or two, the value of $e^{t/G}$ is very nearly 1.0, and so this term can be discarded from the equation. Furthermore, with respect to the unstable RNA fraction, the rate of decay is very nearly equal to the rate of synthesis and both values are constants. Such being the case, they can be moved from under the integral sign and combined into a single value. By incorporating these approximations, equation (16) can be modified to give:

$$(PSun/Run)(SAun_T) \cong \int_0^T (SApre_t - SAun_t)\, dt. \qquad (17)$$

It is important to note that the constants, PSun and Run, are absolute values. In the following equations, I shall signify absolute values by underlining. Terms not underlined refer to relative values. The two terms, $\underline{PSun}$ and $\underline{Run}$, can be further transformed into relative terms by the following manipulations:

Since

$$\underline{PSun} = PSun\ \underline{PStot} \tag{18}$$

and

$$\underline{Run} = Run\ \underline{Rtot}, \tag{19}$$

then

$$\underline{PSun}/\underline{Run} = (\underline{PStot}/\underline{Rtot})(PSun/Run). \tag{20}$$

From equation (12) comes the relationship,

$$(\underline{PStot}/\underline{Rtot})(PSun/Run) = \underline{PStot}/(\underline{Rtot}\ ZI) \tag{21}$$

where ZI refers to the zero time intercept value of the proportional synthesis function.

The net synthesis rate (Rnet) equals inflow minus outflow. From equation (6), one can write

$$\underline{Rnet} = \underline{PStot}/G. \tag{22}$$

Rearranged this gives

$$\underline{PStot} = \underline{Rnet}\ G. \tag{23}$$

By substitution, equation (20) becomes

$$\underline{PSun}/\underline{Run} = G\,\underline{Rnet}/ZI\,\underline{Rtot}. \tag{24}$$

The net synthesis rate can be described in relative terms as follows:

$$Rnet = (1 - Run) + PSun(1 - Run). \tag{25}$$

When the relative pool size of the unstable RNA fraction is small, as for E. coli (approximately 4% by my estimation), then Rnet/Rtot is closely approximated by (1 - Run).

Equation 17 can now be expressed in relative terms as follows:

$$G((1 - Run)/ZI)(SAun_T) \cong \int_0^T (SApre_t - SAun_t)\, dt. \qquad (26)$$

In summary, to find the specific activity of the precursor feeding RNA synthesis at any desired time, T, one would use the following form of equation (26):

$$SApre_T \cong G((1 - Run)/ZI)(\Delta SAun_T/\Delta t) + SAun_T. \qquad (27)$$

Experimentally, one must measure the generation time, G, and both the ZI and Run values. These latter two values can be determined by the methods described earlier in this chapter. One must also measure the specific activity versus time function of the unstable RNA fraction. The slope of this function at time, T, is the value of the term $\Delta SAun_T/\Delta t$. The value of the term, $SAun_T$, is simply the specific activity of the unstable RNA fraction at time T.

Another function of considerable interest is the integral from time zero to time T of the specific activity of the precursor feeding RNA synthesis. This function is of interest because it is directly proportional to the specific activity of the stable RNA function, and at early times after labeling it is nearly proportional to the specific activity of the unstable RNA fraction. Such a function is defined by another form of equation 27.

$$\int_0^T (SApre_t)\, dt \cong G((1 - Run)/ZI)(SAun_T) + \int_0^T (SAun_t)\, dt. \qquad (28)$$

The value of the term, $\int_0^T (SApre_t)\, dt$, is determined by graphical integration of the SAun versus time function.

Figures 24-27, which will be presented in Chapter V, show an application of both equations (27) and (28) to my experimental data.

CHAPTER III

MATERIALS

[5-^{3}H]Uracil (26.2 C/m-mole), [2-^{14}C]uracil (54.9mC/m-mole), carrier-free $H_3{}^{32}PO_4$, and Aquasol were purchased from New England Nuclear, Boston, Massachusetts. Nonradioactive nucleotides (UMP, UDP, UTP, CMP, CDP, CTP, AMP, GMP), uracil, tris(hydroxymethyl)-aminomethane (Trizma base), and pancreatic RNase were purchased from Sigma Chemical Co., St. Louis, Missouri. Millipore filters (0.45 μm pore size, 24 mm diameter) were purchased from Millipore Corp., Bedford, Massachusetts. Schleicher and Schuell Selectron nitrocellulose membrane filters were purchased from Van Waters and Rogers, Brisbane, California. RNase-free sucrose and rifampicin were purchased from Schwarz-Mann, Orangeburg, New York. Diethyl pyrocarbonate was purchased from K+K Laboratories, Inc., Plainview, New York. Acrylamide N,N'—methylenebisacrylamide (bisacrylamide), N,N,N',N'—tetramethylethylenediamine (Temed), and ammonium persulfate were purchased from Canal Industrial Corp., Rockville, Maryland. PEI cellulose F precoated TLC aluminum-backed sheets were purchased from Brinkman Instruments, Inc., Burlingame, California. Large-grain coconut shell charcoal was purchased from Barnebey-Cheney, Columbus, Ohio.

CHAPTER IV

METHODS

Bacterial Cultures

E. coli B was grown in either glucose-salts medium M9 (containing /l. 3 g KH_2PO_4; 6 g Na_2HPO_4; 1 g NH_4Cl; 10^{-3} M-$MgSO_4$; 10^{-4} M-$CaCl_2$; 10^{-6} M-$FeCl_3$; 5 g glucose) or tris-glucose-amino acids medium (containing /l. 5.8 g NaCl; 3.7 g KCl; 1.1 g NH_4Cl; 0.15 g $CaCl_2 \cdot 2H_2O$; 0.1 g $MgCl_2 \cdot 6H_2O$; 10^{-6} M-$FeCl_3$; 0.142 g $NaSO_4$; 12.1 g Trizma base; 5 g glucose; 10 g casamino acids; and adjusted to pH 7.4 with HCl) at 37°C with vigorous aeration. (No phosphate was added to this second medium because the casamino acids preparation supplies sufficient for growth.) Growth of the cultures was followed by measuring the optical density at 550 nm ($O.D._{550}$) in a Beckman DB spectrophotometer. Exponentially growing cultures were started by adding approximately 10^9 cells which had been stored in 50% glycerol at -80°C to 100 ml. of fresh warmed medium. The mass doubling time during exponential growth was 46 minutes in M9 medium and 34 minutes in tris-glucose-amino acids medium. Growth was exponential up to an $O.D._{550}$ greater than 1.0 in M9 medium and up to an $O.D._{550}$ of 0.7 in tris-glucose-amino acids medium.

Radioactive Labeling and Assay of the Specific Activities of RNA Precursor

Radioactive labeling was started by pipetting 10 ml. of M9 culture (having an $O.D._{550}$ of approximately 0.3) into aerated tubes kept at

37°C and containing enough [2-^{14}C]uracil to give a final concentration of 50 μM. Twenty minutes later 250 μC of [5-^{3}H]uracil were added. One ml. samples were pipetted into 4 ml. ice-cold 0.1 M-NH_4HCO_3 and quickly filtered on Millipore filters. These filters were quickly immersed in 1 ml. of extraction mix (by volume: 1% toluene, 39% H_2O, 60% methanol) and stored at 0°C for 15 minutes. Each filter was next removed and washed with 1 ml. of extraction mix. The extract and wash solutions were mixed and centrifuged at 5,000 g for 10 minutes at 4°C. The following steps through the chromatography procedures were carried out at 4°C. The supernatant was frozen and dried under vacuum. The residue was washed with 1 ml. of chloroform/methanol (2:1, v/v). The residue was again dried briefly under vacuum and then resuspended in 50 μl. H_2O containing 10 nmoles each of UMP, UDP, UTP, CMP, CDP, and CTP markers. Twenty μl. of this solution were spotted on each of two PEI thin-layer plates which had been prewashed in 1 M-LiCl and then methanol. Both plates were eluted with methanol, dried, and then eluted with H_2O. After thorough drying, one plate was eluted with 1 M-LiCl and the other plate was eluted with 4 M-sodium formate (pH 3.4). After elution, the plates were dried and the UMP and UDP spots were cut from the LiCl-eluted plate. The UDP and UTP spots were cut from the sodium formate-eluted plate. These spots, still on their aluminum backing, were eluted with 0.5 ml. 2 M-LiCl for 30 minutes at room temperature. The solution was removed and the spots were washed with an additional 0.5 ml. 2 M-LiCl. Elutant and wash were combined and added to 5 ml. Aquasol and counted in a Beckman 3-channel LS-250 scintillation

counter. Figure 10 shows the radioactivity patterns resulting from elution of a sample taken after 4 minutes of labeling with [^{3}H]uracil.

Radioactive Labeling and Assay of the Specific Activities of RNA Fractions

Preparation of DNA Nitrocellulose Filters

DNA was prepared by the procedure of Marmur (1961). E. coli B was grown in 2 l. beef broth to an O.D.$_{550}$ = 0.8. This culture was centrifuged at 5,000 g for 10 minutes. The supernatant was discarded and the pellet resuspended in 100 ml. of saline-EDTA (10^{-1} M-NaCl; 10^{-3} M-EDTA; pH 8). The cells were again centrifuged and resuspended in 6 ml. of saline-EDTA containing 12 mg of lysozyme. This mixture was warmed at 37°C for 15 minutes. Fifty ml. of tris-SDS buffer (0.1 M-Trizma; 1.5% SDS; pH 9) were added, and the mixture was warmed at 60°C for 5 minutes. Fourteen ml. of 5 M-$NaClO_4$ were added, and the mixture was warmed at 60°C for an additional 10 minutes. This mixture was next mixed with an equal volume of chloroform-isoamyl alcohol (24:1, v/v) and thoroughly shaken. The mixture was centrifuged at 1,000 g and the upper phase was carefully decated. This phase was again extracted with chloroform-isoamyl alcohol and next added to 2 volumes of ice-cold ethanol and the DNA spooled out. This spooled DNA was dissolved in 30 ml. of 0.1xSSC (SSC = 0.15 M-NaCl; 0.015 M-trisodium citrate). Six ml. of 6xSSC and 2 ml. of heat-treated RNase (200 µg RNase/ml. SSC, heated in 100°C bath for 10 minutes) were added and the mixture incubated at 37°C for 30 minutes. From this point on, all glassware used had been heated at 110°C for 2 hours to destroy

Figure 10. One-dimensional Separation of Methanol-soluble Pyrimidine Nucleoties

An exponentially growing culture of E. coli was labeled with [^{14}C] uracil and [^{3}H] uracil. Samples were filtered, extracted, and chromatographed as described. The distribution of labels from a sample taken at four minutes is shown. The UV-absorbing spots corresponded in every case to the radioactivity peaks.

(a) Distribution of ^{3}H activity (— ● —) and ^{14}C activity (— ▲ —) on the LiCl-eluted plate.

(b) Distribution of ^{3}H activity (— ● —) and ^{14}C activity (— ▲ —) on the sodium formate-eluted plate.

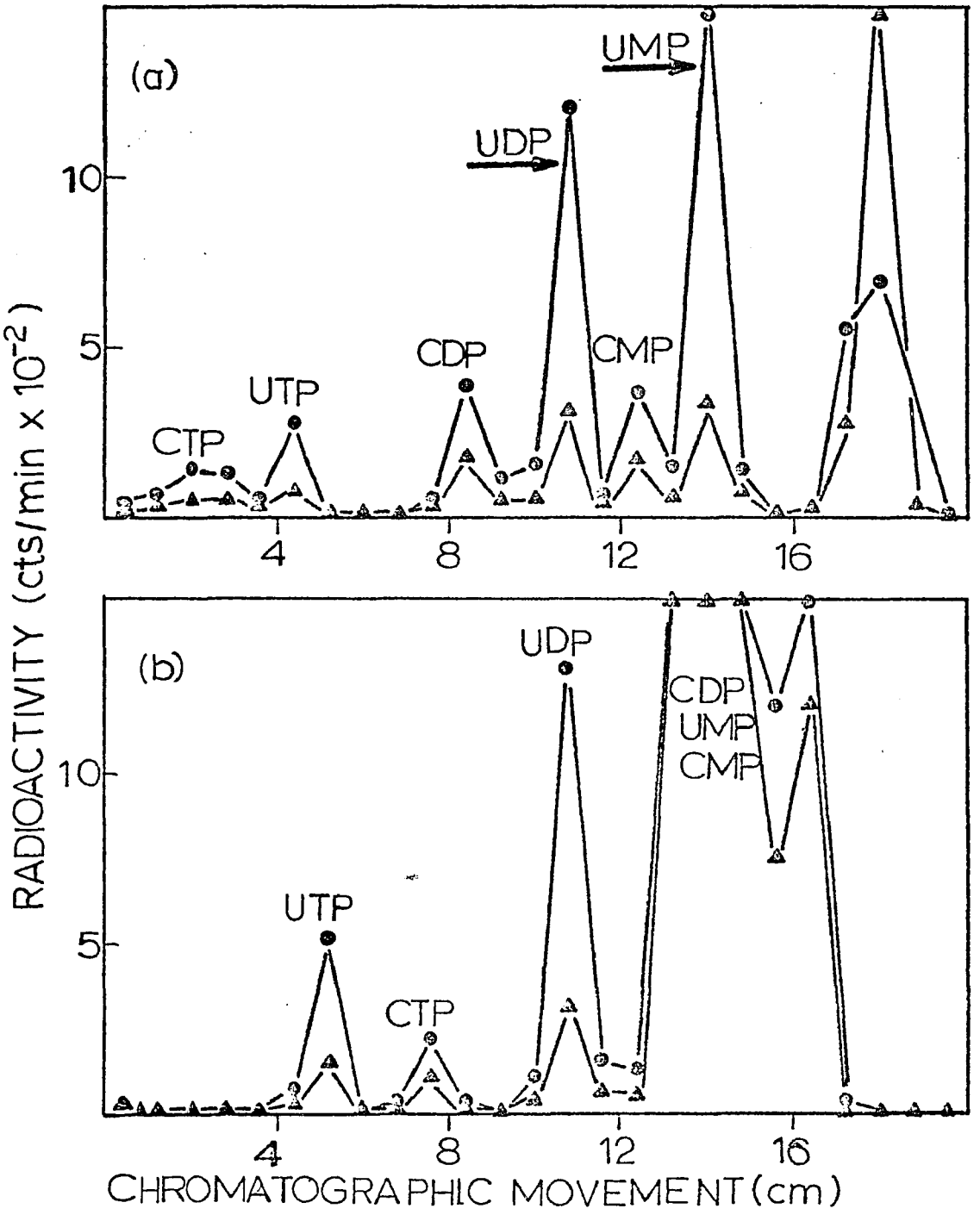

Figure 10. One-dimensional Separation of Methanol-soluble Pyrimidine Nucleotides

any RNase activity. An equal volume of freshly distilled phenol saturated with tris-SDS buffer was added and the mixture shaken vigorously for 10 minutes. The mixture was centrifuged and the aqueous phase was re-extracted with phenol. The aqueous phase was clarified by centrifuging at 10,000 g for 20 minutes at 4°C and then carefully decanted into 2 volumes of 0°C ethanol and the DNA was spooled out. The spooled DNA was washed sequentially in 70%, 80%, and then 90% ethanol. It was next dissolved in 15 ml. of 0.1xSSC, and 3 ml. of 6xSSC were added after dissolution. Two volumes of cold ethanol were added and the spooling and washing steps repeated. The spooled DNA was redissolved in 10 ml. of 0.1xSSC and extracted with two 5-ml. volumes of ether. The residual ether was removed by bubbling with N_2. If the DNA preparation was to be stored for any length of time, it was stored as an alcohol precipitate to prevent breakdown by any residual nuclease. The DNA solution was next diluted to an $O.D._{260}$ of 1.3 with 0.1xSSC. It was heated at 100°C for 10 minutes and then quickly dumped into 9 volumes of ice-cold 2xSSC. This DNA solution should be kept at 4°C to inhibit reannealing and must be used within 8 hours. Nitrocellulose filters were soaked in 2xSSC and then filter-washed with 10 ml. of 2xSSC. Ten ml. of the DNA solution were very slowly filtered through each nitrocellulose filter. These filters were next washed with 20 ml. of 2xSSC and then dried under vacuum. The filters were put in a vacuum desiccator, evacuated, and heated at 80°C for 2 hours. These DNA filters were stored under vacuum. Blank filters were prepared in the same manner with a single exception. A 2xSSC was substituted for the DNA-2xSSC filter-loading solution.

Preparation of Unlabeled Stable RNA
and Preincubation with DNA-
Nitrocellulose Filters

E. coli B was grown to $O.D._{550}$ = 0.8 in 1 l. of beef broth. This culture was centrifuged at 5,000 g for 10 minutes at 4°C. The supernatant was discarded and the pellet resuspended in 100 ml. of saline-EDTA. After 5 minutes, 0.2 ml. of rifampicin (30 mg rifampicin/ml. methanol) was added. This culture was added to 300 ml. of original medium containing 30 μg/ml. rifampicin and incubated at 37°C with aeration for 60 minutes. The culture was centrifuged and the pellet was resuspended in 10 ml. of medium. The resuspended cells were lysed by the procedure of Mueller and Bremer (1968). The cell suspension was added to 20 ml. of 100°C lysis mix (1.5% SDS; 10^{-1} M-EDTA; pH 7) and heated at 100°C for one minute. The lysate was next cooled to room temperature, and 6 ml. of ethanol-diethyl pyrocarbonate (17:3, v/v) were added. This mixture was shaken well and warmed at 37°C for 5 minutes. Eighteen ml. of aqueous NaCl saturated at 0°C were added. Again the mixture was shaken well. The preparation was spun down at 10,000 g for 15 minutes at 4°C. The supernatant was decanted into 50 ml. chloroform-isoamyl alcohol (24:1, v/v) and shaken well. The phases were separated by centrifugation and the upper phase was decanted into an equal volume of freshly distilled phenol saturated with water. After shaking well, the aqueous phase was added to 20 ml. of chloroform-isoamyl alcohol and shaken well. The upper aqueous phase was added to 120 ml. of cold ethanol. The RNA was allowed to precipitate for 4 hours at - 20°C and then centrifuged. The supernatant was discarded and the RNA resuspended in a minimal volume of water. After

resuspension, the RNA solution was diluted with 6xSSC-0.1% SDS to a final RNA concentration of 100 μg/ml. ($O.D._{260} = 2.0$). One DNA-nitrocellulose filter and one blank nitrocellulose filter were added to each thoroughly cleaned and heat-treated scintillation vial, and 0.5 ml. of this stable RNA preparation was added to each vial. The vials were tightly capped and incubated at 66°C for 15 minutes. The vial caps were further tightened and incubation was continued at 66°C for a further 10 hours. These preincubated filters in their unopened vials were stored at -20°C until needed.

Preparation of 15% Polyacrylamide Gels

Acrylamide was recrystallized from chloroform and dried well under vacuum. A solution containing by weight 50% acrylamide, 1% bi-sacrylamide, and 49% water was made up. Five E buffer (containing /l. 24.1 g Trizma base; 8.56 g trisodium acetate; 1.86 g EDTA; 10 ml. glacial acetic acid) and a 20% (w/v) RNase-free sucrose solution were prepared. A solution containing 7.5 ml. of the acrylamide-bisacrylamide solution, 5 ml. of 5 E buffer, 12.5 ml. of 20% sucrose solution, and 4.5 ml. of water was chilled in ice under moderate vacuum. Next, this solution was stirred slowly while 0.02 ml. of Temed and 0.2 ml. of 10% freshly prepared ammonium persulfate were added. This solution was quickly added to plastic tubes (7 mm inside diameter by 16 cm length), and the tubes stored at room temperature for at least 30 minutes. The tops of the tubes were covered with plastic film to prevent dehydration of the gel.

Radioactive Labeling of Cultures

Radioactive labeling was started by pipetting 0.2 ml. of tris-glucose-amino acids culture of $O.D._{550} = 0.1$ into 11 ml. of the same medium maintained at 37°C and containing 700 μC of $H_3{}^{32}PO_4$. At $O.D._{550}$ values of about 0.15, 0.25, and 0.35, 1-ml. samples were removed and their optical densities determined. At an estimated $O.D._{550} = 0.4$, 300 μC of [5-^{3}H]uracil was added.

Preparation of Stable RNA Hydrolysates

At various times samples of double-labeled culture (0.2 ml.) were added to 5 ml. of ice-cold unlabeled medium containing 300 μg/ml. rifampicin and 2×10^{-3} M-EDTA. After 5 minutes, $MgSO_4$ was added to each culture to give a final concentration of 3×10^{-3} M, and the cultures were warmed to 37°C. After 60 minutes at 37°C, the cultures were centrifuged at 5,000 g for 10 minutes at 4°C. Each pellet was resuspended in 0.5 ml. of supernatant and then 0.5 ml. of 100°C lysis mix (0.1 M-EDTA; 1.5% SDS; adjusted to pH 7) was added. This mixture was heated in a boiling water bath for one minute and then cooled to room temperature. The RNA was prepared from this lysate by a procedure similar to one developed by Summers (1970a). After adding 0.2 ml. of ethanol-diethylpyrocarbonate (17:3, v/v), the mixture was shaken and warmed for 5 minutes at 37°C. The mixture was chilled on ice and 0.6 ml. of a saturated NaCl solution was added. After mixing, the precipitate was spun down at 10,000 g for 20 minutes at 4°C. The supernatant was poured into 4.5 ml. of ethanol and chilled at -20° for 4 hours. To the pellet was added 5 ml. of 70% ice-cold ethanol. This solution was

recentrifuged and the supernatant discarded. The pellet was dried briefly under vacuum and then resuspended in 50 µl. of electrophoresis buffer made 10% with RNase-free sucrose. A drop of bromphenol blue marker solution was added and the sample was carefully layered on a 15% polyacrylamide gel and electrophoresed at 5 ma/tube until the bromphenol blue marker had passed completely through the gel. The electrophoresis buffer had the following composition per liter: 4.8 g Trizma base; 1.7 g sodium acetate; 0.37 g EDTA; 2.0 ml. glacial acetic acid; 15 g sodium dodecylsulfate). After electrophoresis the gel was removed from its tube, frozen, and cut into slices 2 mm thick. Each slice was assayed for its ^{32}P activity on a Nuclear Chicago planchet counter. The center slice of the 4 S peak was added to 2 ml. of 0.5 M-NaOH and incubated at room temperature for 8 hours. Next, 2 ml. of 0.8 M-HCl and 20 mg of large-grain charcoal were added and the mixture allowed to stand at room temperature for 1 hour.

Preparation of Total RNA Hydrolysates

Samples of double-labeled cultures (1.0 ml.) were added to 1.0 ml. of 100°C lysis mix and heated at 100°C for 2 minutes and then cooled to room temperature. A 0.4-ml. aliquot of this lysate was added to 2 ml. of ice-cold 10% TCA. The resulting precipitate was spun down and the supernatant discarded. A 5-ml. wash with cold 10% TCA was carried out and then 1 ml. of 0.5 M-NaOH was added to the drained pellet. This hydrolysis step was continued for 2 hours at room temperature. Next, 1 ml. of 0.8 M-formic acid and 20 mg charcoal were added and the mixture allowed to stand at room temperature for 1 hour.

Preparation of Unstable RNA Hydrolysates

To the remaining 1.6 ml. of lysate from the above procedure 0.4 ml. of ethanol-diethylpyrocarbonate was added, and the mixture shaken and warmed at 37°C for 5 minutes. The mixture was chilled and 1.2 ml. of 0°C saturated NaCl solution were added. The precipitate was centrifuged at 10,000 g for 20 minutes at 4°C. The supernatant was discarded and 5 ml. of 70% ice-cold ethanol was added. This solution was recentrifuged and the supernatant discarded. The pellet was dried briefly under vacuum and then resuspended in 0.5 ml. of 6xSSC-0.1% SDS. The solution was warmed at 66°C for 5 minutes and then poured into the scintillation vials containing the preincubated nitrocellulose filters. These vials were incubated at 66°C for 15 hours. When the hybridization step was completed, the vials were quickly chilled in an ice bath and the liquid was discarded from the vials. To each vial, 5 ml. of heat-treated RNase (100 μg/ml. in 2xSSC) was added and the vials were incubated at room temperature for 1 hour. The filters were next removed and washed repeatedly with 2xSSC and then once with 0.2xSSC, and finally each filter was added to a vial containing 2 ml. of water. These vials were heated at 100°C for 15 minutes and the filters removed and discarded. To each vial 0.2 ml. of 6 M-NaOH was added and incubation carried out at room temperatures for 2 hours. Following this hydrolysis step, 0.3 ml. of 8 M-formic acid and 20 mg. large-grain charcoal were added and the mixture was allowed to stand at room temperature for 1 hour.

Fractionation and Counting of Radioactive Nucleotides

The charcoal-bound nucleotides were washed with two 5-ml. aliquots of 10^{-3} M-HCl and then with 5 ml. of 10^{-3} M-formic acid. One ml. of ethanol-NH_4OH-H_2O (7:1:13, v/v/v) was added to the charcoal and the mixture allowed to stand for 30 minutes. This mixture was next filtered and the filtrate was frozen and dried under vacuum. The residue was resuspended in 20 µl. H_2O containing 10 nmoles of both UMP and CMP as optical markers. The solution was spotted on PEI-cellulose thin-layer plates, dried, and then eluted with methanol. After drying, each plate was eluted with H_2O and again dried. These methanol and water elutions remove salts which would interfere in the ion exchange process. Next, the plates were eluted with 1 M-LiCl. The plate was dried and then washed with methanol. After drying, the plate was back eluted (from the original top to the original bottom) with 1 M-acetic acid. This back elution further separates the UMP and CMP spots. The UMP spot was cut out and eluted with 1 ml. of 2 M-LiCl. The elutant was added to 5 ml. of Aquasol and counted in a Beckman 3-channel LS-250 scintillation counter in the automatic quench control mode.

CHAPTER V

RESULTS

Labeling Kinetics of the Uridine Mono-, Di-, and Triphosphates

Enough [2-^{14}C]uracil was added to a culture of growing E. coli to allow a constant rate of uptake for at least 55 minutes. By 20 minutes after [^{14}C] uracil addition, the UMP, UDP, and UTP pools had reached maximum specific activity and therefore from this time to the time at which the exogenous uracil was exhausted, the ^{14}C counts in the uridine-containing nucleotides were directly proportional to their intracellular concentrations. When [5-^{3}H]uracil was added, the ^{3}H/^{14}C ratio of the nucleotides became directly proportional to their specific activities (refer to Discussion section). This relationship holds only if the chemical concentration of [^{3}H]uracil added is small in comparison to the chemical concentration of [^{14}C]uracil present. In these experiments, the amount of [^{3}H]uracil added was approximately 1% of the [^{14}C]uracil present. The ^{3}H/^{14}C ratio can be directly compared between the mono-, di-, and triphosphonucleotides only if each species is completely separated from all radioactive contaminants. In this experiment this criterion was not met. Thymidine diphosphate and thymidine triphosphate will be labeled by [2-^{14}C]uracil but not by [5-^{3}H]uracil. Since the chromatographic system used in the nucleotide fractionation does not separate TDP from UDP and TTP from UTP, some means of correcting for this contamination factor was needed. The cells were in steady-state

growth and both the UDP and TDP pools and the UTP and TTP pools were inseparable in the chromatographic system used; hence, with respect to the ^{14}C label, the ratio, cpm in UDP/cpm in UDP + cpm in TDP, equals some constant value, A, and the ratio, cpm in UTP/cpm in UTP + cpm in TTP, equals some other constant value, B, for all samples taken after 20 minutes of [^{14}C]uracil labeling. Therefore, the true specific activities of all UDP samples were directly proportional to the ratio $^{3}H/A^{14}C$, and the true specific activities of all UTP samples were directly proportional to the ratio $^{3}H/B^{14}C$. Twenty minutes after [5-^{3}H]uracil labeling, the uridine-containing RNA precursors have reached maximal specific activity with respect to both the ^{3}H and the ^{14}C labels and one can use the relationship,

$$\text{specific activity} = \frac{^{3}H/A^{14}C \text{ at time} = T}{^{3}H/A^{14}C \text{ at time} = 20 \text{ minutes}} , \qquad (29)$$

to give the true relative specific activities at time = T. The contamination term, A, cancels out this relationship. These manipulations were used for the UMP, UDP, and UTP data. By using the $^{3}H/^{14}C$ ratio, the specific activity values become totally independent of variations in nucleotide recovery efficiencies. The relative specific activities of the UMP, UDP, and UTP pools in the above-described experiment are presented in Figure 11. As can be seen, the UMP pool labels somewhat more slowly than does the UTP pool. This result is in agreement with the published results of Mueller and Bremer (1968). The UDP pool and the UTP pool label at virtually the same rate in my experimental system. Mueller and Bremer reported that the UTP pool labeled at a substantially faster rate the the UDP pool. However, in a preliminary experiment,

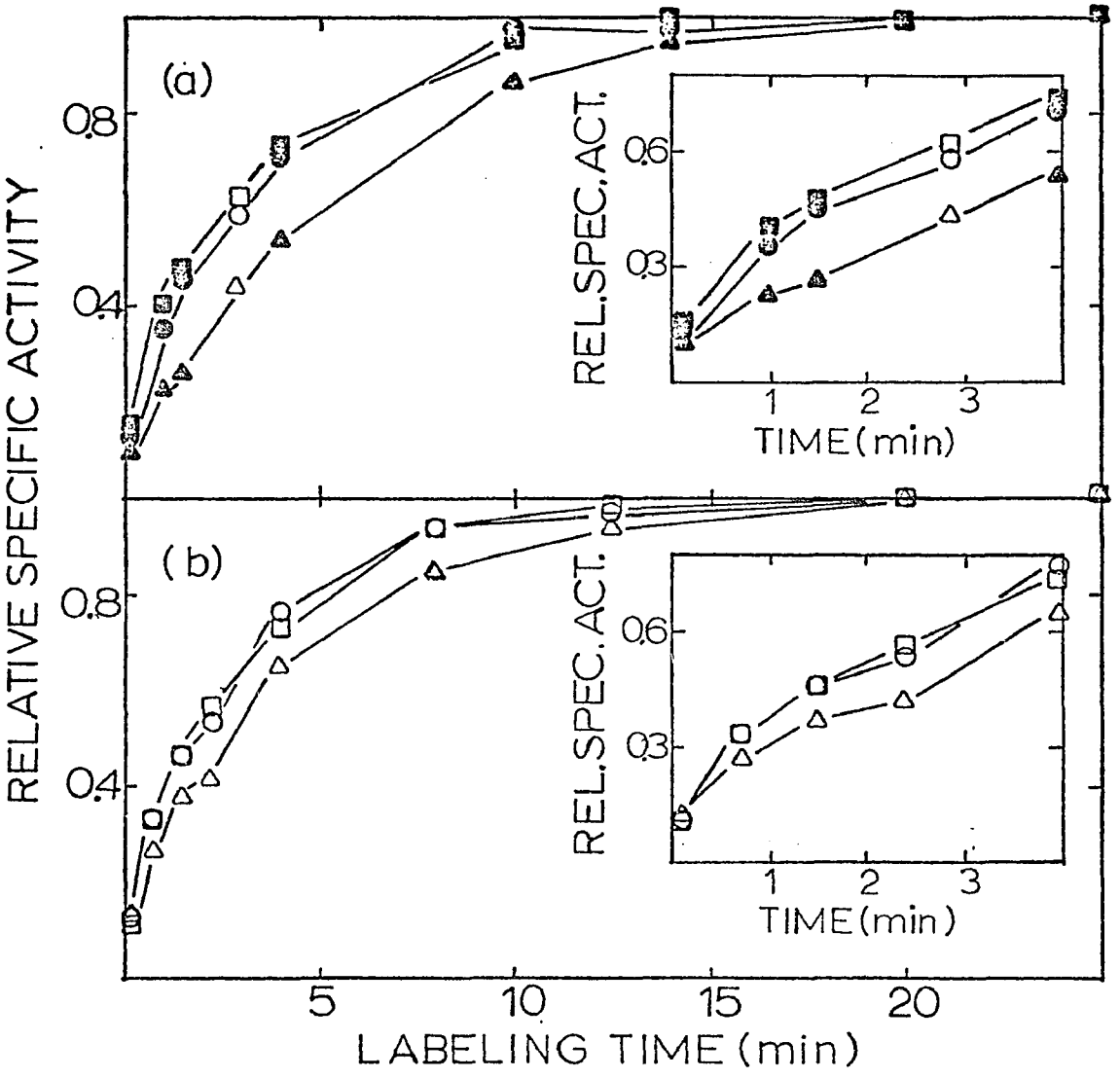

Figure 11. Relative Specific Activities of the UMP, UDP, and UTP Pools in a Continuous Labeling Experiment

An exponentially growing culture of E. coli was labeled with [^{14}C] uracil and [^{3}H] uracil. Samples were filtered, extracted, and the nucleotide extract chromatographed as described in the Methods section.

The UMP (— ▲ —), UDP (— ■ —), and UTP (— ● —) labeling kinetics are shown. The inserts expand the time scale to clarify the early labeling kinetics.

(a) Solid symbols indicate results from one experiment and open symbols indicate results from a second experiment.

(b) Results from a third identical experiment.

they (1968, Fig. 3b) report findings virtually identical to mine. The differences, if any, between our results may be due to a true difference between the strains of bacteria used or may be a consequence of some slight differences in the growth conditions. A second explanation may be that the differences might result from my rather mild conditions for nucleotide extraction and fractionation as compared to the rather harsh conditions used by Mueller and Bremer (100°C temperature and pH down to about 1). It is interesting to note that Salser, Janin, and Levinthal (1968) report that GDP and GTP label at essentially the same rate. These workers also used the $^{3}H/^{14}C$-ratio method but did not correct the data for contamination by deoxyribonucleotides.

Prior to my computer simulation studies, I ran a number of experiments designed to distinguish between Type I and Type II precursor compartmentation. Both the rationales and the results of these experiments are discussed in Appendix B.

Computer-simulated Labeling Kinetics in Three Models

Time-dependent Specific Activities of Precursors and Products

My goal in these modeling studies was to develop methods for experimentally determining the type of, or absence of, RNA precursor compartmentation in growing bacterial culture. I proceeded by comparing the outputs from two variations (both exponentially decaying and linearly decaying unstable RNA fractions) of each of the three models (noncompartmentalized precursors, peripherally compartmentalized precursors, and artifactually compartmentalized precursors) and then looked for

significant differences in some biochemically measurable parameter or set of parameters. In these simulation models, I used the pool size, half-life, and generation time values given by Mueller and Bremer (1968). These values have been used in equations (6), (7), and (8) to calculate the appropriate flow rates between the pools. In the experiments of Figures 12a-h, the specific activity of the exogenous precursor was set at 1.0 for the duration of the experiment. Equation (5) was then used to calculate the time course of the specific activity of each pool. Figure 12 shows the results from a simulated continuous labeling experiment. Figure 13 shows specific activity versus time relationships for various pools in a pulse-chase experiment. This simulated pulse-chase experiment differs from that shown in Figure 12 only in the following manner: the exogenous precursor was set at 1.0 for the first 30 seconds of the experiment and then it was reset to zero for the remainder of the experiment. The arrow in each frame indicates the chase beginning at 30 seconds. From these figures, it is apparent that there are no striking differences between the three models with respect to these particular parameters and labeling schemes.

The Gross Synthesis Function, ΔSAtot/SApre

When Mueller and Bremer (1968) calculated the total rate of RNA synthesis from the precursor specific activity (UTP) and the rate of change of the product specific activity (UMP residues of RNA), they found that their experimental results deviated significantly from that expected in a noncompartmentalized system. In light of their findings, I compared the three models for the value of the function ΔSAtot/SApre

Figure 12. Comparison of the Time Course of the Specific Activities of Several Pools in a Simulated Continuous Labeling Experiment

The pool size values were PSun (pool size unstable RNA) = 7.8; PSst (pool size stable RNA) = 292; PSpre (pool size of total precursor) = 24. The precursor pools were subdivided in the two compartmentalized models. In the peripherally compartmentalized model, the peripheral pool size (PSpre-p) was 8, and the central pool size (PSpre-c) was 16. In the artifactually compartmentalized model, the high flux pool size (PSpre-h) was 8 and the low flux pool size (PSpre-l) was 16. The flow rates (in moles/sec) were Rup (rate of uptake from the exogenous pool) = 0.08499; Run (rate of synthesis of unstable RNA) = 0.05211, Rdecay (rate of decay of unstable RNA) = 0.05006; Rst (rate of stable RNA synthesis) = 0.07664. In the two compartmentalized models, the rate of diffusion between the two precursor pools (Rdif) was 0.91968. In the artifactually compartmentalized model, the rate of uptake from the exogenous pool was subdivided into two rates. The rate of uptake into the low flux pool (Rup - l) was 0.00625 and the rate of uptake into the high flux pool (Rup - h) was 0.07874. In the variations having an exponentailly decaying unstable RNA pool (frames a-d), the half-life of the unstable RNA was 108 seconds. In the variations having a linearly decaying unstable RNA pool (frames e-h), the lifetime of the unstable RNA was 108 seconds. The generation time, G, was 3,590 seconds (doubling time of 44 minutes).

Figures a through d (solid symbols) show the results from models having an exponentially (E) decaying unstable RNA pool while frames e through h (open symbols) show the results from models having a linearly (L) decaying unstable RNA pool.

Results from the noncompartmentalized (— ● —, — ○ —), the peripherally (type I) compartmentalized model (— ▲ —, — △ —), and the artifactually (type II) compartmentalized model (— ■ —, — □ —) are compared in each figure.

(a, e) Total precursor pool.
(b, f) Unstable RNA pool.
(c, g) Stable RNA pool.
(d, h) Total RNA pool.

Specific activity values were calculated at 1-second intervals for the first 30 seconds and then at 5-second intervals thereafter.

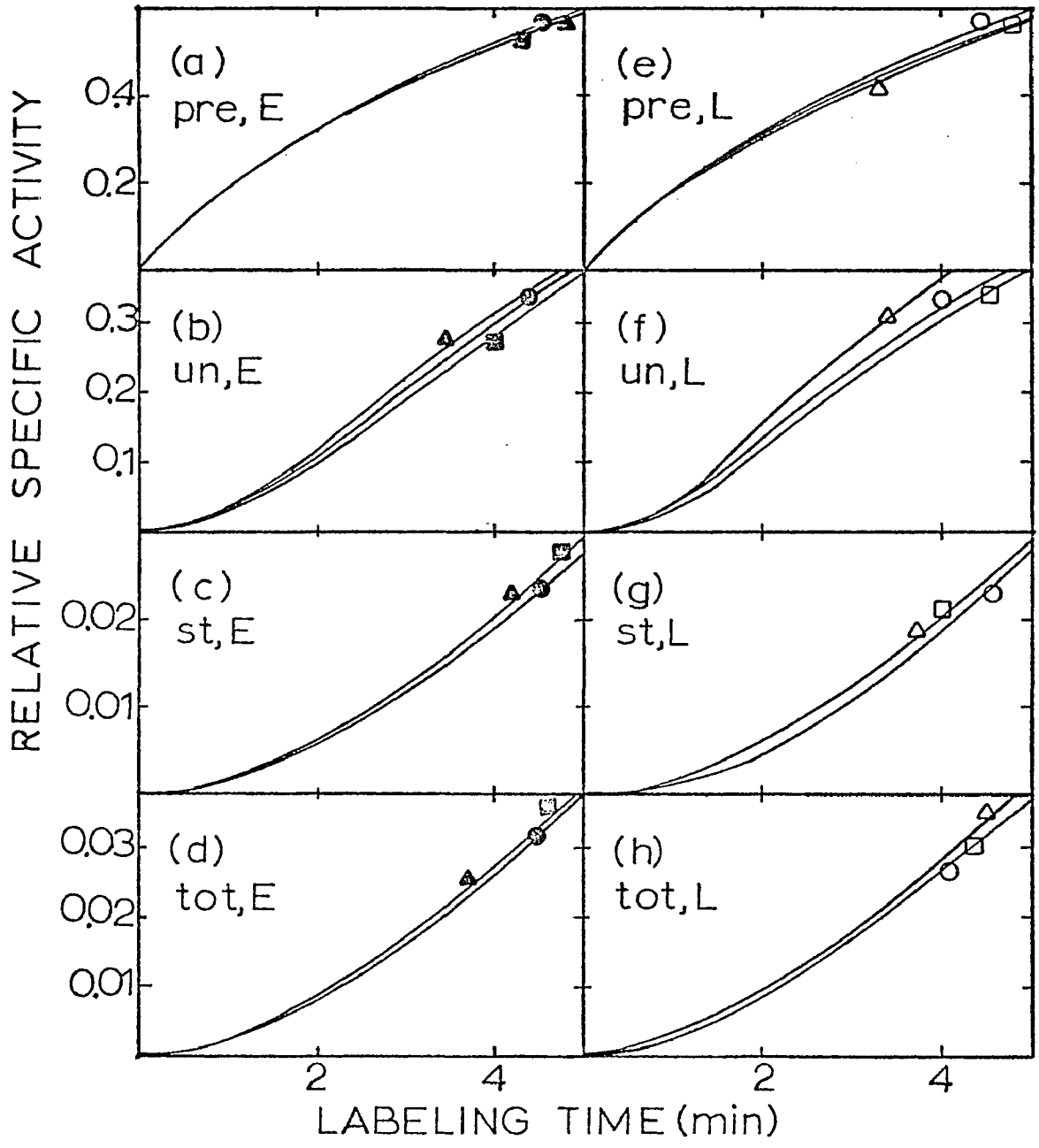

Figure 12. Comparison of the Time Course of the Specific Activities of Several Pools in a Simulated Continuous Labeling Experiment

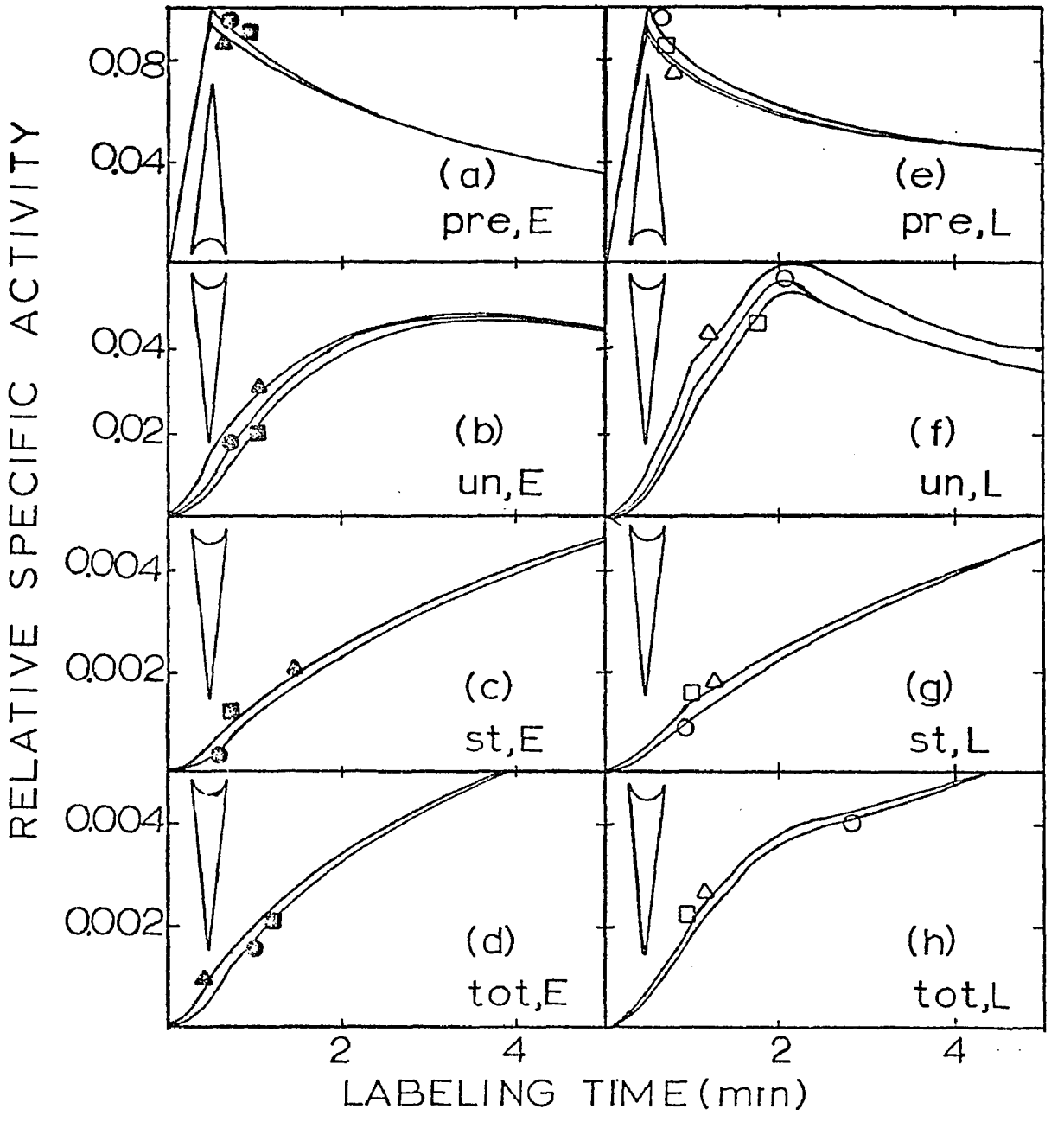

Figure 13. Comparison of the Time Course of the Specific Activities of Several Pools in a Simulated Pulse-chase Labeling Experiment

This experiment differs from that shown in Figure 12 only in the following manner: the exogenous precursor was set at 1.0 for the first 30 seconds of the experiment and then it was reset to zero for the remainder of the experiment. The arrow in each frame indicates the chase beginning at 30 seconds.

versus time after labeling. This output is shown in Figure 14. With respect to this function, the two compartmentalized models differ markedly from the noncompartmentalized model. I believe this function can, with the reservations to be discussed later, be used to detect the presence of RNA precursor compartmentation. It cannot, however, be used to discriminate between the two types of compartmentation.

The Proportional Synthesis Function, SAun/SAtot

A close inspection of the basic difference between the two types of compartmentation led me to compare the three models with respect to the value of the function SAun/SAtot versus time. Figure 15 shows a very substantial difference between the two compartmentation models with respect to this function. The values of this function in the noncompartmentalized model and in the peripherally compartmentalized model are, however, virtually indistinguishable.

Briefly, I can now generalize that a plot of the function ΔSA(product)/SA(precursor) versus time can serve to distinguish between a compartmentalized system and a noncompartmentalized system. Furthermore, if compartmentation is indicated by the above function, then a plot of the function SAun/SAtot versus time can be used to indicate the type of compartmentation present in the system.

In the simulation experiments thus far, I have considered two variations of each of the three models: one variation having an exponentially decaying unstable RNA fraction and the other variation having a linearly decaying unstable RNA fraction. In a later section, I show my

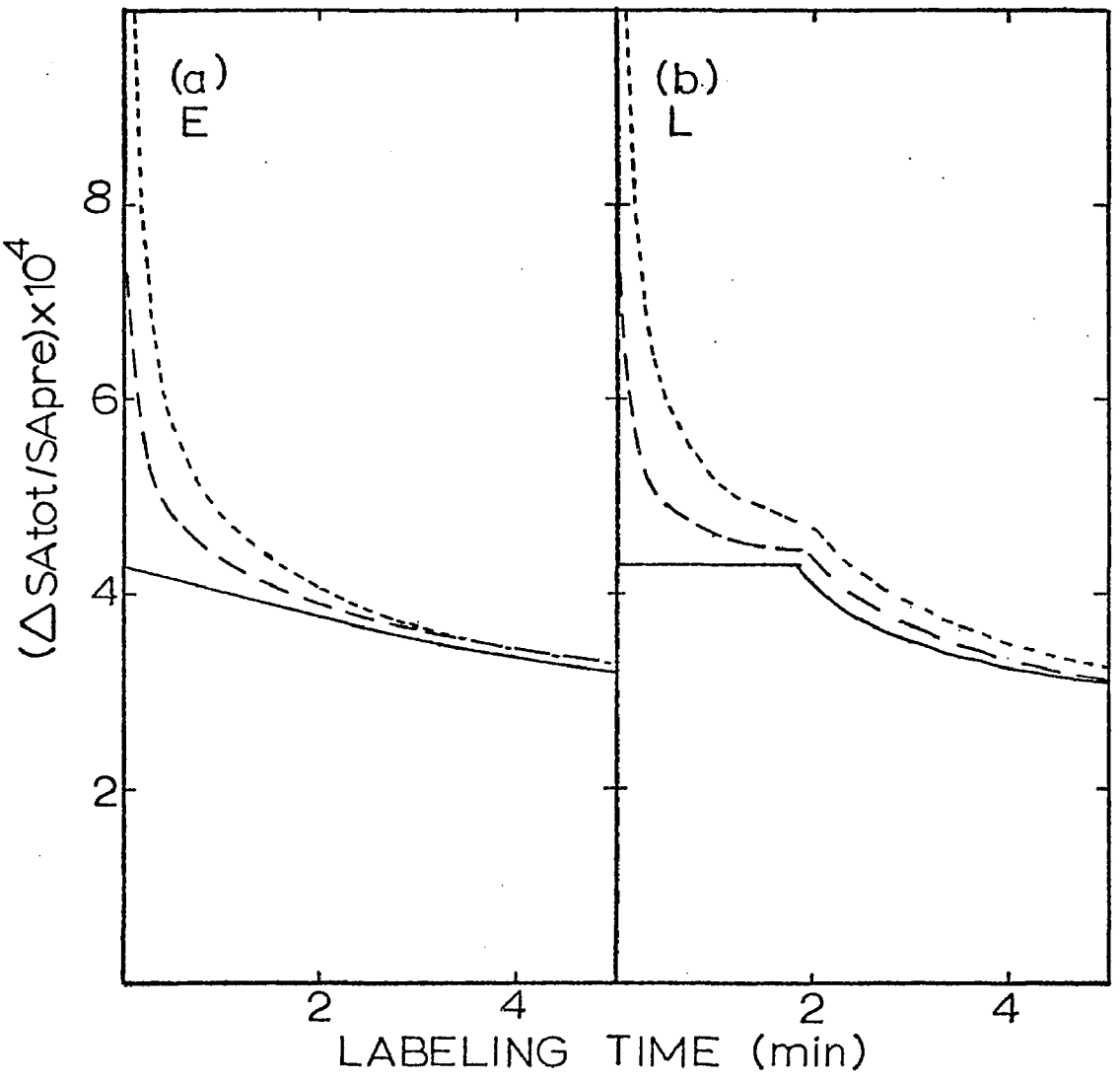

Figure 14. The Gross Synthesis Function

In the experiment of Figure 12, the rate of incorporation of uracil into RNA was plotted versus time after labeling. In each frame, the solid line (—) represents output from the noncompartmentalized model, the dotted line (...) represents output from the peripherally compartmentalized model, and the dashed line (---) represents output from the artifactually compartmentalized model.

(a) Exponentially decaying unstable RNA models.
(b) Linearly decaying unstable RNA models.

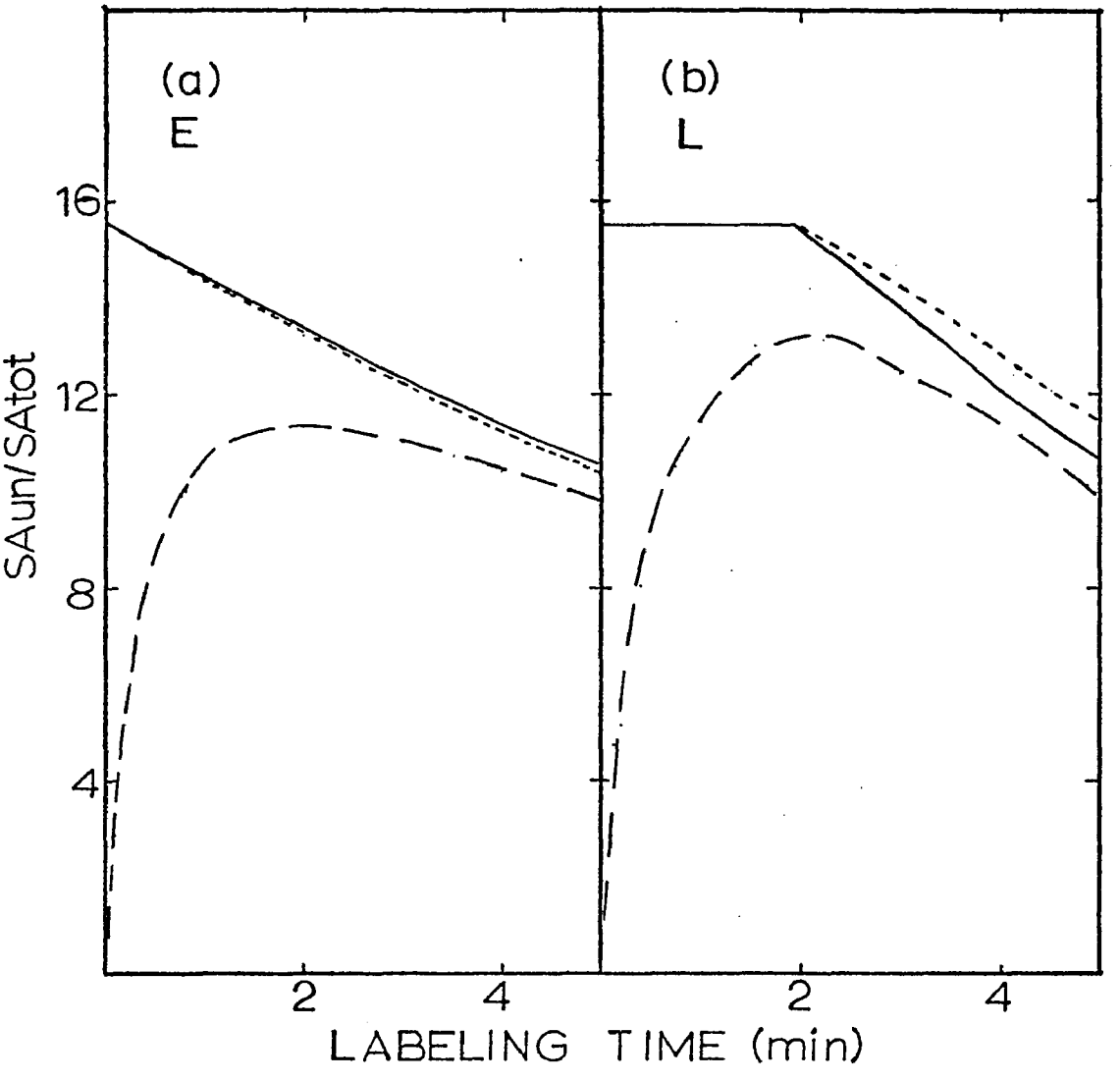

Figure 15. The Proportional Synthesis Function

In the experiment of Figure 12, the specific activity of the unstable RNA pool was divided by the specific activity of the total RNA pool. This ratio was plotted versus time after labeling. The solid, dotted, and dashed lines signify, respectively, output from the same models as in Figure 14.

(a) Exponentially decaying unstable RNA models.
(b) Linearly decaying unstable RNA models.

experimental determinations of the proportional synthesis function. When these experimental results are compared to the results from the simulation experiment shown in Figure 15, the model involving linear decay of the unstable RNA fraction is clearly discounted. Thus, I shall henceforth deal only with models entailing an exponentially decaying unstable RNA fraction.

Effects of Relative Precursor Pool Sizes and Diffusion Rate on Both the Gross Synthesis Function and the Proportional Synthesis Function

I next addressed myself to a more detailed analysis of the gross synthesis function and the proportional synthesis function in the two compartmentalized models. In these two models, both the diffusion rate between the two cellular precursor pools and the relative size of each precursor compartment were chosen in a rather arbitrary manner. I therefore checked to see if the values for these two functions remained qualitatively similar with higher and lower diffusion rates and changes in the relative sizes of the precursor compartments. Figure 16 shows the effects of varying the diffusion rate in the two compartmentalized models with respect to the gross synthesis function (ΔSAtot/SApre). Figure 17 shows the effects of varying the relative sizes of the precursor compartments with respect to this same function.

Figure 18 shows the effects of varying the diffusion rate on the function SAun/SAtot in the two compartmentalized models. Figure 19 shows the effects of varying the relative sizes of the precursor compartments with respect to this same function.

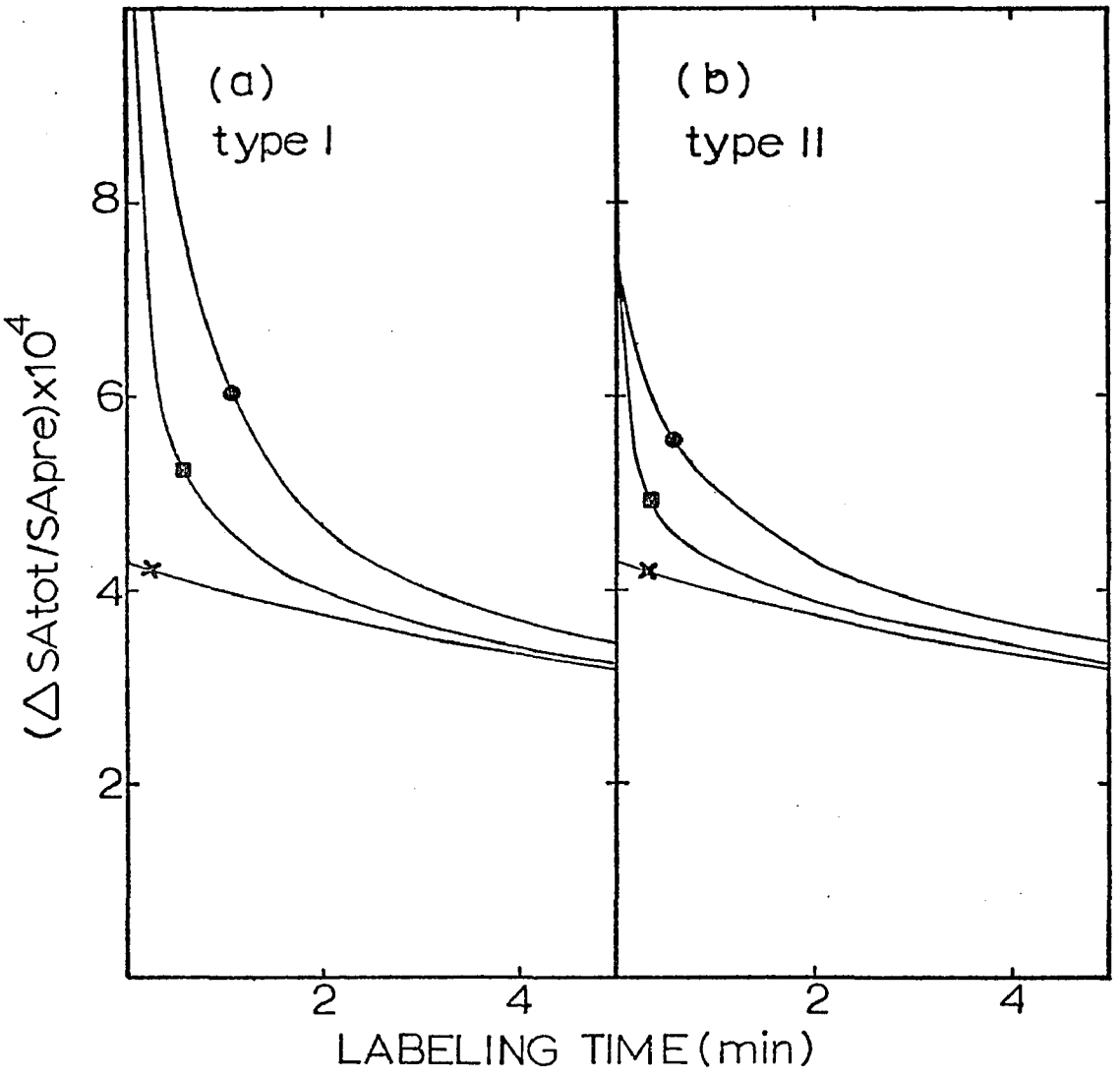

Figure 16. The Effect on the Gross Synthesis Function of Varying the Intercompartment Diffusion Rate

These experiments differ from that shown in Figure 12 in the following manner. In the compartmentalized models, the rate of diffusion between the two precursor compartments was varied. The diffusion rates were Rdif = 4 x Rst (— ● —), Rdif = 12 x Rst (— ■ —), Rdif = ∞ Rst (— × —).

(a) Peripherally compartmentalized model.
(b) Artifactually compartmentalized model.

Figure 17. The Effect on the Gross Synthesis Function of Varying the Relative Sizes of the Precursor Compartments

These experiments differ from that shown in Figure 12 in the following manner: in the two compartmentalized models, the relative sizes of the precursor compartments were varied.

(a) The precursor pool sizes in the peripherally compartmentalized model were PSpre - p = 4, PSpre - c = 20 (— ● —); PSpre - p = 12, PSpre - c = 12 (— ▲ —); PSpre - p = 18, PSpre - c = 6 (— ■ —).

(b) The precursor pool sizes and corresponding exogenous uptake rates in the artifactually compartmentalized model were PSpre - h = 4, PSpre - l = 20, Rup - h = 0.07769, Rup - l = 0.00730 (— ● —); PSpre - h = 12, PSpre - l = 12, Rup - h = 0.07070, Rup - l = 0.00520 (— ▲ —); PSpre - h = 18, PSpre - l = 6; Rup - h = 0.08136, Rup - l = 0.00362 (— ■ —).

The gross synthesis function in the noncompartmentalized model is given for reference in both frames a and b (— + —).

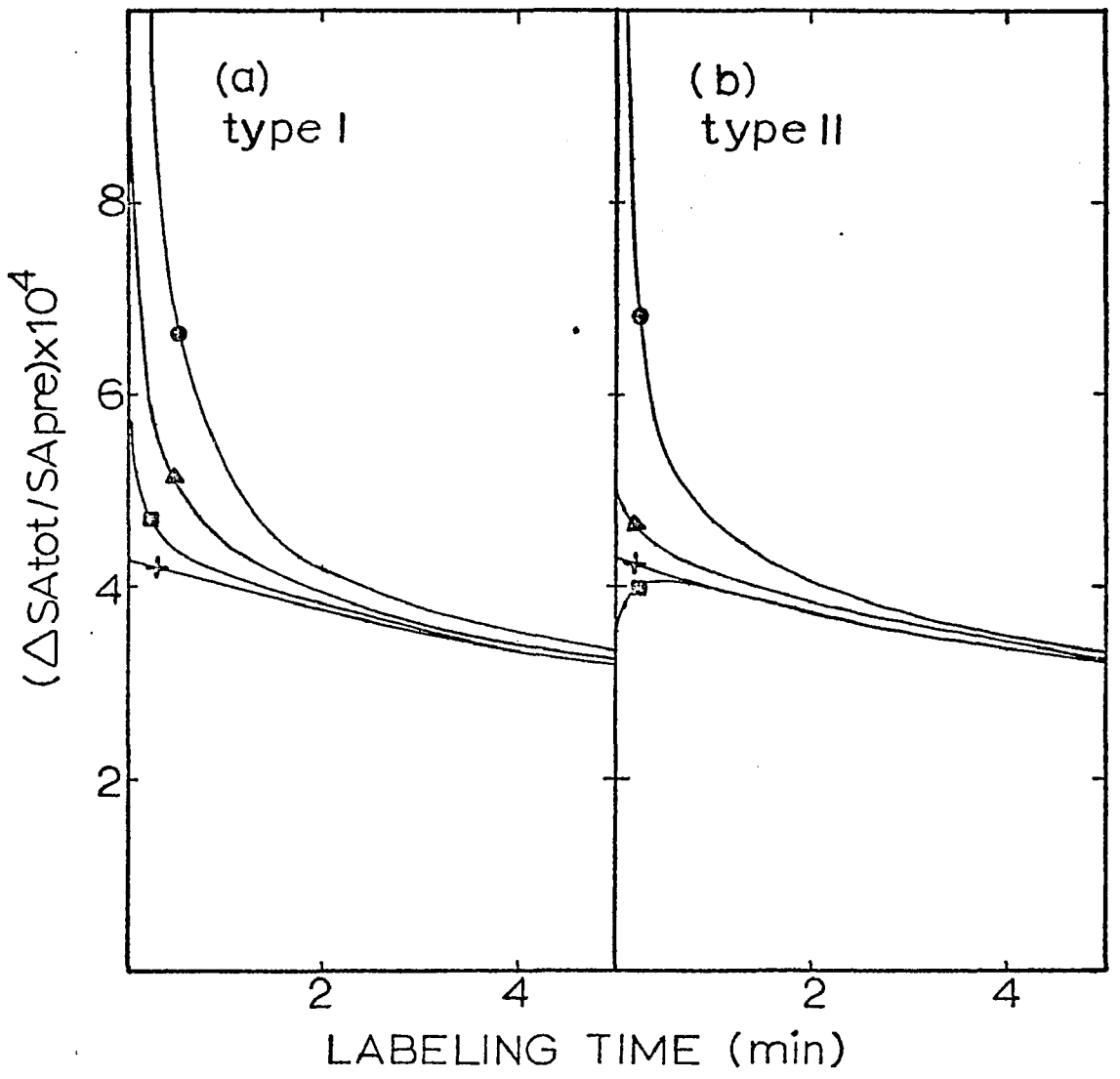

Figure 17. The Effect on the Gross Synthesis Function of Varying the Relative Sizes of the Precursor Compartments

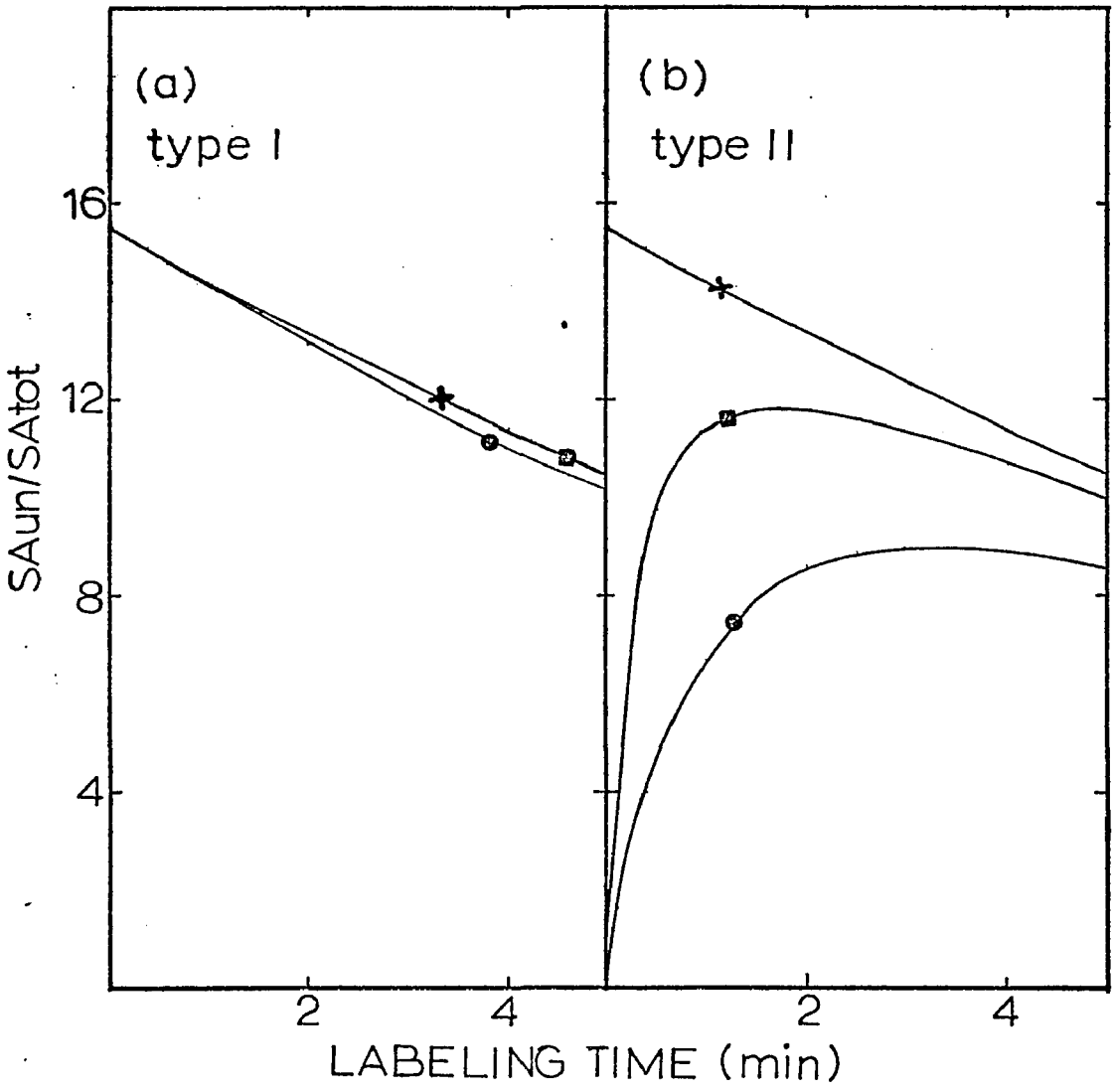

Figure 18. The Effect on the Proportional Synthesis Function of Varying the Intercompartment Diffusion Rate

These experiments differ from that shown in Figure 12 in the following manner: in the compartmentalized models, the rate of diffusion between the two precursor compartments was varied. The diffusion rates were Rdif = 4 x Rst (— ● —), Rdif = 12 x Rst (— ■ —), Rdif = ∞ Rst (— + —).

(a) Peripherally compartmentalized model.
(b) Artifactually compartmentalized model.

Figure 19. The Effect on the Proportional Synthesis Function of Varying the Relative Sizes of the Precursor Compartments

These experiments differ from that shown in Figure 12 in the following manner: in the compartmentalized models, the relative sizes of the precursor compartments were varied.

(a) The precursor pool sizes in the peripherally compartmentalized models were PSpre - h = 4, Pspre - c = 20 (— ● —); PSpre - h = 12, PSpre - 1 = 12, Rup - h = 0.07979, Rup - 1 = 0.00520 (— ▲ —); PSpre - h = 18, PSpre - 1 = 6; Rup - h = 0.08136, Rup - 1 = 0.00362 (— ■ —).

The proportional synthesis function in the noncompartmentalized model is given for reference in both frames a and b (— + —).

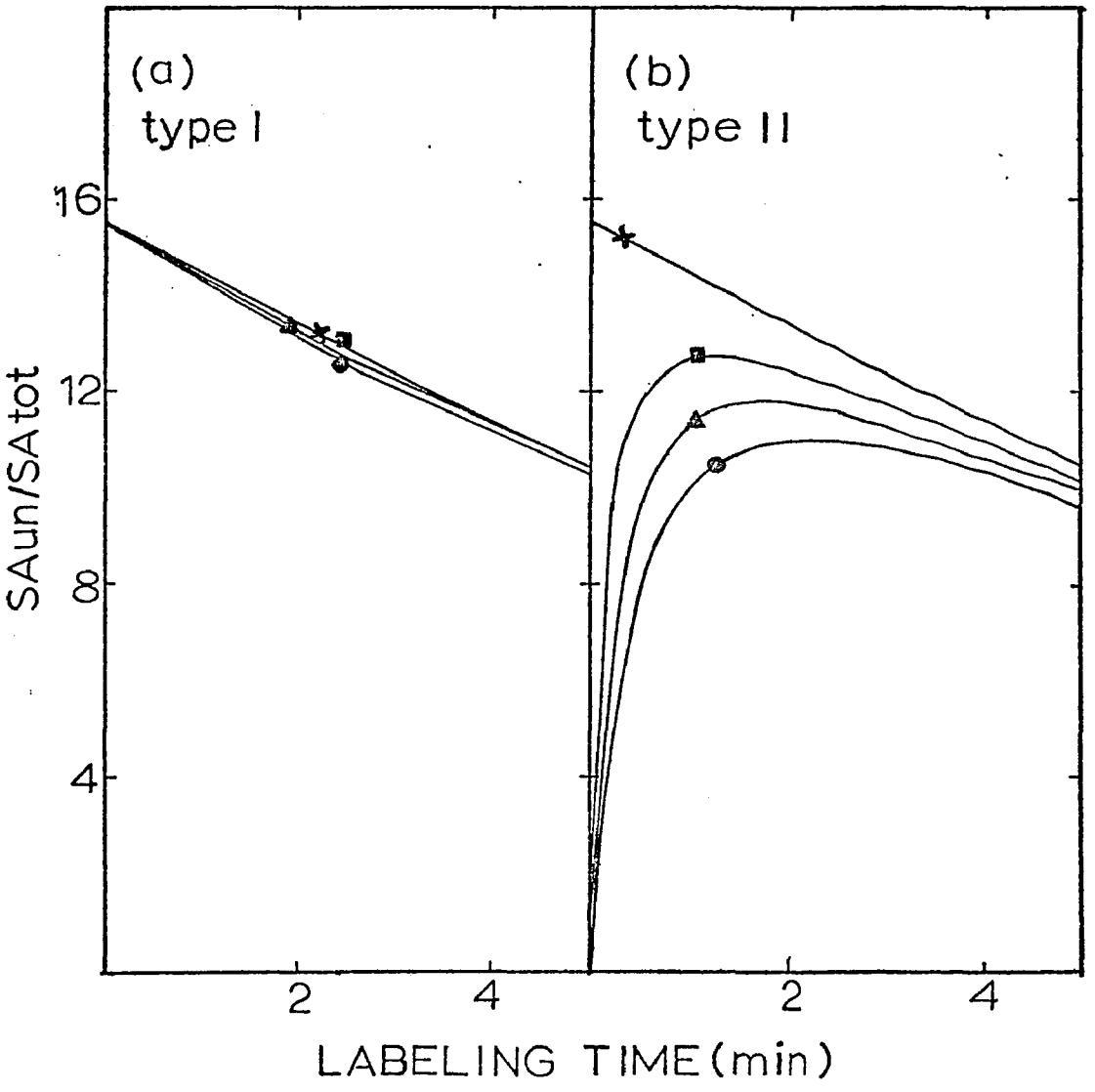

Figure 19. The Effect on the Proportional Synthesis Function of Varying the Relative Sizes of the Precursor Compartments

From these figures one can conclude that over a wide range of diffusion rates and relative precursor compartment sizes, the values of these two functions remain qualitatively similar.

Degree of Dependence on Precursor Specific Activity of Both the Gross Synthesis Function and the Proportional Synthesis Function

If the zero time intercept of a function is independent of precursor specific activity, then a simulation experiment should give the same zero time intercept for that function irrespective of the initial precursor specific activity. Figure 20 compares the three models with respect to the gross synthesis function in two simulation experiments. In one experiment, the precursor had an initial specific activity of zero and in the second experiment the precursor had an initial specific activity of one. Figure 21 compares the three models with respect to the proportional synthesis function in the two above-described initial conditions experiments. The results indicate that in both the noncompartmentalized and the Type I compartmentalized models, the zero time intercepts of the proportional synthesis function are independent of precursor specific activity. On the other hand, both types of precursor compartmentation render the zero time intercept of the gross synthesis function sensitive to variations in precursor specific activity.

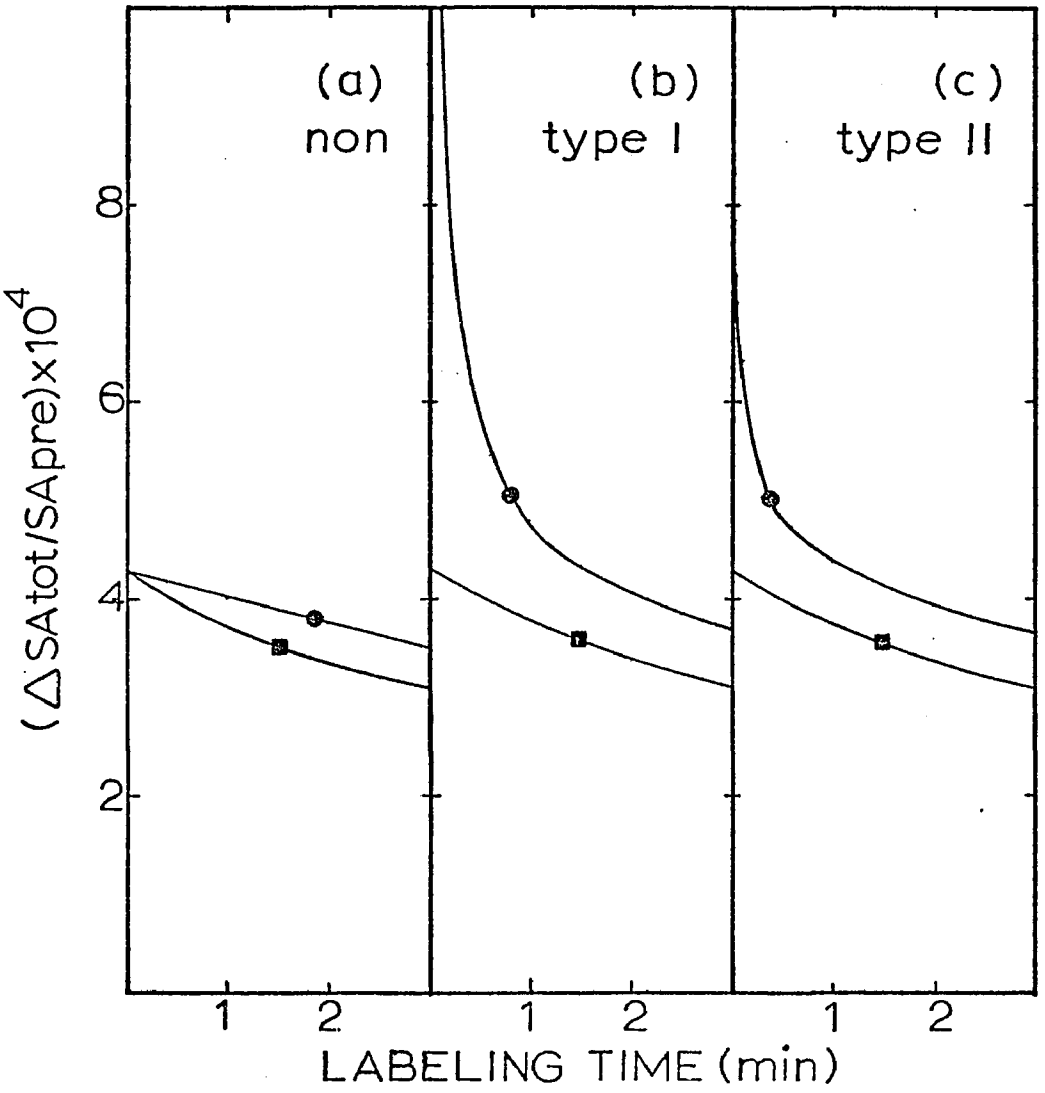

Figure 20. Dependence of the Gross Synthesis Function on Precursor Specific Activity

In the experiment of Figure 12 the specific activity of the total precursor pool had an initial value of zero (— ● —) or an initial value of 1.0 (— ■ —).

(a) Noncompartmentalized model.
(b) Peripherally compartmentalized model.
(c) Artifactually compartmentalized model.

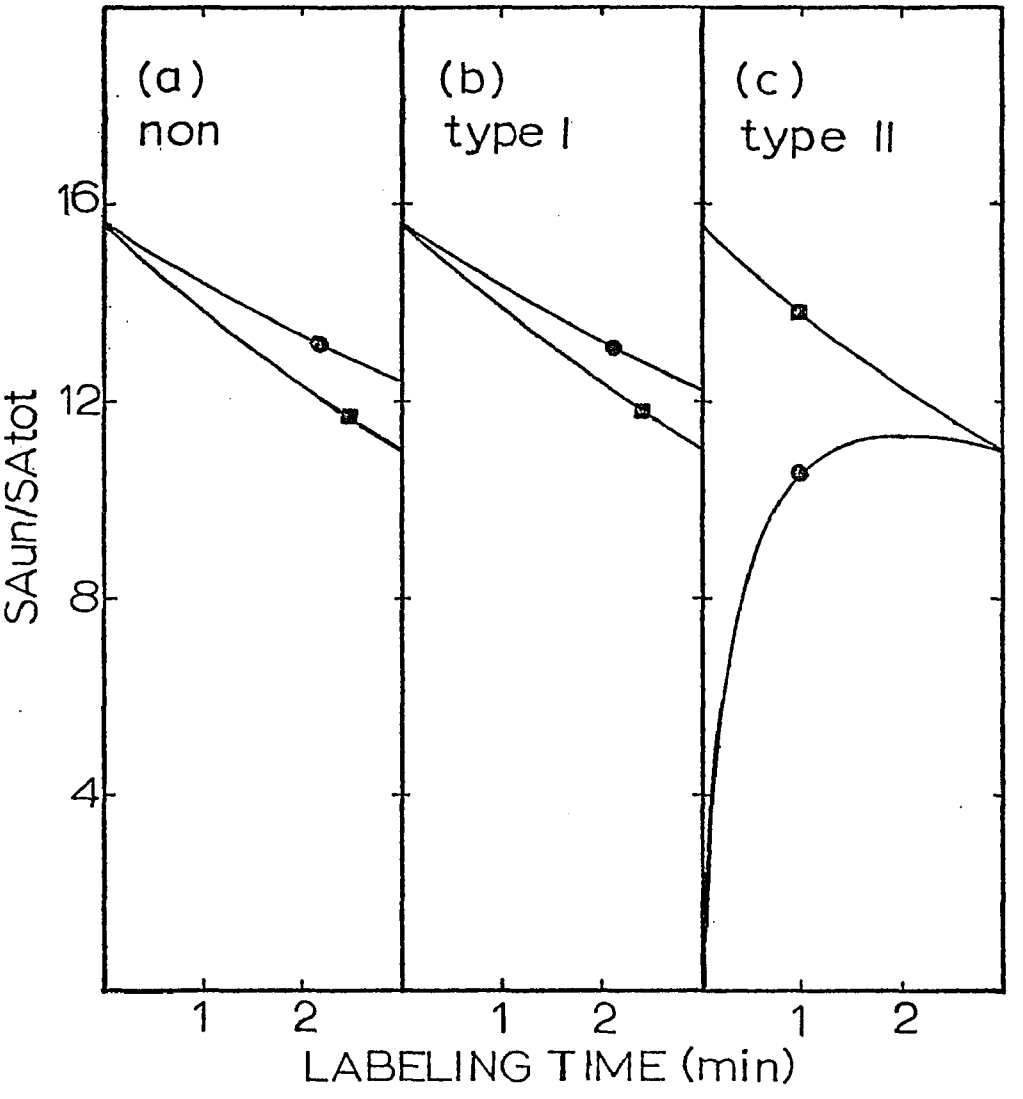

Figure 21. Dependence of the Proportional Synthesis Function on Precursor Specific Activity

In the experiment of Figure 12 the specific activity of the total precursor pool had an initial value of zero (— ● —) or an initial value of 1.0 (— ■ —).

(a) Noncompartmentalized model.
(b) Peripherally compartmentalized model.
(c) Artifactually compartmentalized model.

Experimental Determination of the Relative Rate of Synthesis and of the Relative Pool Size of the Unstable RNA Fraction

Experimental Measurement of the Proportional Synthesis Function

Figure 22 shows an experimental measurement of the proportional synthesis function. The culture from which these samples were taken had been pregrown in unlabeled uracil in order to pre-expand the precursor pools and shut off endogenous synthesis of uracil. This procedure insures steady-state labeling conditions. Figure 23 shows a second experimental measurement of the proportional synthesis function. This experiment differs from that of Figure 22 in that this second culture was not pregrown in unlabeled uracil before labeling with [5-^{3}H]uracil.

In this second labeling scheme, there is probably a much more rapid rise in precursor specific activity due to the rapid influx of labeled precursor leading to an expanded precursor pool. Such a phenomenon has been reported by several workers (Salser et al., 1968; Bremer and Yuan, 1968b). Not surprisingly, the zero time intercept values are indistinguishable in these two experiments. Such an equivalence of zero time intercept values in the presence of differing precursor specific activities was predicted by both equation (11) and by the simulation experiments of Figure 21.

In these experimental determinations of the proportional synthesis function, the zero time intercept value is somewhat questionable because of the need for extrapolating a curved line. In the computer-simulated experiments, a straight line results when one plots the value, log ((SAun/SAtot) - 1), versus time. This is to be expected if the

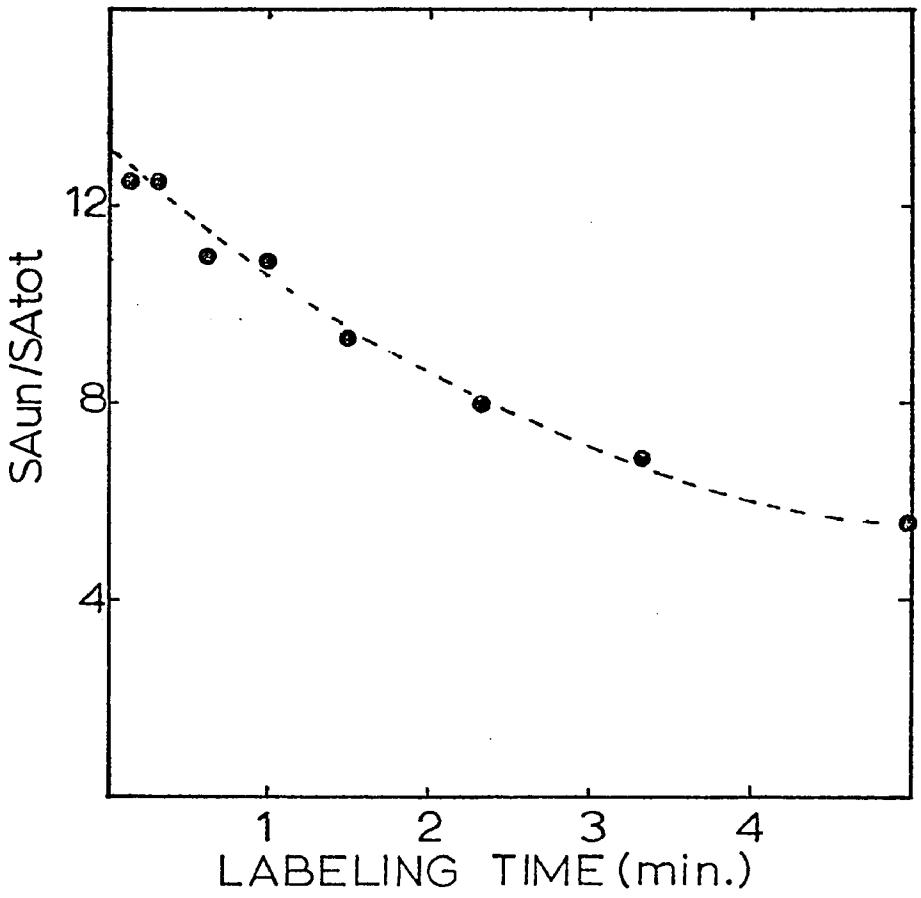

Figure 22. Experimental Measurement of the Proportional Synthesis Function in a Culture Pregrown in Uracil

An exponentially growing culture of E. coli was labeled with $H_3{}^{32}PO_4$ for 7.5 doublings. Unlabeled uracil was added to preexpand the nucleotide pools and 15 minutes later [^{3}H]uracil was added. RNA was extracted, fractionated, and counted as described in the Methods section. The ratios of the specific activities, unstable RNA/total RNA, were plotted versus their sampling time.

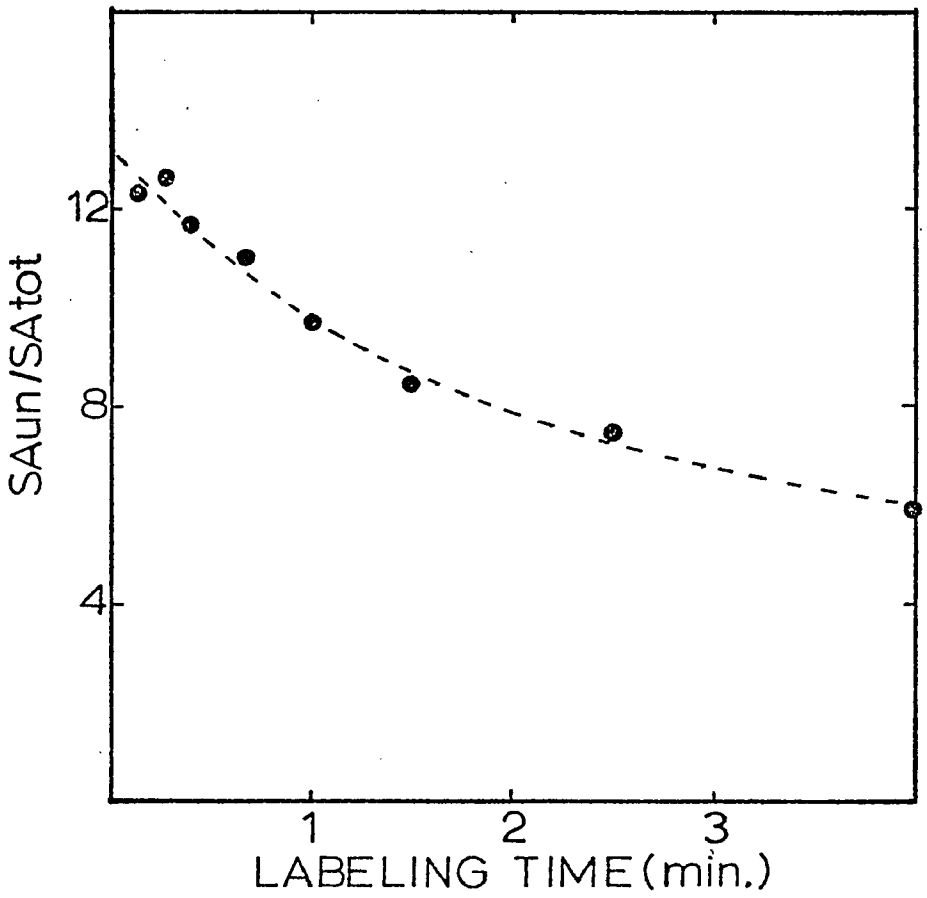

Figure 23. Experimental Measurement of the Proportional Synthesis Function

An exponentially growing culture of E. coli was incubated as in Figure 22 except that no unlabeled uracil was added prior to ^{3}H labeling. The remaining procedures were identical.

unstable RNA is decaying in an exponential fashion. The quantity, one, is subtracted from the specific activities ratio since this ratio asymtotically approaches a limit of one rather than zero. A plot of the experimental data from the experiment of Figure 23 in the form just discussed is shown in Figure 24. The zero time intercept in this plot has a value of 12.2 and hence the zero time intercept of the proportional synthesis function has a value of 13.2. When this zero intercept value is multiplied by the pool size (covered in the next section), it will give the proportion of the total uridine nucleotides incorporated into the unstable RNA fraction (see equation 12).

Relative Pool Size of the Unstable RNA Fraction

Figure 25 shows the unstable RNA pool size calculated (see equation 15) from four sampling times. The average value is 4.4% $\pm$ 0.36% of the total RNA. This means that 4.4% of those UMP residues in the total RNA pool are in the unstable RNA fraction. UMP residues compose 21.5% of the nucleotides in stable RNA and 23.5% of the nucleotides in unstable RNA (Cox, 1968). When these base ratio data are taken into account, the percentage of the total RNA nucleotides in the unstable RNA fraction is 4.1%.

With this pool size value and the previously determined zero time intercept value of the proportional synthesis function, 13.2, it is a simple matter to calculate from equation (12) the proportion of the total uridine nucleotides incorporated into the unstable RNA fraction. This proportion is 58%. When this value is adjusted with the base ratio data

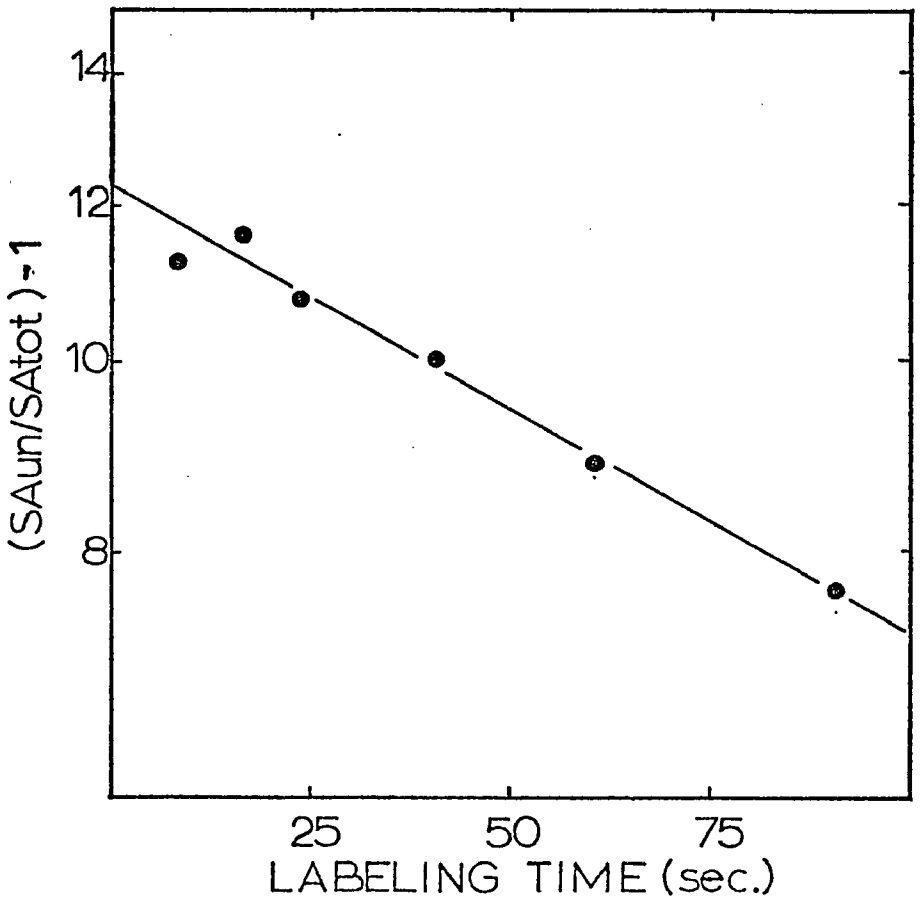

Figure 24. Semilogarithmic Plot of an Experimentally Measured Proportional Synthesis Function

A value of 1 was subtracted from each ratio of the specific activities, unstable RNA/total RNA, shown in Figure 23. These new values were plotted on a semilogarithmic scale versus their sampling times.

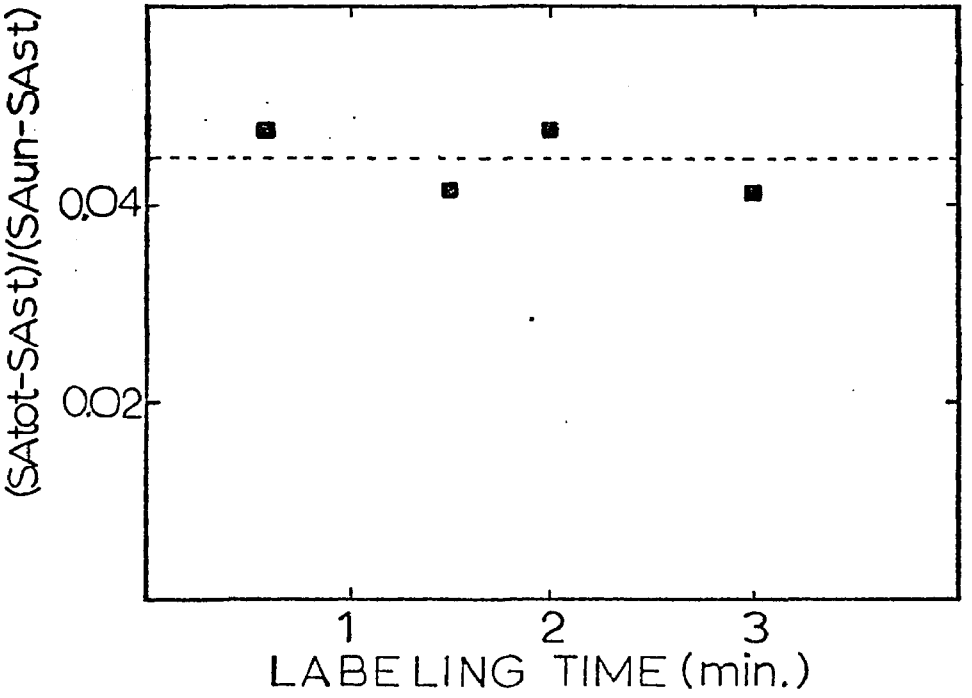

Figure 25. Relative Pool Size of the Unstable RNA Fraction

Specific activity values from the experiment of Figure 23 were substituted into the equation

$$PSun = \frac{SAtot - SAst}{SAun - SAst}.$$

These PSun values were plotted versus their sampling times. The dashed line represents the mean PSun value.

of Cox (1968), one finds that 56% of the total nucleotide incorporation into RNA is into the unstable RNA fraction.

Calculation of the Specific Activity of the Precursor Feeding RNA Synthesis

Figure 26 shows a plot of the specific activity versus time after labeling of unstable RNA, total RNA, and RNA precursor. The values for unstable RNA and total RNA were measured directly in the experiment of Figure 23. The values for the RNA precursor were calculated using the data from the experiment of Figures 23 and 25 and equation (27). In this experiment, the calculated precursor specific activity shows a very substantial rise by the first sampling time (8 seconds). By one minute the label in the medium appears to be exhausted and the rate of rise of the precursor specific activity begins decreasing and becomes negative at 90 seconds. The rapid exhaustion of exogenous precursor occurs because of the very small amount of labeled uracil used in these experiments. I used such small amounts because my primary interest lay in the events occuring during the first minute or two of labeling.

Figure 27 shows a plot of the integral of the specific activity versus time after labeling of unstable RNA, total RNA, and RNA precursor. The values for unstable RNA and total RNA are direct graphical integrations of the data from the experiment of Figure 23. The values for the RNA precursor were calculated using equation (28) and the data from the experiments of Figures 23 and 25.

Figure 28 shows plots of the specific activity versus time after labeling of unstable RNA and the corresponding calculated values for RNA precursor from three separate experiments. In these experiments

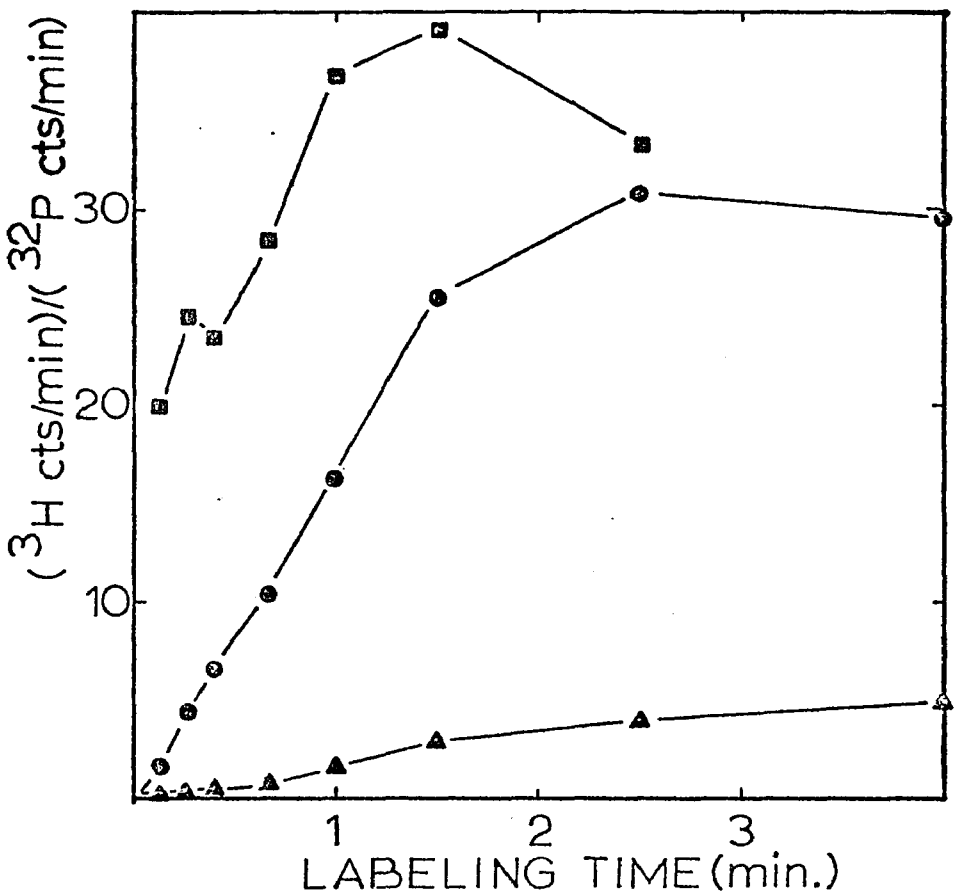

Figure 26. The Time Course of the Specific Activities of Total RNA, Unstable RNA, and RNA Precursor

Specific activity values for total RNA (— ▲ —) and unstable RNA (— ● —) were plotted directly and used in equation (27) to calculate the specific activity values for RNA precursor (— ■ —).

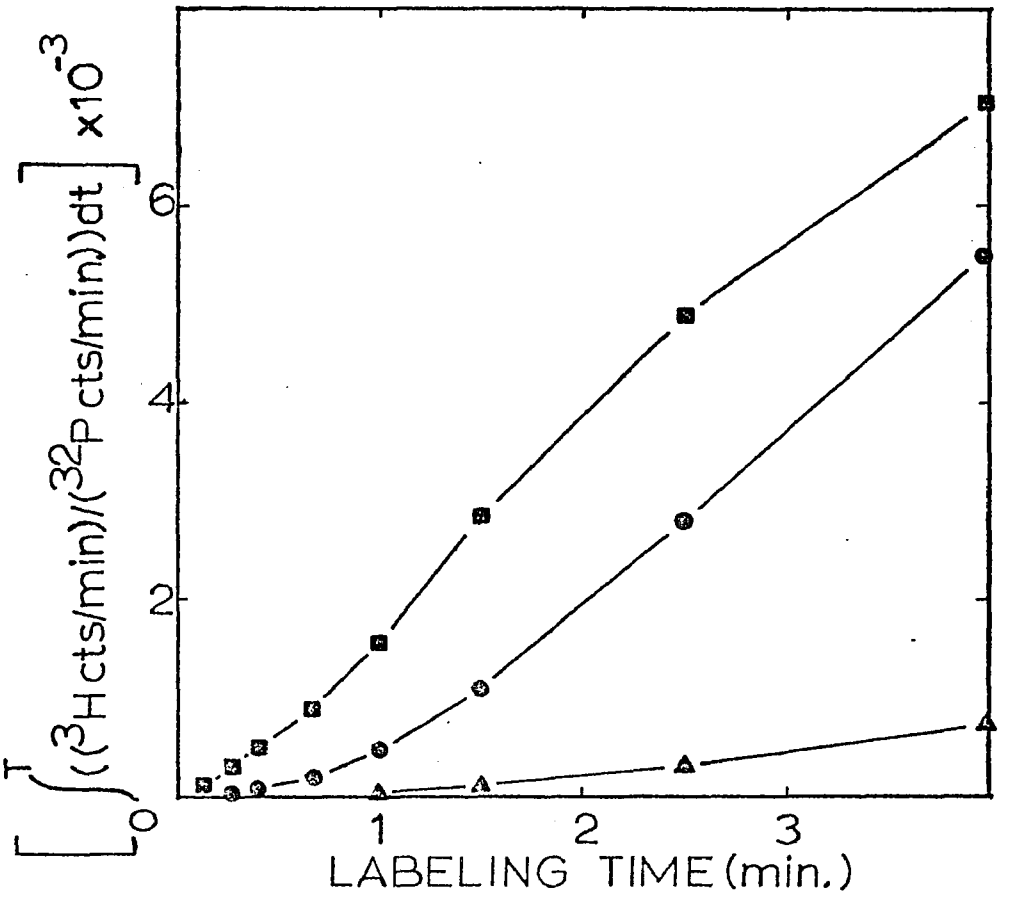

Figure 27. The Time Course of the Integral of the Specific Activities of Total RNA, Unstable RNA, and RNA Precursor

Specific activity values from the experiment of Figure 23 were graphically integrated over time. These integral values for total RNA (— ▲ —) and unstable RNA (— ● —) are plotted versus labeling time. Calculated integral values for RNA precursor (— ■ —) are also plotted versus labeling time.

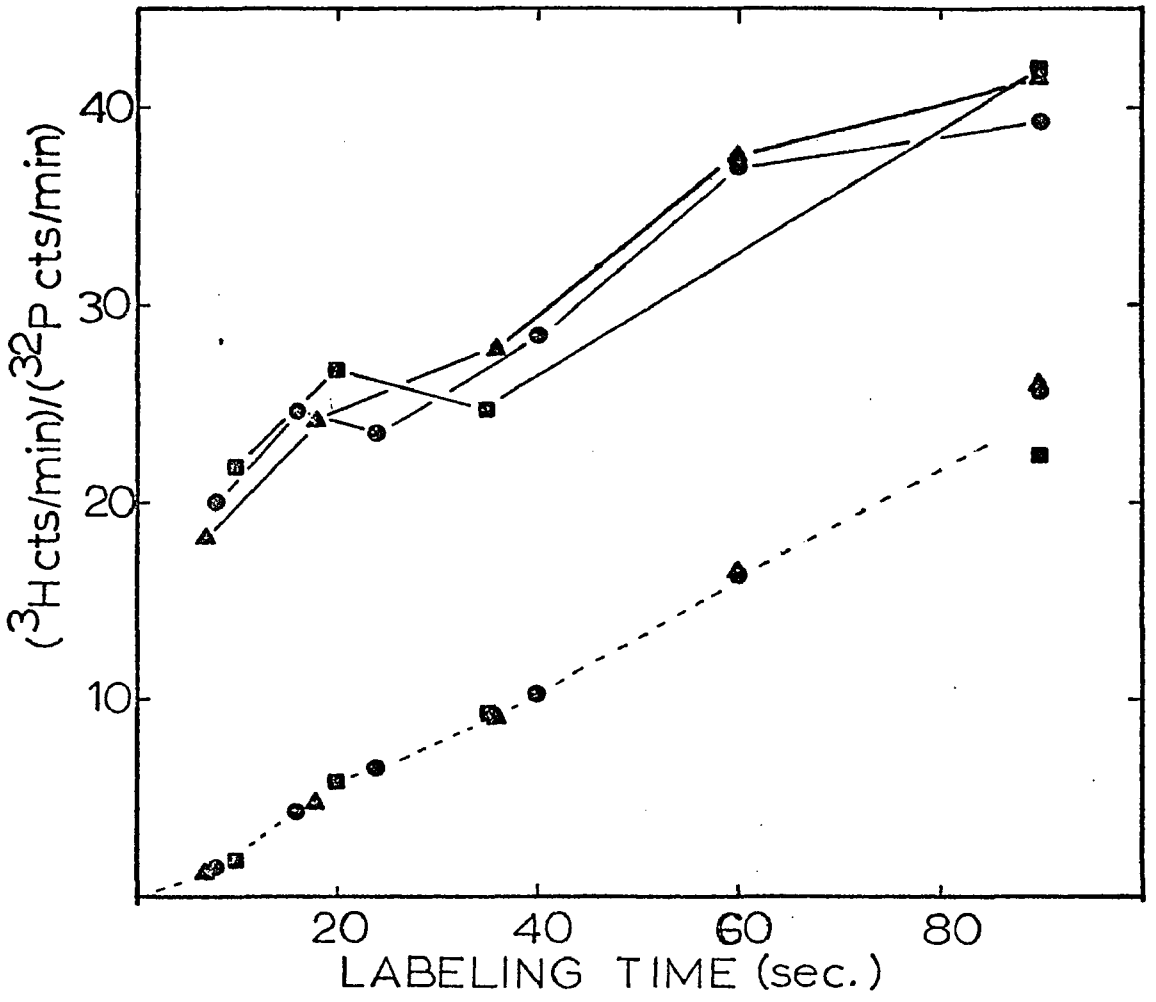

Figure 28. The Time Course of the Specific Activities of Unstable RNA and RNA Precursor in Three Experiments

The specific activities of the unstable RNA fraction (---) from the experiments of Figure 22 (--- ▲ ---), Figure 23 (--- ● ---), and an identical experiment (--- ■ ---) were plotted versus labeling time. The respective RNA precursor specific activities (——) were calculated as in Figure 26.

In one experiment (▲) the culture was pregrown in unlabeled uracil before [^{3}H] uracil labeling, whereas in the other two experiments (●, ■) the cultures were not pregrown in uracil.

there is an exceedingly rapid rise in calculated precursor specific activity during the first 7 to 10 seconds followed by a substantially reduced rate of rise up to about 20 seconds. Between 20 and 35 seconds after labeling, the precursor specific activity rises more slowly or even decreases to a small extent. At about 30 seconds after labeling, the precursor resumes its earlier rate of labeling. It should be noted that the two experiments in which the calculated precursor specific activity showed a decrease between 20 and 35 seconds were ones entailing no pregrowth in unlabeled uracil and hence no pre-expansion of the precursor pools. The one experiment depicted in which the culture was pregrown in uracil may or may not dip in this time period; an additional sample at 25 seconds would have clarified this point.

Figure 29 shows a plot of the calculated precursor specific activity in an experiment entailing pregrowth in unlabeled uracil. Also depicted are the results from three other experiments in which UTP specific activity was measured directly. The cultures used in these three experiments were also pregrown in unlabeled uracil. The data from one of these UTP specific activity experiments were kindly supplied by Karl Mueller (written communication, 1971). These data have been published previously as part of Figure 5 of the paper by Mueller and Bremer (1968). The experiment from which the precursor specific activity was calculated involved a culture growing with a doubling time of 34 minutes, whereas the three experiments in which precursor (UTP) specific activities were measured directly involved cultures growing with doubling times of 44 and 46 minutes. Because of this discrepancy in growth rates, I have plotted the specific activity values versus fraction of a generation time

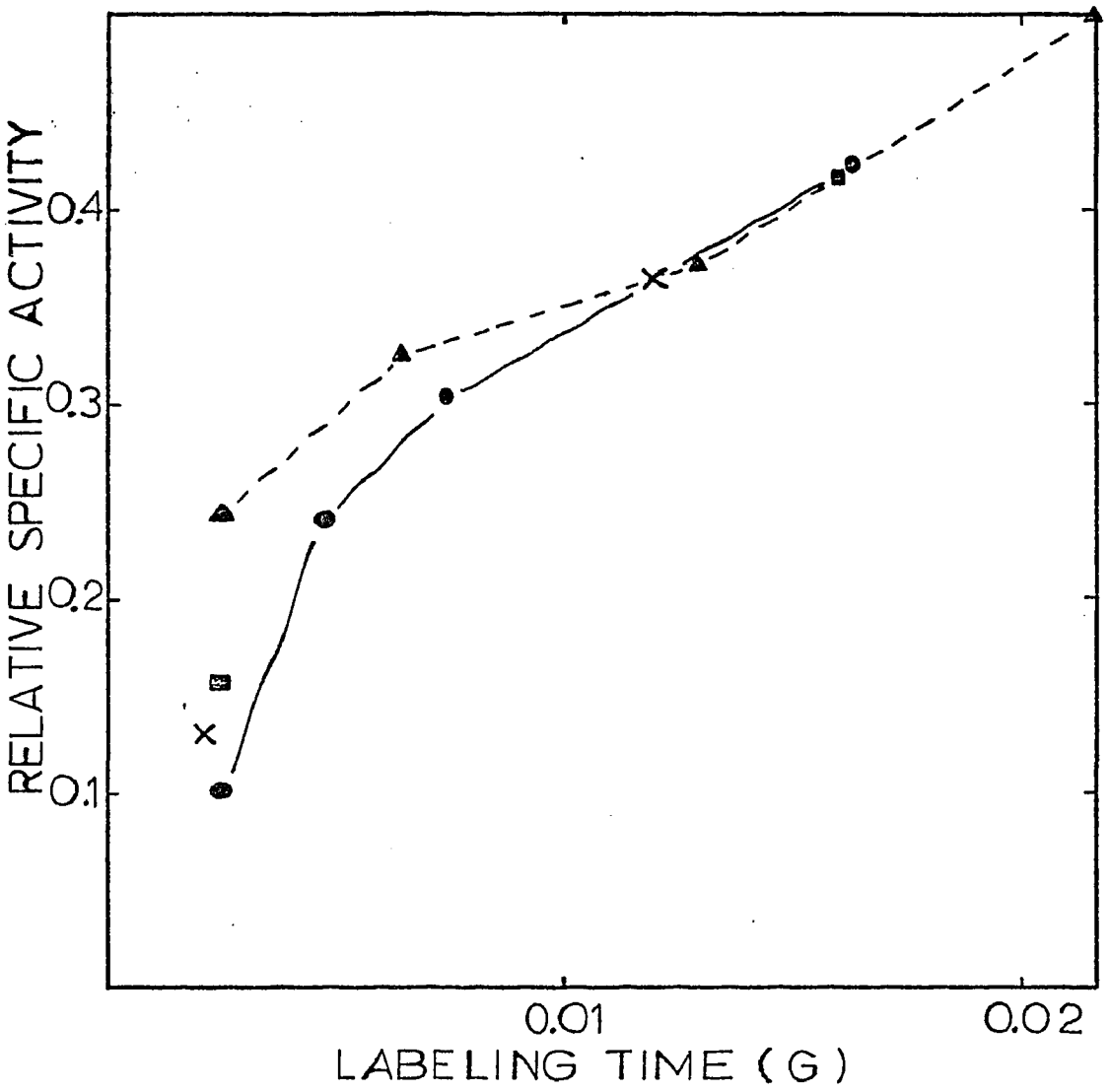

Figure 29. Comparison of the Time Course of the Calculated and Measured RNA Precursor Specific Activities

Specific activity values of the unstable RNA pool in the experiment of Figure 22 were used to calculate the time course of the specific activity of RNA precursor (--- ▲ ---). Measured UTP specific activities from the experiment of Figure 11 (— X —) and of an identical experiment (— ■ —) and of a similar experiment performed by Mueller and Bremer (1968) (— ● —) are plotted versus labeling time.

rather than versus seconds. The results from the three experiments entailing direct measurement of precursor specific activities were normalized to the calculated precursor specific activity function between 0.011 and 0.022 of a generation time (between 33 and 60 seconds in a culture doubling every 34 minutes). I believe that this normalization is valid because when Mueller and Bremer (1968, Figure 7a) calculated the gross synthesis function, the error introduced by precursor compartmentation appeared to be significant only during the first 20 to 30 seconds after labeling. This corresponds to less than 0.01 of a generation time.

This composite figure indicates that the measured precursor activity is only about half of the calculated precursor specific activity at the earliest sampling time (0.0025 generations) and the two functions converge at about 0.011 generations. This time of convergence corresponds to 30 seconds for a culture doubling every 34 minutes and to 40 seconds for a culture doubling every 45 minutes.

CHAPTER VI

DISCUSSION

Precursor Compartmentation

Presence of Precursor Compartmentation

Mueller and Bremer (1968) found, and my results confirm (see Figure 11), that UTP labels faster than UMP after the first 10 seconds of labeling with uracil. This finding constitutes evidence that the UMP and probably the UDP pools are compartmentalized. Such being the case, it is also likely that the UTP pool is compartmentalized.

McCarthy and Britten (1962), Buchwald and Britten (1963), and recently Koch (1971a) have asserted that the lag in incorporation of label into RNA is somewhat shorter than would be expected considering the size of the precursor pool. Such a phenomenon is characteristic of a system in which the precursor is compartmentalized into a main precursor pool and a bypass precursor pool.

Mueller and Bremer (1968) found that the calculated gross synthesis rate of RNA drops precipitously during the first few seconds after labeling. This indication of a component with an unreasonably high turnover rate is a classical manifestation of precursor compartmentation. (See Garfinkel and Heinmets, 1969, for a discussion of the possible ways in which compartmentation may manifest itself.) This rapid drop in the gross synthesis rate of RNA is not seen when calculated from the CTP pool and the CMP residues of RNA, nor is it seen when one uses a labeling function--the proportional synthesis function (see Figures 22 and 23)--which is relatively unaffected by fluctuations in precursor specific activity (see Figure 21).

I find that the experimentally measured precursor specific activity is at early times after labeling substantially lower than the precursor specific activity calculated from the rate of labeling of the unstable RNA pool (see Figure 29).

I believe that the above arguments constitute proof that in E. coli cells labeled with uracil the RNA precursor, UTP, is compartmentalized with respect to label at early times after labeling.

Type of Precursor Compartmentation

I originally defined the two types of precursor compartmentation in such a manner that they were mutually exclusive and exhaustive alternatives, i.e., both stable RNA and unstable RNA must be either synthesized from the same precursor compartment or, alternatively, they must be synthesized from different compartments. The results from my experimental measurements of the proportional synthesis function (Figs. 22 and 23) clearly exclude any significant amount of Type II precursor compartmentation (compare with Figs. 15, 18, and 19).

Since in the previous section I have presented evidence indicating precursor compartmentation and since Type II compartmentation has been ruled out, the compartmentation must therefore be Type I. I cannot say with certainty that the variation of Type I compartmentation used in the computer simulation studies is the correct one, but the statements and conclusions regarding this precursor compartmentation are unaffected by variations within the type--they only depend on the fundamental characteristic of the type, i.e., that both classes of RNA are synthesized from the same precursor pool.

It is interesting to note that while the UTP pools have equilibrated by about 0.011 generations, the UMP pool and probably the UDP pool remain significantly compartmentalized for about 0.3 generations

(Fig. 11, and Mueller and Bremer, 1968). This may mean that the UTP compartments can mix relatively rapidly, while the UMP and UDP compartments are prevented from intermixing by some physical barrier, such as the cell membrane which separates the periplasmic space from the cytoplasm or possibly a mesosomal membrane. The very restricted mixing could be explained if the exogenous uracil is taken up and remains bound to some structure during reaction with phosphoribosylpyrophosphate and the subsequent addition of the β and γ phosphates.

Degree of Precursor Compartmentation

Figure 29 shows the experimentally measured specific activity of the total cellular UTP and the calculated specific activity of the UTP compartment feeding unstable RNA synthesis. (Since the precursor compartmentation is of Type I, this UTP compartment feeding unstable RNA also feeds stable RNA synthesis.) In a system in which precursors are compartmentalized, this calculated precursor specific activity function is the desired one since the directly measured specific activity function is a combined measure of both the compartment feeding RNA synthesis and the compartment not feeding RNA synthesis. The difference between these two precursor specific activity functions is greatest at very early labeling times. At 9 seconds (for a culture doubling every 45 minutes), the measured specific activity has a value of only about 40% to 60% that of the calculated value. By 0.011 of a generation time, the two functions have converged. As mentioned earlier, this convergence time is about 40 seconds for a culture doubling every 45 minutes. There is an even greater discrepancy in the integrals of these functions. For example, by the time the two precursor specific activity functions converge, the integral of the experimentally measured function is still only about 80% of the integral of the calculated function.

Effects of Precursor Compartmentation

Since I have found that the precursor compartmentation in E. coli is Type I rather than Type II, this compartmentation phenomenon will not introduce error into those labeling schemes involving fractionation of RNA into its component classes or species followed by a comparison of the amount of label incorporated into each fraction. Type I precursor compartmentation will, however, introduce error into those experiments centered around the relationship between precursor and product.

Experiments which require a measurement of the specific activity or total activity (Salser et al., 1968; Mueller and Bremer, 1968; Pato and Meyenburg, 1970; Winslow and Lazzarini, 1969) of the precursor will be in error since the desired precursor compartment mixes with the total cellular precursor during the extraction process and thereby becomes inaccessible to direct measurement. Furthermore, the discrepancy between the desired precursor activity value and the measured precursor activity value will be greatest during the most critical period of the experiment.

Those experimental methods which rely on a measure of the precursor pool size (Salser et al., 1968; McCarthy and Britten, 1962; Koch, 1971a) are also adversely affected by precursor compartmentation since the precursor pool feeding RNA synthesis is substantially smaller than the total precursor pool. The labeling kinetics of this desired precursor fraction will be exceedingly complex because of rapid mixing with the remaining cellular precursor.

Two labeling procedures which rely on the precursor-product relationship but which are not affected by the compartmentation discussed herein are an ^{18}O labeling scheme devised by Chaney and Boyer (1972) and a labeling scheme used by Nazar and Wong (1972). Both of these schemes rely on relatively long-term labeling and therefore any compartmentation effect during the first 1% of a generation time would have an insignificant effect on the results.

In summary, in RNA labeling experiments with E. coli which utilize either precursor activity or pool size measurements one should not rely on experimental measurements of samples taken during the first 0.011 of a generation time after labeling. In cases where the integral of the precursor specific activity is calculated from measurements of the precursor specific activity, the value of the integral should not be relied upon for 0.02 of a generation time after labeling.

Mode of Decay of Unstable RNA

The discovery of RNase V and its ribosomal translocation-linked activity (Kuwano et al., 1969) lent credence to the widely held belief that decay of most, if not all, unstable RNA species proceeds from the 5' to the 3' end of the molecule. Since RNA synthesis also proceeds from the 5' to the 3' end, it is likely that the predominant order of decay is the same as the order of synthesis.

If a nucleotide at the 5' end of a molecule must be removed before its 3' neighbor can be cleaved, the loss of labeled nucleotides from that molecule will be described by the linear decay kinetics discussed in Chapter II. Since it is likely that each unstable RNA chain

is decaying with linear kinetics, it would seem reasonable to expect an experimental determination of the gross synthesis function to resemble one of the simulation plots shown in Figure 14b and an experimental determination of the proportional synthesis function to resemble one of the simulation plots shown in Figure 15b. Mueller and Bremer (1968) have experimentally measured a function which is in essence the gross synthesis function (Fig. 7a of their paper). Their plot clearly resembles one of the simulated exponential decay plots shown in Figure 14a and does not resemble any of the simulated linear decay plots shown in Figure 14b. Likewise, my experimental determinations of the proportional synthesis function (Figs. 22 and 23) clearly show exponential rather than linear decay kinetics (compare Figs. 15a and 15b).

If one presumes that RNase V is the agent responsible for the decay of the unstable RNA fraction and that this decay proceeds in the manner envisioned by Kuwano et al. (1969), then the decay of the unstable RNA fraction can be divided into two kinetically distinct processes. One process is the initiation of decay at the 5' end of a chain. The other process is the actual decay proceeding toward the 3' end of the chain. That process which is rate limiting (slowest) is the one whose kinetics will be seen experimentally. Therefore, I believe, in light of my results and the results of numerous other workers who have found exponential decay of the unstable RNA fraction, that the rate limiting step in the decay of unstable RNA is the initiation of decay. Furthermore, essentially every intact 5' terminus of the unstable RNA fraction must have an equal chance (weighted for its stability) for the

initiation of decay during any time interval. Only such a random jeopardy phenomenon can give the exponential decay kinetics seen.

Scope and Limitations of the Experimental Techniques

Necessity of Assaying Component Nucleotides Rather Than Intact RNA

[5-^{3}H] Uracil labels both the UMP residues and the CMP residues of RNA. Bolton and McCarthy (1962) and Mueller and Bremer (1968) have shown that in cells labeled with uracil the ratio of label entering RNA as UMP to that entering RNA as CMP varies radically in the first few minutes after labeling. Furthermore, the distribution of labeled UTP to labeled CTP in that fraction of the precursors which is being used for RNA synthesis is indeterminable by direct measurement due to the precursor compartmentation. The stable RNA fraction, and in particular the 4 S subfraction, has a UMP to CMP ratio substantially different from the UMP to CMP ratio of the unstable RNA fraction, UMP/CMP of 4 S stable RNA = 0.77; UMP/CMP of unstable RNA = 0.95 (Cox, 1968). In light of this unknown ratio of label entering RNA as UMP to label entering RNA as CMP, one cannot correct the experimental data for variations in base ratio among the RNA fractions. Separation of the various RNA fractions into their component nucleotides followed by assessment of the specific activities of either the UMP or the CMP residues removes this unknown factor from the system.

Applicability of the Isotope Ratio Method

If one wishes to measure the relative amounts of labeled precursor incorporated into the various components of a biological system, it is necessary to measure the final recovery efficiencies very carefully. If any hybridization procedures are involved, the efficiencies of hybridization must be accurately determined. The specific activity of a component is independent of both recovery efficiency and hybridization efficiency. However, in measuring the specific activity, a new set of problems is encountered. Specific activity is defined as labeled material/total material. If the total material is to be measured by optical methods, it must be both quite pure and in reasonably large quantity. In the case of the unstable RNA fraction, it would be necessary to run a rather large-scle experiment in order to have an accurately measurable quantity for the specific activity assay.

When an exponentially growing culture is labeled for eight doublings, all components will have a relative specific activity of 0.996 or greater. In this situation there is essentially a one-to-one rleationship between the amount of material and the amount of label in every labeled component. Now, if a second label is introduced, the ratio, short-term label/long-term label, is directly proportional to the ratio, short-term label/total material, i.e., specific activity.

Two conditions must be satisfied if this proportionality is to hold. First, the short-term label must neither change the rate of uptake of the long-term label nor in any way displace the normal utilization of the long-term label. Second, both labels must enter the component whose specific activity is to be measured. For RNA labeling $H_3{}^{32}PO_4$

is a most satisfactory long-term label and [5-^{3}H]uracil performs well as a short-term label. This combination satisfies the conditions discussed above and has an added advantage in that these two isotopes have widely differing β energies and hence are easily resolved in a multichannel scintillation counter.

In conclusion, the problems of variable recovery efficiency and variable hybridization efficiency can be reduced by utilization of an apprropriate double-labeling scheme to the much simpler problem of dual isotope counting.

Theoretical Considerations Concerning the Proportional Synthesis Function

The relationship given in equation (15) can be used to determine the relative pool size of the unstable RNA fraction if the following criteria are met:

1. If there is heterogeneity in the decay rates of the various unstable RNA species, as indicated by the work of Salser (1966) and more recently by Blundell and Wild (1971), then each stability class (includes all of those species having the same decay constant) must be represented in the unstable RNA specific activity assay in proportion to its in vivo concentration.
2. If that fraction of RNA remaining after 60 minutes incubation in the presence of rifampicin (stable RNA fraction) does indeed have a slow but significant turnover for some or all of its component species, as suggested by Norris and Koch (1972), then each stability class of this "stable" fraction must be

represented in the specific activity assay in proportion to its *in vivo* concentration.

3. No species should be represented in both the unstable RNA and the stable RNA specific activity assays.

If a valid unstable RNA pool size can be determined, then the relationship given in equation (12) can be used to determine the relative rate of synthesis of the unstable RNA fraction if the following conditions are met:

1. The RNA precursors must be either noncompartmentalized or compartmentalized in a Type I fashion. Type II precursor compartmentation must not be present to any significant extent.
2. Each stability class of the unstable RNA fraction must be represented in the specific activity assay in proportion to its *in vivo* concentration.

Preparation of the Unstable RNA Fraction

When the entire cellular complement of DNA is used in an RNA-DNA hybridization procedure, RNA is fractionated on the basis of the number of RNA chains per complementary DNA sequence. As a general rule, stable RNA species will be abundant relative to their complementary DNA sequences, while unstable RNA species will be rare relative to their complementary DNA sequences. Fractionation of the RNA occurs when a limited amount of DNA is incubated with excess RNA. Under these conditions, rare species will have an excess of complementary DNA sequences available for hybridization and hence most rare copies of RNA will hybridize. In contrast, abundant species will be in great excess

over their available complementary DNA sequences and therefore only a small percentage will hybridize.

The rule that stable RNA species will be abundant and unstable RNA species will be rare is based on the premise that gene transcription frequencies are reasonably similar for all species. It is conceivable that a gene for an unstable RNA species might be transcribed at an unusually high frequency. During hybridization this unstable RNA species would saturate its complementary DNA sequences and the excess non-hybridized chains would be classed as stable RNA. Kennell (1968) has estimated that as little as 10% of the E. coli genome codes for approximately 70% of the unstable RNA, while 20% codes for about 99.85% of the unstable RNA. This indicates a rather wide range in gene transcription frequencies.

A second problem may arise as a result of rarely transcribed stable species. Such species would, because of their limited abundance, be classed as unstable in a fractionation based on hybridization. It seems reasonable to belive that there are stable messengers which code for constitutive protein synthesis or which are controlled at the level of translation. Stable species of RNA (not ribosomal or transfer) have been found in phage-infected bacteria (Summers, 1970b; Adesnik and Levinthal, 1970). In mammals, the messenger RNA coding for hemoglobin is stable for several days.

Data on protein synthesis in rifampicin-treated cultures has been presented by Schwartz et al. (1970) and Blundell and Wild (1971). These workers interpret their data as evidence that essentially all template RNA is unstable with a maximum half-life of about 8 minutes. It

should be noted that these experiments actually measure net rather than total protein synthesis. Numerous workers have shown that there is a significant amount of protein turnover in E. coli (Willetts, 1967; Pine, 1966; Mandelstam, 1963). Under the conditions resulting from rifampicin treatment there could be a significant amount of protein synthesis continuing from stable messenger species, but such synthesis would go undetected because amino acids from protein decay would be used in preference to exogenous labeled amino acids.

In summary, the problem one must solve is how to get a representative sample of the unstable RNA fraction while avoiding contamination of this fraction with any RNA from the stable fraction.

Three factors must be adequately dealt with if an unstable RNA fraction prepared by a hybridization procedure is to meet the criteria discussed in a previous section. First, when RNA is hybridized to DNA which has been bound to a nitrocellulose filter, some RNA binds nonspecifically to the filter. Since most RNA is of the stable type, most of this nonspecifically bound RNA is likely to be of the stable type and hence must be corrected for. This factor was handled by hybridizing in the presence of both a DNA filter and a blank filter. If the amount of nonspecifically bound RNA was the same on both filters, then subtraction of the blank filter counts from the DNA filter counts should have effectively cancelled the error introduced by the nonspecifically bound RNA.

The second factor is the necessity of insuring proportional representation of each stability class of the unstable RNA fraction. This can probably be accomplished by providing enough DNA so that no gene

site for any unstable RNA species is saturated by the amount of RNA presented for hybridization. Kennell (1968) has shown that an RNA to DNA ratio of about 0.5 fulfills this requirement for E. coli B under normal growth conditions. Mueller and Bremer (1968) have found that under their growth conditions, 10^9 cells ($O.D._{550}$ = 1.35) contain 380 nmoles of RNA. From these data I calculate that the RNA to DNA ratio in my hybridization preparations was about 0.5. I am assuming here that if sufficient DNA is present for hybridization, then all stability classes will hybridize with the same efficiency. This may not be true. It is possible that if there are differing degrees of stability in the unstable RNA fraction, this stability may be achieved by means of a secondary structure based on self-complementarity. Labowitz, Weissman, and Radding (1971) have determined the sequence of a 6 S RNA chain synthesized in vitro from λ phage DNA. Judging from the sequence of this RNA chain, which is presumably at least in part messenger RNA, it appears to have extensive regions of base pairing between terminal and internal sequences. It is quite possible that there is a direct correlation between amount of base repairing and resistance to degradation. If intramolecular or intermolecular hybrid formation by unstable RNA species prevents their hybridization to DNA, then it is conceivable that there is an inverse relationship between hybridization efficiency and half-life. If this were the case, then the more stable classes of unstable RNA would be underrepresented in the specific activity assay in spite of the precautions taken for their proportional representation in the hybridization procedure.

The third problem which arises in using hybridization procedures for preparing the unstable RNA fraction involves the prevention of hybridization of stable RNA to its gene sites. Kennell (1968) has shown that at an RNA to DNA ratio of 0.5, approximately 20% of hybridized E. coli RNA is of the stable type. In a pulse labeled RNA preparation, the amount of label in this 20% is negligible since stable RNA has such a low specific activity (about 2% of that of the unstable RNA fraction). On the other hand, with respect to a long-term label, this hybridized stable RNA fraction introduces a very serious error into the specific activity assay. Kennell (1968) has calculated that all of the stable RNA species saturate their gene sites at an RNA to DNA ratio of about 1/160. I have avoided contamination of the unstable RNA fraction with stable RNA by prehybridizing the DNA with a 125-fold excess of unlabeled stable RNA (50 μg stable RNA with 65 μg DNA).

Preparation of the Stable RNA Fraction

Norris and Koch (1972) have presented evidence which seems to indicate that all classes of RNA in the stable fraction are reasonably stable in cultures doubling in less than an hour. They also conclude that some or all classes of the stable RNA fraction may have a significant amount of turnover at much slower growth rates (5 hours or longer). It should be noted that these workers are limiting growth rates by partial glucose starvation and so their purported instability in the stable RNA fraction at slow growth rates may be an artifact of their growth conditions. Strange, Dark, and Ness (1961) have shown that RNA species which are stable under normal growth conditions are degraded during starvation of bacterial cultures.

In light of the above, I believe it is safe to assume essentially no decay of the stable species in cultures doubling every 34 minutes. If this is true, then the specific activity of the 4 S stable RNA peak can be taken as representative of the total stable RNA fraction.

An important requirement in the preparation of a stable RNA fraction by treatment with rifampicin is that synthesis of that fraction must be terminated very soon after rifampicin treatment. Pato and Meyenburg (1970) have estimated that the synthesis of 4 S RNA continues for 5 to 10 seconds after rifampicin has stopped new initiations. Their estimation of the lag in cessation of RNA syntheis is based on an assay of both the amount of label in the 4 S RNA peak and the specific activities of the UTP and CTP pools. Because of Type I precursor compartmentation, this estimated 5- to 10-second lag is probably twofold to threefold overestimated. A more accurate estimate of the time from initiation to termination of 4 S RNA synthesis is probably 2 to 5 seconds. If samples labeled for 30 seconds or longer are used for the unstable RNA pool size determination, the error introduced should be within acceptable limits. If a serious error was introduced by continued synthesis of the 4 S fraction after rifampicin treatment, the slope of the line in Figure 25 should be positive. This does not appear to be the case and, thus, I believe it is safe to assume that any error due to continued synthesis is negligible.

If rifampicin prevented the processing steps which lead to stabilization of 4 S RNA, then newly synthesized 4 S could decay during the subsequent incubation in the presence of rifampicin and thereby severely perturb the specific activity assay. Two lines of evidence run counter

to this argument. First, Blundell and Wild (1971) has shown that newly synthesized stable RNA species appear to be stable when incubated with rifampicin. Secondly, the slope of the line in Figure 25 should be negative if newly synthesized 4 S RNA decayed when incubated in the presence of rifampicin. This does not appear to be the case, and so the new 4 S RNA is probably processed normally and thus remains stable for the duration of the incubation period.

Generalizations Concerning the Specific Activity Ratios Method for Determining Relative Pool Sizes and Synthesis Rates

The most serious potential problem in my method for determining the kinetic parameters of RNA metabolism is the possibility of getting nonrepresentative samples with respect to their specific activities. Fortunately, such nonrepresentative samples would manifest themselves as a time-dependent change in the calculated value of the PSun, such a phenomenon is not seen in my experimental data (Fig. 25).

The zero time intercept value of the proportional synthesis function (SAun/SAtot) is rather insensitive to any error introduced by the assumption of homogeneity in the half-lives of the unstable species. This is also the case for the zero time intercept value of the gross synthesis function (ΔSAtot/SApre) but unlike the proportional synthesis function the gross synthesis function (as well as those other methods based upon the precursor-product relationship) is seriously perturbed by Type I precursor compartmentation. Furthermore, with respect to the gross synthesis function, if an unexpected component with a high synthesis rate and very fast turnover is indicated, there is no simple way

to determine if this is a real component or an artifact caused by precursor compartmentation.

The specific activity ratios method detailed in this paper would be classified with those methods in which labeled RNA is fractionated into its component classes or species followed by assessment of the label in each fraction. The method shares with the other methods of this type the advantage of not requiring a measurement of the specific activity of the immediate precursor to RNA. In fact, methods of this type do not even require a knowledge of the identity of this precursor. My method also avoids (as do most other methods involving hybridization) the unknown effects on metabolism which plague studies based upon inhibition of RNA synthesis.

When RNA is hybridized to a great excess of DNA such that there are more copies of each DNA sequence than there are of complementary RNA copies, then one would expect that all copies of the RNA would hybridize. Such is not the case. Under optimal conditions and in the presence of an excess of DNA sequences per RNA copy for every species the maximum amount of RNA which binds to DNA-nitrocellulose filters seldom exceeds 80%. Furthermore, of that 80% bound only about 8/10 of it appears to be in the form of true hybrid. The remaining material can be removed by treatment with pancreatic RNase, a nuclease which will not attack RNA complexed to its complementary single-stranded DNA. It is very difficult to determine the stability characteristics of either the bound but RNase-sensitive RNA or the unbound RNA. If either the nonbound fraction of RNA or the bound but RNase-sensitive fraction of RNA is not representative of total RNA, then serious bias

would be introduced into those hybridization-based methods which rely on measurements of the proportion of label hybridized. On the other hand, the specific activity value of the hybridized fraction is, in contrast to the proportion of the label hybridized, independent of the efficiency of hybridization.

A serious problem in many methods for determining the pool size of the unstable RNA fraction is that they require subtraction of a very small number from a very large number (Zimmerman and Levinthal, 1967; Kennell, 1968; Midgley, 1969; Norris and Koch, 1972). Generally, the uncertainty in the large number is of the same order of magnitude as the total value of the small number. Because of this problem, the uncertainty of the pool size determination is rather great. In my experimental procedure this problem is substantially reduced because the specific activities of the various pools differ from one another (during the time periods in which the measurements were made) far less than do the sizes of the various pools.

Other Systems Where Precursor Compartmentation May Play a Role

Werner (1971a) has presented evidence which indicates that in a thymine auxotroph of E. coli, thymine and thymidine do not compete as precursors for DNA synthesis. Furthermore, he has shown that the labeling rate of TTP derived from thymidine correlates with the labeling rate of DNA, whereas the labeling rate of TTP derived from thymine does not correlate with the labeling rate of DNA. Werner (1971b) has also shown that there is a TCA-insoluble slowly sedimenting (about 4 S) component which is labeled by thymine but not by thymidine.

Billen et al. (1971) have shown that in freeze-treated B. subtilis, exogenously added TTP feeds "repair"-type DNA synthesis, while thymidine feeds DNA replication (semiconservative synthesis).

I believe that all of the above findings are compatible with a system having Type II precursor compartmentation. In this system, I propose that thymine (or TTP in the case of freeze-treated cells) is used for the synthesis of metabolically unstable DNA ("repair" synthesis), while thymidine is preferentially used for DNA replication. It is quite possible that this "repair"-type synthesis is involved in some manner with RNA transcription because rifampicin treatment has a dramatic effect on this "repair" synthesis (R. Sternglanz, personal communication, 1972) but not on replication synthesis (Sugino, Hirose, and Okazaki, 1972). I would also like to suggest that DNA replication occurs in a mesosomal structure (Ryter, 1968) and that exogenously added thymidine has facilitated access to this compartment. On the other hand, DNA "repair"-type synthesis occurs either in the cytoplasm or, as proposed by Billen et al. (1971), in the periplasmic space and may involve resynthesis of a short (4 S) single strand of DNA at the promotor site of each transcripton. I propose this because one strand of the DNA double helix at the operator size may be degraded to allow binding of the RNA polymerase and/or to allow unwinding of the transcripton during transcription. There is some evidence that this "repair"-type synthesis comprises a very substantial portion of the total DNA synthesis rate but only a small portion of the net DNA synthesis rate, possibly because the "repaired" sequences are rapidly turning over. I base the above

statements on the fact that the 4 S DNA component described by Werner (1971b) and further characterized by Sternglanz (personal communication, 1972) does not appear to chase into any other class of DNA.

Most eucaryotic cells probably have compartmentalized precursors because of their organization into membrane-limited organelles. Plagemann (1972) has presented evidence for separate nucleotide pools for nuclear and cytoplasmic RNA synthesis in mammalian cells growing in suspension culture. He has shown that exogenously added precursor appears to enter the nuclear pool directly without first mixing with the cyrtoplasmic pool.

In conclusion, if one wishes to measure the kinetic parameters of some cellular component, one should first test for precursor compartmentation. If compartmentation is found, it must be characterized, and then experiments must be designed which will avoid or minimize the uncertainties introduced by this compartmentation.

CHAPTER VII

SUMMARY

I have developed a nucleotide extraction and fractionation technique in which the nucleotide-containing sample is maintained throughout at neutral pH and between 0°C and 4°C. Using this technique, I have verified the results of Mueller and Bremer (1968) in which they find that after 10 seconds of labeling with [^{3}H]uracil the UTP pool has a higher specific activity than the UMP pool.

A series of computer simulation models of RNA metabolism were used as an aid in designing experiments which could differentiate between compartmentalized and noncompartmentalized precursors and which could characterize any compartmentation indicated. One model was based on a noncompartmentalized model. A second model assumed precursor compartmentalized in such a manner that both stable and unstable classes of RNA were synthesized from the same precursor compartment. A third model involved stable RNA synthesized from one precursor compartment and unstable RNA synthesized from a different compartment. With the aid of the output from these computer simulations, I have settled upon two labeling functions for detecting and characterizing RNA precursor compartmentation. One function, the gross synthesis function, can be used to differentiate between systems having and systems lacking compartmentation of their precursor. The other function, the proportional synthesis function, can be used to characterize any precursor compartmentation detected by the first function.

Experimental measurement of the proportional synthesis function in E. coli B indicated that both classes of RNA (stable and unstable) are synthesized from precursors of equivalent specific activities.

After characterizing the precursor compartmentation present in uracil-labeled E. coli, a method was developed for measuring the relative pool size and the relative rate of synthesis of the unstable RNA fraction in the presence of this previously characterized type of precursor compartmentation. This new method relies heavily on a precise measurement of the specific activity of the stable RNA fraction. A new technique for making this measurement is covered in detail. The size of the unstable RNA fraction was found to be 4.1% of the total RNA pool, and its rate of synthesis was 56% of the total RNA synthesis rate.

Finally, equations were developed for determining the specific activity of that portion of the precursor pool which is being incorporated into RNA. Using these equations and my earlier experimental results, I find that precursor compartmentation is only significant during the first 0.01 of a generation time after labeling. Such compartmentation can introduce significant error into the results from experiments which rely on measurements of samples taken during this first 1% of a generation time.

The method presented for measuring the pool size and rate of synthesis of the unstable RNA fraction is essentially independent of both DNA-RNA hybridization efficiencies and of precursor compartmentation. Since low hybridization efficiencies and the presence of precursor compartmentation have been major obstacles in measuring RNA pool sizes and synthesis rates in eucaryotic organisms, I suggest that this new

method will be of significant value in experimental measurements of eucaryotic organisms.

APPENDIX A

DERIVATION OF KINETIC EQUATIONS USED IN THE COMPUTER SIMULATIONS

Derivation of Equation (2)

Using the format of equation (1), the change in specific activity of pool B over the time interval T to $T + \Delta T$ is:

$$\Delta SAB = \frac{\int_0^{T+\Delta T} e^{t/G}(RAB \cdot SAA_t - RBC \cdot SAB_t)\, dt}{PSB\, e^{(T+\Delta T)/G}}$$

$$- \frac{\int_0^{T} e^{t/G}(RAB \cdot SAA_t - RBC \cdot SAB_t)\, dt}{PSB\, e^{T/G}} . \tag{30}$$

If we let $X_t = e^{t/G}(RAB \cdot SAA_t - RBC \cdot SAB_t)$, (31)

then

$$\Delta SAB = \frac{\int_0^{T+\Delta T} X_t\, dt}{PSB\, e^{(T+\Delta T)/G}} - \frac{\int_0^{T} X_t\, dt}{PSB\, e^{T/G}} . \tag{32}$$

Since

$$e^{(T+\Delta T)/G} = e^{T/G}\, e^{\Delta T/G} \tag{33}$$

and

$$\int_0^{T+\Delta T} X_t\, dt = \int_0^{T} X_t\, dt + \int_T^{T+\Delta T} X_t\, dt, \tag{34}$$

then

$$\Delta SAB = \frac{\int_0^{T} X_t\, dt}{PSB\, e^{T/G}\, e^{\Delta T/G}} - \frac{\int_0^{T} X_t\, dt}{PSB\, e^{T/G}} + \frac{\int_T^{T+\Delta T} X_t\, dt}{PSB\, e^{(T+\Delta T)/G}} \tag{35}$$

and

$$\Delta SAB = \frac{\int_0^T X_t\,dt}{PSB\,e^{T/G}}(e^{-\Delta T/G} - 1) + \frac{\int_T^{T+\Delta T} X_t\,dt}{PSB\,e^{(T+\Delta T)/G}} . \tag{36}$$

Since

$$SAB_T = \frac{\int_0^T X_t\,dt}{PSB\,e^{T/G}}, \tag{37}$$

then

$$\Delta SAB = SAB_T(e^{-\Delta T/G} - 1) + \frac{\int_T^{T+\Delta T} X_t\,dt}{PSB\,e^{(T+\Delta T)/G}} . \tag{38}$$

When the time interval ΔT is constant and small, one can make the approximation:

$$SAA_{T+\Delta T} - SAA_T \cong SAA_T - SAA_{T-\Delta T} \tag{39}$$

and

$$SAB_{T+\Delta T} - SAB_T \cong SAB_T - SAB_{T-\Delta T} . \tag{40}$$

This says that the specific activities of pools A and B are changing at a nearly constant rate over $2\Delta T$. If this is true, then the terms SAA_t and SAB_t in the integral, $\int_T^{T+\Delta T} X_t\,dt$, can be considered constants with the values

$$SAA_t \cong SAA_T + \frac{SAA_T - SAA_{T-\Delta T}}{2} \tag{41}$$

and

$$SAB_t \cong SAB_T + \frac{SAB_T - SAB_{T-\Delta T}}{2} . \tag{42}$$

The integral can now take the form

$$\int_{T}^{T+\Delta T} X_t\,dt = \left[RAB\left(SAA_T + \frac{SAA_T - SAA_{T-\Delta T}}{2}\right)\right.$$

$$\left. - RBC\left(SAB_T + \frac{SAB_T - SAB_{T-\Delta T}}{2}\right)\right]\int_{T}^{T+\Delta T} e^{t/G}dt. \quad (42)$$

and by substituting, one can arrive at

$$\Delta SAB = SAB_T(e^{-\Delta T/G} - 1) + G(1 - e^{-\Delta T/G})$$

$$\left[\frac{RAB\left(SAA_T + 1/2\left(SAA_T - SAA_{T-\Delta T}\right)\right)}{PSB}\right.$$

$$\left. - \frac{RBC\left(SAB_T + 1/2\left(SAB_T - SAB_{T-\Delta T}\right)\right)}{PSB}\right]. \quad (2)$$

Derivation of Equation (6)

During growth, any pool can be defined by three rates: inflow, outflow, and accumulation. It is obvious that when the rate of flow out of a pool is subtracted from the rate of flow into it, one is left with the rate of accumulation. One can write:

$$Rinflow - Routflow = Raccumulation. \quad (43)$$

The generation time, G, is the time required to increase the mass of a culture e-fold. If a culture has a mass of x at some given time, then after a period of time, G, the mass will be xe and the amount of growth will have been $xe - x$, or $x(e - 1)$.

In a nonsynchronous steady-state exponentially growing culture, all cellular pools are growing at the same rate and hence any pool of pool size, PS, will, during one generation time, increase by the amount

PS(e - 1), and one can write:

$$PS(e - 1) = \int_0^G ((\text{Raccumulation}) e^{t/G})\, dt. \tag{44}$$

Integration gives:

$$PS(e - 1) = (\text{Raccumulation})\, G(e - 1),$$

or more simply:

$$\text{Raccumulation} = \frac{PS}{G}. \tag{45}$$

Equation (43) now becomes:

$$\text{Rinflow} = \frac{PS}{G} + \text{Routflow}. \tag{6}$$

Using this equation, it becomes a simple matter to calculate the synthesis rates of stable pools, such as ribosomal RNA and transfer RNA. Since stable pools have no outflow, one needs only to measure their pool size and the generation time of the culture. An additional parameter is needed (either inflow or outflow) to describe the kinetics of an unstable pool.

Derivation of Equations (7) and (8)

It is often difficult or impossible to measure directly the outflow from a pool. A parameter which is generally more amenable to measurement is the half-life of the pool. For an exponentially decaying pool (i.e., during any given time increment every molecule present in the pool has an equal chance of leaving that pool), the half-life, $T_{1/2}$, is defined as follows:

$$T_{1/2} = \frac{0.693}{\lambda} \tag{46}$$

where λ is the decay constant. The decay constant is related to the outflow rate in the following way:

$$\lambda = \frac{\text{Routflow}}{\text{PS}} \quad . \tag{47}$$

Combining equations (6), (46), and (47), one can write:

$$\text{Rinflow} = \text{PS}\left(\frac{1}{G} + \frac{0.693}{T_{1/2}}\right) \tag{48}$$

or

$$\text{PS} = \frac{(\text{Rinflow})\, T_{1/2}}{0.693 + \frac{T_{1/2}}{G}} \quad . \tag{7}$$

In the case of an unstable pool containing many species with heterogeneous half-lives, the half-life value in equations (48) and (7) must correspond to the mass average half-life value.

In a linearly decaying pool, every molecule has a set lifetime in the pool. In this situation, equation (46) is replaced by

$$\text{lifetime} = \frac{1.0}{\lambda} \quad , \tag{49}$$

and equation (48) is replaced by

$$\text{Rinflow} = \text{PS}\left(\frac{1}{G} + \frac{1.0}{\text{lifetime}}\right) . \tag{50}$$

Equation (7) is replaced by

$$\text{PS} = \frac{(\text{Rinflow})\,(\text{lifetime})}{1.0 + \frac{\text{lifetime}}{G}} \quad . \tag{8}$$

For the case of heterogenous lifetimes, the lifetime values used must correspond to the mass average lifetime.

Given that a culture is undergoing nonsynchronous steady-state exponential growth, then equation (6) holds irrespective of either the mode of decay of the pool or the presence or absence of heterogeneity in decay constants. On the other hand, when the relationships described by equations (7) and (8) are applied to the unstable RNA fraction, caution must be exercised. This is because heterogeneity in the half-lives of the species comprising this unstable RNA fraction has been indicated by Salser (1966).

APPENDIX B

EARLY EFFORTS TOWARD CHARACTERIZATION OF THE PRECURSOR COMPARTMENTATION IN E. COLI

In this appendix, I describe the early experiments in which I attempted to characterize the precursor compartmentation discovered by Mueller and Bremer (1968). In essence, I was looking for an experimental system which would clearly distinguish between Type I and Type II precursor compartmentation. As will be seen herein, these early experiments were rather nondecisive and produced apparently contradictory results. It was because of these problems that I developed the computer simulation programs. The hope was that the simulations would suggest some experiment or set of experiments which would give a definitive characterization of the precursor compartmentation in E. coli. These did indeed fulfill this hope (see Chapter V), and I am detailing these earlier experiments only for the sake of completeness.

My first experiments involved double labeling E. coli with [^{3}H]uracil and $H_3{}^{32}PO_4$ for 75 seconds. I then extracted polysomes and ribosomal subunits on the assumption that new messenger RNA (the unstable RNA fraction is probably mostly or all messenger RNA) would be in the polysomes and new ribosomal RNA (ribosomal RNA constitutes a majority of the stable RNA fraction) would be in the 30 S and 50 S regions. This latter assumption is based on the work of Nomura (1970) in which he found that newly synthesized ribosomal RNA does not enter polysomes

for approximately 5 minutes after synthesis. Presumably this amount of time is required for processing and packaging of the newly synthesized ribosomal RNA.

I measured the ratio, $^{3}H/^{32}P$, of both the polysome fraction and the ribosomal subunits fraction. Figure 30 shows a typical polysome profile, and Table 1 gives the results from four separate experiments.

Table 1. $^{3}H/^{32}P$ Ratios of Ribisomal Subunits and Polysomes

	$^{3}H/^{32}P$ Ratios				
				Ribosome/Polysome	
Experiment	30 S RNA + 50 S RNA	50 S RNA	Polysome RNA	Experimental	Theoretical
1	5.62		4.77	1.18	0.91
2	5.33		4.68	1.14	0.91
3		1.19	0.80	1.49	0.94
4		0.89	0.79	1.13	0.94

The rationale for this experiment is as follows. Endogenously synthesized RNA precursors should not be compartmentalized, whereas exogenously acquired precursors probably will be for at least the first minute or so. When cells are fed both $H_3{}^{32}PO_4$ and [^{3}H]uracil, then the ^{32}P entering RNA via ATP, CTP, and GTP should enter in a noncompartmentalized manner, while essentially all of the ^{3}H should enter in a compartmentalized manner. If this were the case, then one would predict

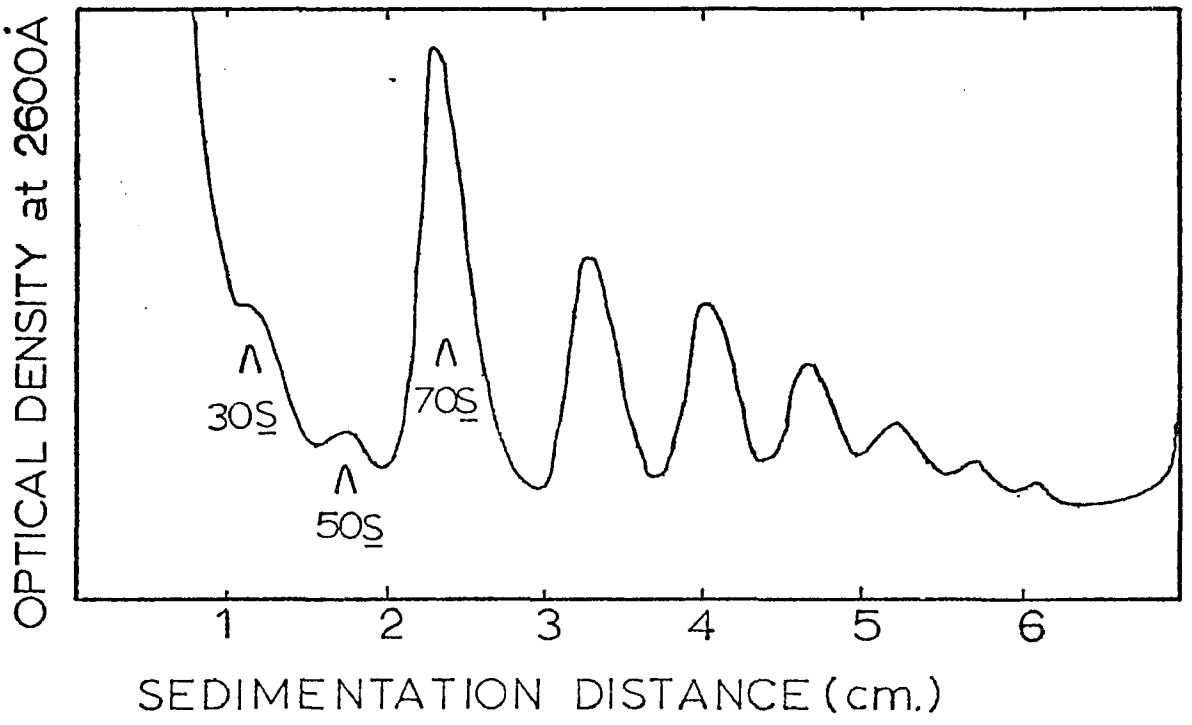

Figure 30. Typical Polysome Profile

Exponentially growing cultures (minimal medium) of E. coli at an O.D.$_{600}$ = 0.3 were labeled with [5-^{3}H]uracil (10 μM, 0.26 C/mmole) and $H_3{}^{32}PO_4$ (carrier-free, 0.1 μC/ml.) for 75 seconds, and 90 ml. of this culture were poured onto 50 g of -20°C crushed ice. The cells were centrifuged at 6,000 rpm for 4 minutes at 4°C. The drained pellet was vortexed and 0.4 ml. of sucrose buffer (20%, RNase-free sucrose, 10^{-2} M $MgSO_4$, 6 x 10^{-2} M KCl, 5 x 10^{-3} M tris, pH 7.2) was added. One-tenth ml. of protoplasting mixture (10^{-1} M tris, 1.75 mM EDTA, 1.5 mg/ml. lysozyme-3x recrystallized, pH 8.1) was added followed by 0.5 ml. lysing mixture (2 x 10^{-2} M $MgSO_4$, 1% Brij 58, 0.4% deoxycholate, 2 x 10^{-3} M tris, 0.1 mg/ml. DNase-electrophoretically pure, pH 8.1). After 5 minutes incubation at 4°C, the preparation was centrifuged at 100,000 g for 5 minutes, and 0.5 ml. of the supernatant was carefully layered onto a 32-ml. sucrose gradient (sucrose buffer--15% to 30% sucrose) and centrifuged at 4°C in a Beckman SW25 head for 7 hours at 25,000 rpm.

The gradient was collected by a peristaltic pump and scanned at 2600 A while passing through a continuous-flow photo cell. Appropriate fractions were precipitated with 5% cold TCA and counted in Aquasol.

that in either a noncompartmentalized system (Fig. 4a) or a Type I compartmentalized system (Fig. 5a), the ratio ($^3H/^{32}P$ ribosomal RNA/ $^3H/^{32}P$ polysomal RNA) should be around 0.91 (this value is less than 1.0 because of the differences in base ratio between ribosomal and messenger RNA's). In the case of Type II precursor compartmentation (Fig. 6a), one would predict a substantially higher value for this ratio.

In the series of four experiments (Table 1), the value of the ratio ranged from 1.13 to 1.49. This corresponds to a value of 30% to 70% higher than predicted for either a noncompartmentalized or a Type I compartmentalized system. These results appear to favor the Type II compartmentalized model but are open to a very serious criticism.

A fundamental assumption in this experiment was that ^{32}P labels all four ribonucleotides at about the same rate or, alternatively, that ribosomal RNA and messenger RNA have equivalent base ratios. Messenger RNA and ribosomal RNA are known to differ markedly in base ratio, and Price et al. (1967) have shown that the rate of ^{32}P labeling in the α position of the four ribonucleotides varies considerably. In light of these findings, it is quite possible that the value of the ratio ($^3H/^{32}P$ ribosomal RNA)/($^3H/^{32}P$ polysomal RNA) is higher than predicted for the Type I compartmentalized model simply because ^{32}P is entering the polysomal RNA faster than expected.

My next set of experiments involved the use of the antibiotic rifampicin. This antibiotic prevents the initiation of new RNA chains but allows the completion of previously initiated chains. Unstable RNA appears to decay normally in rifampicin-treated cultures. Experimentally, I added [^3H]uracil and rifampicin simultaneously and then assayed for

trichloroacetic acid (TCA) insoluble label as a function of time after labeling. A typical experiment gives the characteristic plot shown in Figure 31.

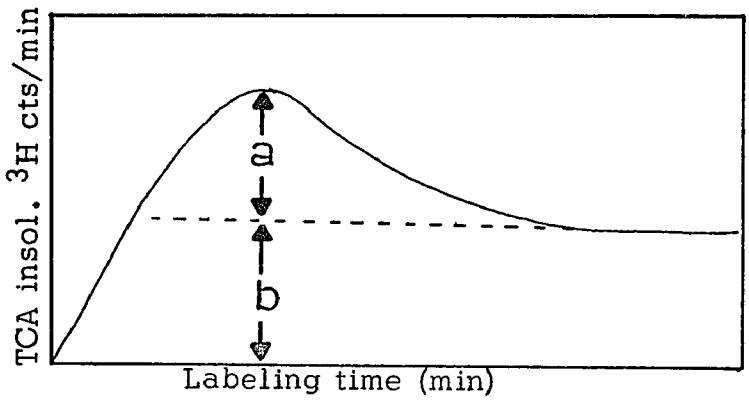

Figure 31. Incorporation of Labeled Precursor into RNA in the Presence of Rifampicin

In this plot, the height b is taken as the proportion of label in stable RNA and the height a is taken as the proportion of label in unstable RNA. The Q value is defined as a/(a + b) and is assumed to be proportional to the relative rate of unstable RNA synthesis. In both compartmentalized models there is a competition between utilization of RNA precursor and diffusion of RNA precursor. If utilization is dominant, then compartmentation is favored. If diffusion is dominant, then one would expect a decreased degree of compartmentation. In a Type II compartmentalized system such as is shown in Figure 6a, a decreased degree of compartmentation should result in a higher Q value, whereas in a Type I compartmentalized system the Q value is unaffected by the degree of compartmentation. Diffusion is a first-order phenomenon, whereas the phosphorylation and polymerization steps comprising the

utilization of precursor are second or higher order reactions. Because of this disparity in reaction orders, a decrease in temperature should slow utilization of precursor much more than diffusion of precursor and thereby effectively decompartmentalizes.

I ran two experiments involving simultaneous addition of rifampicin and [^{3}H]uracil. One culture was incubated at 37°C and one culture at 25°C. The respective Q values were 0.38 and 0.43. These experimental results are shown in Figure 32.

Again, the results appear to support Type II compartmentation but are equivocal for the following reasons. It is possible that either the relative rate of unstable RNA synthesis goes up as the growth rate decreases or that the rate of unstable RNA decay is decreased to a greater extent than the rate of synthesis at the lower temperature. Either of these factors would result in an increased Q value with decreased temperature.

In an effort to avoid growth rate changes which might change the relative rate of unstable RNA synthesis and/or decay, I ran the following experiment. To one of two identical cultures, I added unlabeled uracil to give a concentration of 50 μM. The second culture had no exogenous uracil. After 10 minutes (well before the first culture would have exhausted its exogenous uracil), I added to each culture labeled uracil and rifampicin. The results are shown in Figure 33. The Q values were identical in these two cultures.

The rationale behind this experiment was that those cells grown in the absence of exogenous uracil should have undergone a larger precursor pool expansion concurrent with labeling and that this rapid influx

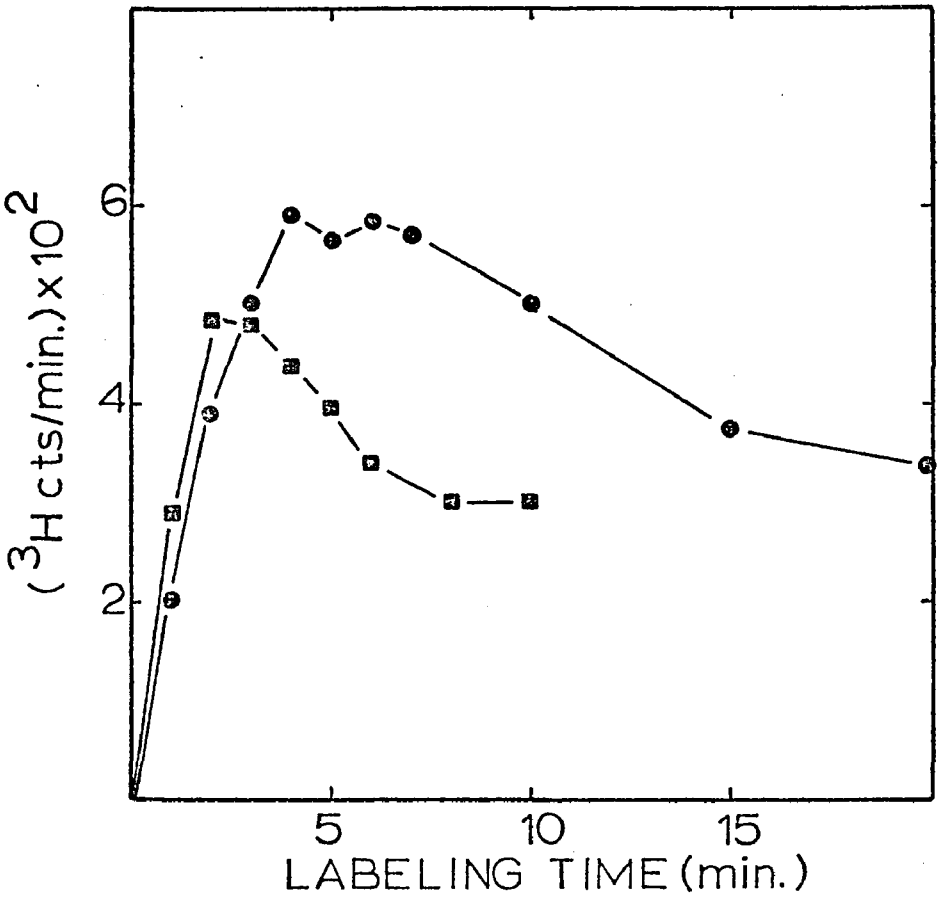

Figure 32. Temperature-dependent Incorporation of Labeled Precursor into RNA in the Presence of Rifampicin

To 10 ml. of an exponentially growing culture (minimal medium) of E. coli at $O.D._{600}$ = 0.25, 0.7 ml. of R-U-A (3 mg rifampicin in 0.1 ml. methanol, 0.1 ml. [5-^{3}H] uracil (20 μC/ml, 0.26 C/mmoles) and 0.5 ml. 1% bovine serum albumin) was added, and 0.5-ml. samples were taken into 5 ml. of cold 5% TCA. The precipitate was hydrolyzed with 0.5 N NaOH and the hydrolysate was counted in Aquasol. One culture was maintained at 37°C (— ■ —); a second culture was maintained at 25°C (— ● —).

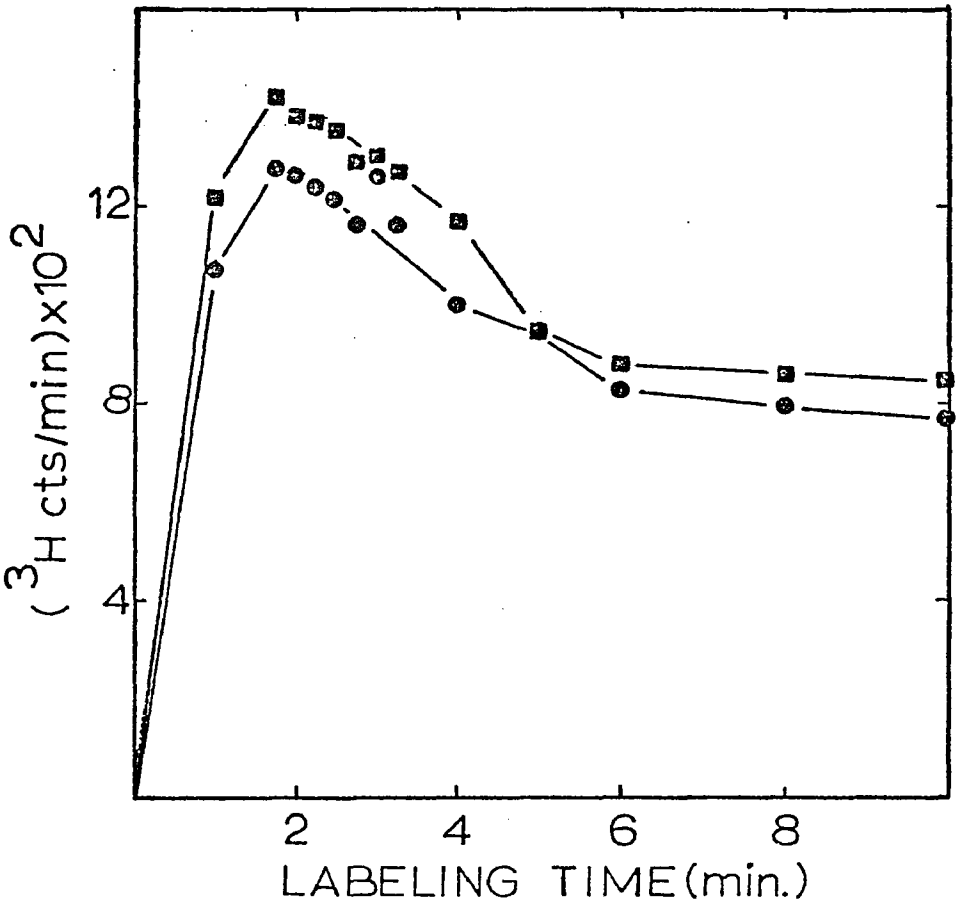

Figure 33. Effect of Pregrowth with Precursor on the Incorporation of Labeled Precursor into RNA in the Presence of Rifampicin

Two exponentially growing cultures of E. coli were incubated at 37°C as in the experiment of Figure 32. One culture was pregrown in 50 μM uracil for 10 minutes before labeling (— ● —); the other culture received no uracil before labeling (— ■ —). Both cultures were labeled, treated, and counted as in the experiment of Figure 32.

of labeled uracil would have been relatively noncompartmentalized. On the other hand, those cells grown in the presence of exogenous uracil should have undergone no significant precursor pool expansion concurrent with labeling. If the above were indeed true, thenone would predict identical Q values in the case of a Type I compartmentalized system and nonidentical Q values in the case of a Type II compartmentalized system. The experimental results therefore appear to favor the Type I compartmentation model.

Because of all of the above equivocations and apparently contradictory results, I began work on the computer simulations detailed in Chapter II.

REFERENCES

Adesnik, Milton and Levinthal, Cyrus (1970). RNA metabolism in T4-infected Escherichia coli. J. Mol. Biol. 48, 187.

Berlin, R. D. and Stadtman, E. R. (1966). A possible role of purine nucleotide pyrophosphorylases in the regulation of purine uptake by Bacillus subtilis. J. Biol. Chem. 244, 2679.

Billen, Daniel, Carreira, L. B., Hadden, C. T. and Silverstein, S. J. (1971). Evidence suggestive of compartmentalization of deoxyribonucleic acid--synthesizing systems in freeze-treated Bacillus subtilis. J. Bact. 108, 1250.

Birnbaum, L. S. and Kaplan, Sam (1971). Localization of a portion of the ribosomal RNA genes in Escherichia coli. Proc. Nat. Acad. Sci., Wash. 68, 925.

Blundell, M. R. and Wild, D. G. (1971). Altered ribosomes after inhibition of Escherichia coli by rifampicin. Biochem. J. 121, 391.

Bolton, E. T. and McCarthy, B. J. (1962). A general method for the isolation of RNA complementary to DNA. Proc. Nat. Acad. Sci., Wash. 48, 1390.

Borek, Ernest and Srinivasan, P. R. (1966). The methylation of nucleic acids. Ann. Rev. Biochem. 35, 275.

Bothwell, A. L. and Apirion, David (1971). Is RNase V a manifestation of RNase II? Biochem. Biophys. Res. Comm. 44, 844.

Bremer, Hans, Konrad, M. W., Gaines, Kathleen, and Stent, G. S. (1965). Direction of chain growth in enzymatic RNA synthesis. J. Mol. Biol. 13, 540.

Bremer, Hans and Yuan, Dorothy (1968a). Uridine transport and incorporation into nucleic acids in Escherichia coli. Biochim. Biophys. Acta 169, 21.

Bremer, Hans and Yuan, Dorothy (1968b). Chain growth rate of messenger RNA in Escherichia coli infected with bacteriophage T4. J. Mol. Biol. 34, 527.

Buchwald, M. and Britten, R. J. (1963). Incorporation of ribonucleic acid bases into the metabolic pool and RNA of E. coli. Biophys. J. 3, 155.

Chaney, S. G. and Boyer, P. D. (1972). Incorporation of water oxygens into intracellular nucleotides and RNA: II. Predominantly hydrolytic RNA turnover in Escherichia coli. J. Mol. Biol. 64, 581.

Cox, R. A. (1968). Macromolecular structure and properties of ribonucleic acids. Quart. Rev. (London) 22, 499.

Cutler, R. G. and Evans, J. E. (1967). Relative transcription activity of different segments of the genome throughout the cell division cycle of Escherichia coli. The mapping of ribosomal and transfer RNA and the determination of the direction of replication. J. Mol. Biol. 26, 91.

Darnell, J. E. (1968). Ribonucleic acids from animal cells. Bact. Rev. 32, 262.

Davidson, J. N. (1969). The Biochemistry of the Nucleic Acids. London Methuen and Co., Ltd.

Fan, D. P., Higa, Akiko and Levinthal, Cyrus (1964). Messenger RNA decay and protection. J. Mol. Biol. 8, 210.

Garfinkel, David and Heinmets (1969). Application of computers to the study of protein metabolism. In Mammalian Protein Metabolism, vol. III, p. 264, ed. by H. N. Munro, New York, Academic Press.

Garfinkel, David and Lajtha, Abel (1963). A metabolic inhomogeneity of glycine in vivo. I. Experimental determination. J. Biol. Chem. 238, 2429.

Geiduschek, E. P. and Haselkorn, Robert (1969). Messenger RNA. Ann. Rev. Biochem. 28, 647.

Gillespie, David and Spiegelman, S. (1965). A quantitative assay for DNA-RNA hybrids with DNA immobilized on a membrane. J. Mol. Biol. 12, 829.

Holmes, R. K. and Singer, J. F. (1971). Inability to detect RNase V in Escherichia coli and comparison of other ribonucleases before and after infection with coliphage T7. Biochem. Biophys. Res. Comm. 44, 837.

Hurwitz, Jerard and August, J. T. (1963). The role of DNA in RNA synthesis. Progress in Nucleic Acid Res. 1, 59.

Huzyk, Lydia and Clark, D. J. (1971). Nucleoside triphosphate pools in synchronous cultures of Escherichia coli. J. Bact. 108, 74.

Jacob, Francois and Monod, Jacques (1961). Genetic regulatory mechanisms in the synthesis of proteins. J. Mol. Biol. 3, 318.

Kennell, David (1968). Titration of the gene sites on DNA by DNA-RNA hybridization. II. The Escherichia coli chromosome. J. Mol. Biol. 34, 85.

Koch, A. L. (1968). The evaluation of the rates of biological processes from tracer kinetic data. II. RNA metabolism in growing bacteria. J. Theor. Biol. 18, 105.

Koch, A. L. (1971a). Evaluation of the rates of biological processes from tracer kinetic data. III. The net synthesis lemma and exchangeable pools. J. Theor. Biol. 32, 429.

Koch, A. L. (1971b). Evaluation of the rates of biological processes from tracer kinetic data. IV. Digital simulation of nucleic acid metabolism in bacteria. J. Theor. Biol. 32, 451.

Kuwano, Michihiko, Kwan, C. N. and Apirion, David (1969). Ribonuclease V of Escherichia coli. I. Dependence on ribosomes and translocation. Proc. Nat. Acad. Sci., Wash. 64, 693.

Labowitz, Paul, Weissman, S. M. and Radding, C. M. (1971). Nucleotide sequence of a ribonucleic acid transcribed in vitro from λ phage deoxyribonucleic acid. J. Biol. Chem. 246, 5120.

Leive, Loretta (1965). Actinomycin sensitivity in Escherichia coli produced by EDTA. Biochem. Biophys. Res. Comm. 18, 13.

Leive, Loretta and Kollin, Virginia (1967). Synthesis, utilization and degradation of lactose operon in RNA in Escherichia coli. J. Mol. Biol. 24, 247.

Levinthal, Cyrus, Keynan, Alex, and Higa, Akiko (1962). Messenger RNA turnover and protein synthesis in B. subtilis inhibited by actinomycin D. Proc. Nat. Acad. Sci., Wash. 48, 1631.

Lindahl, Lasse and Forchhammer, Jes (1969). Evidence for reduced breakdown of messenger RNA during blocked transcription or translation in Escherichia coli. J. Mol. Biol. 43, 593.

Mandelstam, J. (1963). Protein turnover and its function in the economy of the cell. Ann. New York Acad. Sci. 102, 621.

Mangiarotti, Giorgio and Schlessinger, David (1967). Polyribosome metabolism in Escherichia coli. II. Formation and lifetime of messenger RNA molecules, ribosomal subunit couples and polyribosomes. J. Mol. Biol. 29, 395.

Marmur, J. (1961). A procedure for the isolation of deoxyribonucleic acid from micro-organisms. J. Mol. Biol. 3, 208.

Maruo, B., Seto, H. and Nagata, Y. (1969). Inducible synthesis of β-galactosidase in disrupted spheroplast of Escherichia coli. J. Bact. 100, p. 209.

McCarthy, B. J. and Britten, B. J. (1962). The synthesis of ribosomes in E. coli. I. The incorporation of C^{14}-uracil into the metabolic pool and RNA. Biophys. J. 2, 35.

Midgley, J. E. (1969). The messenger ribonucleic acid content of Bacillus subtilis 168. Biochem. J. 115, 171.

Mosteller, R. D. and Yanofsky, Charles (1970). Transcription of the tryptophan operon in Escherichia coli: rifampicin as an inhibitor of initiation. J. Mol. Biol. 48, 525.

Mueller, Karl and Bremer, Hans (1968). Rate of synthesis of messenger ribonucleic acid in Escherichia coli. J. Mol. Biol. 38, 329.

Nazar, R. N. and Wong, J. T. (1972). Nucleotide changes and the regulation of ribonucleic acid accumulation during growth rate shifts in Escherichia coli. J. Biol. Chem. 247, 790.

Nierlich, D. P. (1968). Amino acid control over RNA syntheis: a reevaluation. Proc. Nat. Acad. Sci., Wash. 60, 1345.

Nierlich, D. P. and Vielmetter, Walter (1968). Kinetic studies on the relationship of ribonucleotide precursor pools and ribonucleic acid synthesis. J. Mol. Biol. 32, 135.

Nomura, Masayasu (1970). Bacterial ribosome. Bact. Rev. 34, 228.

Norris, T. E. and Koch, A. L. (1972). Effect of growth rate on the relative rates of synthesis of messenger, ribosomal and transfer RNA in Escherichia coli. J. Mol. Biol. 64, 633.

O'Donovan, G. A. and Neuhard, Jan (1970). Pyrimidine metabolism in microorganisms. Bact. Rev. 34, 278.

Pastan, Ira and Perlman, L. (1969). Stimulation of tryptophanase synthesis in Escherichia coli by cyclic 3'5'-adenosine monophosphate. J. Biol. Chem. 244, 2226.

Pato, M. L. and Meyenburg, Kaspar (1970). Residual RNA synthesis in Escherichia coli after inhibition of initiation of transcription by rifampicin. Symposia on Quantitative Biology, 35, 497.

Pine, J. J. (1966). Metabolic control of intracellular proteolysis in growing and resting cells of Escherichia coli. J. Bact. 92, 847.

Plagemann, P. G. (1972). Nucleotide pools in Novikoff rat hepatoma cells growing in suspension culture. III. Effects of nucleosides in medium on levels of nucleotides in separate nucleotide pools for nuclear and cystoplasmic RNA synthesis. J. Cell Biology 52, 131.

Pollock, M. R. (1963). The differential effect of actinomycin D on the biosynthesis of enzymes in Bacillus subtilis and Bacillus cereus. Biochim. Biophys. Acta 76, 80.

Price, T. D., Darmstadt, R. A., Hinds, H. A. and Zemenhof, Stephen (1967). Mechanism of synthesis of deoxyribonucleic acid in vivo. The heterogeneity of incorporation of ^{32}P into the deoxyribonucleotidyl units in Escherichia coli. J. Biol. Chem. 242, 140.

Randerath, Jurt and Randerath, Erika (1967). Thin-layer separation methods for nucleic acid derivatives. Methods in Enzymology 12A, 323.

Rogers, Dexter (1970). Dissociation of a galactose transport system by warm-water treatment. Biochim. Biophys. Acta 211, 255.

Roth, G. S. and Daneo-Moore, Lolita (1971). Intracellular localization of ribosome biosynthesis in osmotically fragile forms of Streptococcus faecalis. Biochim. Biophys. Acta 240, 575.

Ryter, Antoinette (1969). Structure and functions of mesosomes of gram positive bacteria. Current Topics in Microbiology and Immunology 49, 151.

Salser, W. A. (1966). The metabolism of unstable RNA and its relation to protein synthesis. Ph.D. thesis, Massachusetts Institute of Technology.

Salser, Winston, Janin, Joël, and Levinthal, Cyrus (1968). Measurement of the unstable RNA in exponentially growing cultures of Bacillus subtilis and Escherichia coli. J. Mol. Biol. 31, 237.

Schaechter, M., Previc, E. P. and Gillespie, M. E. (1965). Messenger RNA and polyribosomes in Bacillus megaterium. J. Mol. Biol. 12, 119.

Schwartz, Thom, Craig, Elizabeth and Kennell, David (1970). Inactivation and degradation of messenger ribonucleic acid from the lactose operon of Escherichia coli. J. Mol. Biol. 54, 299.

Shigeura, H. T. and Boxer, G. E. (1964). Incorporation of 3'-deoxyadenosine-5'-triphosphate into RNA by RNA polymerase from Micrococcus lysodeikticus. Biochem. Biophys. Res. Comm. 17, 758.

Spadari, S. and Ritossa, F. (1970). Clustered genes for ribosomal ribonucleic acids in Escherichia coli. J. Mol. Biol. 53, 357.

Sternglanz, Rolf (1972). Biochemistry Department, State University of New York at Stony Brook, Stony Brook, N.Y. Personal communication.

Strange, R. E., Dark, F. A. and Ness, A. G. (1961). The survival of stationary phase Aerobacter aerogens stored in aqueous suspension. J. Gen. Microbiol. 25, 61.

Sugino, Akio, Hirose, Susumu and Okazaki, Reiji (1972). RNA-linked nascent DNA fragments in Escherichia coli. Proc. Nat. Acad. Sci., Wash. 69, 1863.

Summers, W. C. (1970a). A simple method for extraction of RNA from E. coli utilizing diethyl pyrocarbonate. Anal. Biochem. 33, 459.

Summers, W. C. (1970b). The process of infection with coliphage T7. IV. Stability of RNA in bacteriophage-infected cells. J. Mol. Biol. 51, 671.

Thomas, E., Weissbach, H. and Kaback, H. (1971). Department of Biochemistry, Roche Institute of Molecular Biology, Nutley, N.J. Personal communication.

Umezawa, Hamao, Mizuno, Satoshi, Yamazaki, Hisaji and Nitta, Kazuo (1968). Inhibition of DNA-dependent RNA synthesis by rifamycins. J. Antibiotics 21, 234.

Varricchio, Frederick (1972). "Compartmentalization" of Escherichia coli ribosomes and ribonucleic acid. J. Bact. 109, 1284.

Wahba, A. J., Salas, Margarita and Stanley, W. M. (1966). Studies on the translation of the genetic message. II. Translation of oligonucleotide messengers of specified base sequence. Cold Spr. Harb. Symp. Quant. Biol. 31, 103.

Werner, Rudolf (1971a). Mechanism of DNA replication. Nature 230, 570.

Werner, Rudolf (1971b). Nature of DNA precursors. Nature New Biology 233, 99.

Willetts, N. S. (1967). Intracellular protein breakdown in non-growing cells of Escherichia coli. Biochem. J. 103, 453.

Winslow, R. M. and Lazzarini, R. A. (1969). The rates of synthesis and chain elongation of ribonucleic acid in Escherichia coli. J. Biol. Chem. 244, 1128.

Zimmermann, R. A. and Levinthal, Cyrus (1967). Messenger RNA and RNA transcription time. J. Mol. Biol. 30, 349.